UNIVERSIDAD DE SALAMANCA

Instituto de Biología Funcional y Genómica

(USAL/CSIC)

Pheromone-dependent cell cycle arrest in the

phytopathogenic fungus *Ustilago maydis*

PhD Thesis

Paola Bardetti

Salamanca 2018

UNIVERSIDAD DE SALAMANCA

Instituto de Biologia Funcional y Genomica

(USAL/CSIC)

Pheromone-dependent cell cycle arrest in the phytopathogenic fungus *Ustilago maydis*

Memoria presentada por Paola Bardetti para optar al grado de Doctor en Biología.

Director de tesis: Prof. Dr. José Pérez-Martín

Salamanca 2018

ABBREVIATIONS

bE: bEast

bW:bWest

C: DNA content

cAMP: Cyclin adenosine monophosphatase

Cbx: Carboxin

CDK: Cyclin-dependent kinase

CKI: Cdk inhibitor

cDNA: Coding DNA

CFW: calcofluor white

CMD: Complete medium with glucose

CMA: Complete medium with arabinose

DIC: Differential interference contrast microscopy

DNA: Deoxyribonucleic acid

dNTP: Deoxyribonucleotide

FACS: Fluorescence-acticated cell sorting

G418: Geneticin

GFP: Green fluorescent protein

Hyg: Hygromycin

MAPK: Mitogen-activated protein kinase

$MMNO_3$: Minimal medium with nitrate

mRNA: Messenger RNA

NLS: nuclear localization signal

OD_{600}: Optical density at 600nm

PCR: Polymerase chain reaction

Phleo: phleomycin

RNA: Ribonucleic acid

rpm: Revolution per minute

RT-PCR: Reverse transcription polymerase chain reaction

SDS: Sodium dodecyl sulphate

SSC: Salin-sodium citrate buffer

DMSO: Dimethil-sulfoxide

DTT: 1,4-ditiotreitol

EDTA: Ethylenediaminetetracetic acid

h: Hour

min: Minute

kb: Kilobase

kDA: Kilodalton

Tyr: tyrosine

Thr: Threonine

TABLE OF CONTENTS

INTRODUCTION

1. AIM OF THE WORK

All living cells use signal transduction pathways to respond to the environmental changes. Signaling cascades are involved in the transmission of an external stimulus to intracellular targets allowing cells to adapt to the new conditions. The comprehension of these signaling pathways is pivotal to understand important mechanisms such as cellular growth, differentiation and cell death. Since Fungi are simple organisms and their internal signals pathways are evolutionary conserved, they represent on of the best model to provide insights into these processes also in higher Eukaryotes. Moreover, in the past decades the knowledge about fungal signaling pathways has increased and it has emerged their importance in determine pathogenicity in human and plant pathogens (Zhao *et al.* 2007; Perez-Nadales *et al.* 2014). For this reason these cascades and their intracellular targets are often studied to understand the mechanism of pathogenicity and develop drugs and compounds that can arrest the infection.

Ustilago maydis is a basidiomycota phytopathogen that causes smut disease in *Zea mais* plant, causing big economic loses (Topp *et al.* 2002). Thanks to the development of techniques that make easier the genetic and molecular manipulation, nowadays *U. maydis* represents a good model to study phytopathogenity (Bolker 2001; Kamper 2004; Terfruchte *et al.* 2014). This fungus has a no pathogenic saprophytic yeast-like phase and a pathogenic phase that is triggered by the mating of two compatible cells in response to pheromone. The fusion results in the formation the infective hyphae that can infect corn plants and cause tumor. In other words, in *U. maydis* virulence is strictly associated with sexual life and pheromone signal triggers the activation of the virulence program. In order to mate *U. maydis* needs to form the sexual structures, called conjugative tube and synchronize the cell cycle of both cells in the same phase. In the no-pathogenic ascomycete fungus *S. cerevisiae,* the

mechanism of cell cycle synchronization induced by pheromone is quite well characterized and results in a cell cycle arrest in G1 phase (Chang and Herskowitz 1990). In *U.maydis* it has been extensively described that a conserved MAPK cascade transmits the pheromone signal, as happens in *S. cereviase*, but how this cascade is able to govern the arrest of the cell cycle is poorly understood. The aim of this study is to elucidate the mechanism by which the pheromone signal can modulate the cell cycle machinery through the MAPK cascade in a pathogenic fungus.

2. U. maydis LIFE CYCLE

U. maydis has a dimorphic life cycle. During the saprophytic no pathogenic phase, haploid cells grow in a yeast-like manner, dividing by budding. In order to complete its life cycle *U. maydis* has to pass through the pathogenic phase in which it grows like a dykarion mycelium inside the plant eventually producing diploid spores

The transition to the pathogenic form starts when two haploid cells of the opposite mating type fuse together. Cells recognition depends on a pheromone/receptor system that consists of seven trans-membrane domain receptors and small lipopeptide pheromone (*pra1/2* and *mfa1/2,* respectively) encoded at the biallelic *a* mating type locus (Felbrugge, 2004). Active pheromone signal results in the formation of the sexual structure, called conjugative tube, and in a cell cycle arrest in G2 (Garcia-Muse *et al.* 2003). These structures appear on one of the cell tip and they grow in a polarized way following the pheromone gradient until they fuse together. After the fusion of the two conjugative tubes, the dykariotic infective filament starts to form (Figure 1E). This developmental switch resulting in the hyphae formation is controlled by the transcription factors bE/bW, composed of two separate subunits bW and bE encoded at the multiallelic *b* mating type locus. Plasmogamy is pitoval for the functionality of the b-factor because it is active only like a heterodimer with subunits derived from different mating partners. The dykariotic

hypha grows over the plant surface in a polar manner accumulating all the cell content on the tip and leaving vacuolated empty sections behind (Steinberg and Perez-Martin 2008). Such kind of growth enables the fungus to find the appropriate point of entry. To penetrate successfully the plant epidermis, the hyphae swells at the tip to generate a structure called appressorium (Lanver *et al.* 2010) (Figura 1F). Once the filament enters into the plant, cell cycle arrest is finally released but the dykariotic status of the growing filament is maintained thanks to the clamp structures that allow the correct sorting of two genetically distinct nuclei during the mitotic cell division (Figure 1I). Subsequently, the massive proliferation and the hypha fragmentation occur inside the plant resulting in tumors formation (Figure 1J). After karyogamy, black diploid teliospores develop and once the tumors dry up and break, mature spore are spread by the wind. Under favorable conditions, teliospores germinate and release haploid cells closing the life cycle of *U. maydis* (Banuett 1995; Lanver *et al.* 2017)(Figure 1K)
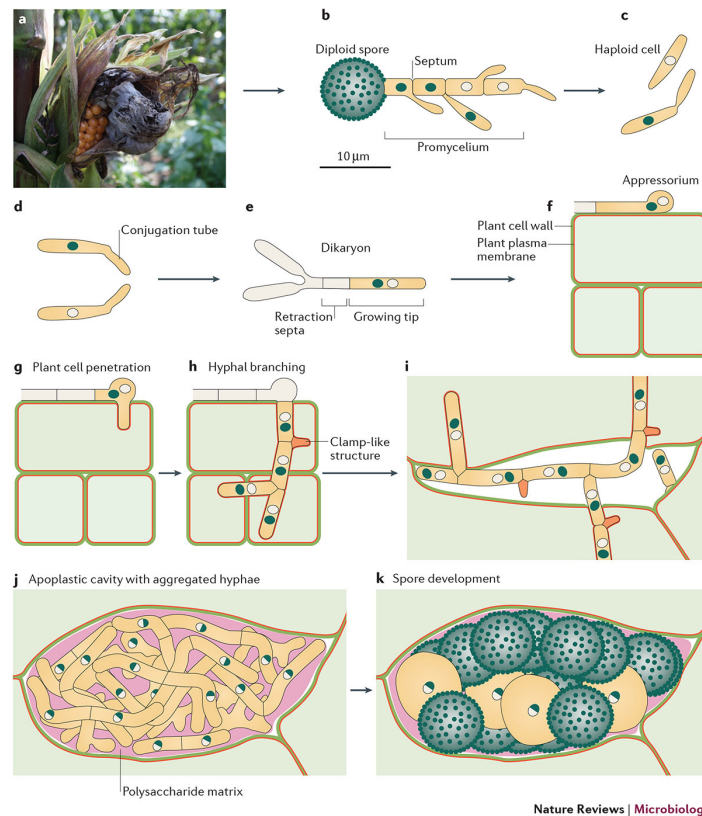
Figure 1: Life cycle of *U.maydis* (Lanver *et al.* 2017)In yeast stage, cells grow by budding and they are no pathogenic. Pheromone recognition between two cells of the opposite mating type takes place on the plant surface. Cells arrest cell cycle and switch to polar grow in order to form the conjugative tube. Once the cell fuse together, the dicaryotic infective filament forms and grows on the plant surface until it reaches the correct point of entry. To penetrate inside the plant *U.maydis* forms a structure called appressorium. Once inside, the cell cycle is released and the infective hypha continues to proliferate. The dycariotic status is maintained thanks to the formation of the clamp structure. Massive proliferation gives rise to the tumors formation. Inside tumors, hypha breaks and nuclear fusion takes place. When tumors dry up, mature black diploid spores are able to germinate and release haploid cells.

3. FORMATION OF THE INFECTIVE FILAMENT BY THE b-FACTOR

In *U.maydis* the infective filament is formed when two haploid cells of the opposite mating type recognize each other through pheromone signal and fuse together. The resulting infective hypha is the structure able to growth in a hyperpolarized way on plant surface and to enter inside. These filaments are arrested in G2 phase (Mielnichuk *et al.* 2009) and cell cycle is not released until the fungus penetrates inside the plant. This arrest in cell cycle is

determined by the bW/bE heterodimer that is formed when two haploid cells mate. For this reason in *U.maydis* sexual development, cell cycle and pathogenicity are strictly related to each other.

3.1 Control of sexual development and pathogenicity in *U.maydis*

Many pathogenic fungi are able to undergo sexual reproduction that is governed by their mating type locus (Bolker and Kahmann 1993). *U. maydis* is a heterothallic fungus (two compatible mating types are required to complete sexual cycle) and its sexual reproduction is regulated by the *a* and *b* loci . In order to mate two cells need to recognized themselves and this depends on the mating type determinants encoded in the locus *a*. In each locus, *a*1 and *a*2, two genes encode for the lipopeptide-pheromone receptor (*mfa*) and a seven transmembrane receptor (Gillissen *et al.* 1992). Pheromone recognition by its receptor results in the activation of the MAPK cascade that triggers the formation of the conjugative tube and, eventually, the cellular fusion (Muller *et al.* 2003)(Figure 2A).

Once the cytoplasmatic fusion is achieved the second mating type determinant, encoded by the *b* locus, induces the sexual progression. The *b* locus is composed of two genes that encode for two unrelated homeodomains transcription factors bE and bW. These two proteins can form a heterodimer only in the case that the two homodimers derive from two different alleles. In this way the formation of this heterodimer is linked to the sexual process and only after the cell fusion can be reached (Kamper *et al.* 1995). The formation of bE/bW homeodomain is the key factor for the formation of the infective hyphae and the initiation of the virulence program. The b factor is able to control the expression of genes that are involved in the dimorphic transition, cell cycle regulation and establishment of the biotrophic phase. The activation of the *a* and *b* loci are cross-controlled: activation of the pheromone-dependent signalling pathways results in the induction of bE and bW genes through the *pfr1* transcription factor while the formation of an active bE/bW

heterodimer after cell fusion leads to the down regulation of the a-pathway (Heimel *et al.* 2010; Heimel *et al.* 2010) (Figure 2B).
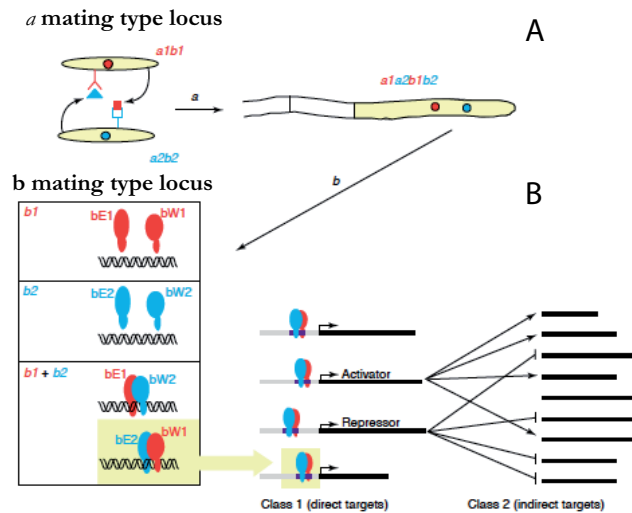
Figura 2: Control of sexual development and pathogenicity in *U. maydis* by *a* and *b* mating type loci (Adapted from (Feldbrugge *et al.* 2004). A) Schematic representation of the interaction pheromone-receptor between two cells of opposite mating type. B) The multi-allelic b locus encoded for a pair of unrelated homodomain proteins, bE and bW. Only the combination between bW and bE of two different alleles is active. An active b transcription factor activates a transcriptional cascade involving more than 200 genes involved in cell cycle regulation, morphology and biotrophic growth.

3.2 Cell cycle arrest triggered by the b-factor.

Interestingly, it has been observed that in *U. maydis* the infective hyphae formed upon the formation of the b-factor is arrested in G2. The cell cycle arrest is a consequence of the accumulation of the inhibitory phosphorylation of Cdk1. This mechanism is dependent of the kinase Wee1, since down-regulation in Wee1 or the expression of an allele of Cdk1 refractory to the phosphorylation result in the formation of the infective hypha that is not arrested in G2 (Castanheira *et al.* 2014). The accumulation of the phosphorylated form of Cdk1 is due to the prevention of nuclear accumulation of Cdc25 in the nucleus. Cdc25 is retained in the cytoplasm by the Bmh1, a protein of the 14-3-3 family (Mielnichuk and Perez-Martin 2008). Cdc25 needs to be phosphorylates in its Bmh1 recognition sites and it has been observed that this phosphorylation is performed by Chk1, a kinase generally

involved in the DNA damage response. Therefore Chk1 is transiently activated during the formation of the infective hyphae (Mielnichuk *et al.* 2009). Recently, it has been described that also Hsl1, a Nim-family kinase that negatively regulates Wee1, is down regulated upon the activation of the b-factor. This down regulation of *hsl1* results in an increase of the inhibitory phosphorylation of Cdk1. The imbalance between the activity of Wee1 and Cdc25 results in the arrest of the cell cycle during the formation of the infective hyphae (Castanheiro *et al.* 2014) (Figure 3).
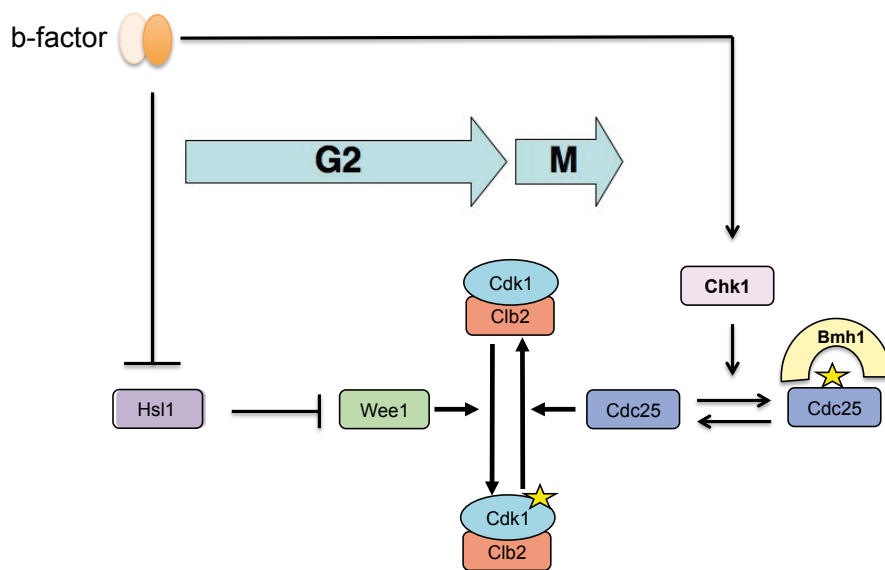
Figure 3: G2 cell cycle arrest induced by the b-factor in *U. maydis*. The kinase Wee1 is responsible of the inhibitory phosphorylation of Cdk1. The phosphatase Cdc25 removes the inhibitory phosphorylation driving the cell into mitosis. Upon the activation of the b-factor, the kinase Chk1 phosphorylates Cdc25 on its Bmh1 sites causing the retention of Cdc25 in the cytoplasm. Moreover Wee1 activity increases due to the down regulation of Hsl1. This balance between Cdc25 and Wee1 is responsible of the G2 cell cycle arrest induced by b-factor.

4 PHEROMONE RESPONSE AND MATING IN *U.maydis*

In *U.maydis* the virulence is strictly associated to sexual development. In fungi able to reproduce sexually, pheromone signal triggers the mating response. This is a crucial point for cells that have to decide whether or not to arrest cell cycle, originate the sexual

structure and eventually fuse together. When pheromone binds the receptors, it leads to the activation of the MAPK cascade that is able to regulate cell cycle machinery and therefore arrest the cell cycle progression.

4.1 Pheromone response pathway and MAPK cascade in U.maydis

U. maydis haploid cells are non-pathogenic and they grow like an yeast, dividing by budding. Key components of the pheromone-signaling pathway are the G-protein-coupled receptors, Pra1/2, seven trans-membrane receptors situated in the plasma membrane that recognize cognate peptide pheromone Maf1/Maf2. Pheromone and receptor are both encoded by the biallelic *a* mating type locus (Feldbrugge *et al.* 2004). The activation of the pheromone system relies with the activation of the evolutionary conserved MAPK cascade module. This intracellular transduction module is composed of three mitogen-activated protein kinases: the MAPKKK Kpp4, the MAPKK Fuz7 and the MAPK Kpp2. The catalytic activation of the MAPK Kpp2 requires the phosphorylation on a serine/threonine residues by the MAPKK Fuz7, which is it phosphorylates by the MAPKKK Kpp4 on a conserved serine/threonine residues (Muller *et al.* 2003). In addition to MAPK cascade, the PKA pathway plays also an important role in response to the external cues. These two cascades integrate nutritional and pheromone signal in order to control sexual development. The integration of both signals occurs through the HMG box transcription factor Prf1. Prf1 is directly phosphorylated by the MAPK kinase Kpp2 and by PKA (Kaffarnik *et al.* 2003). The phosphorylation by PKA triggers the expression of the *a* genes, whereas the phosphorylation by MAPK and PKA induces the expression of the *b* genes. (Heimel *et al.* 2010) (Figure 4).
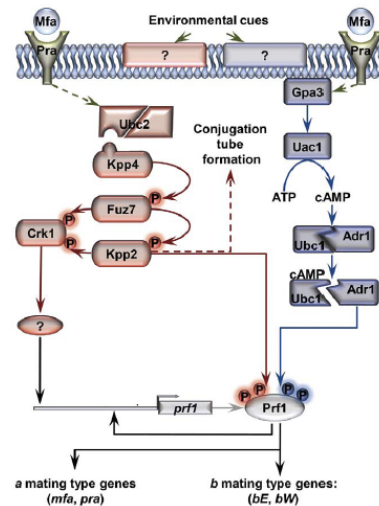
Figure 4: Schematic representation of the pheromone pathway and PKA pathway. (Adapted from Elias-Villalobos, 2011). Pheromones bind to their receptors and activating the MAPK cascade and the PKA pathway. The MAPK cascade module is composed of the MAPKKK Kpp4, the MAPKK Fuz7 and the MAPK Kpp2. The MAPK cascade is able to directly regulate the kinase Crk1, an Ime2-related kinase. Other environmental signals are sensed by unknown receptors and they also contribute to activate both pathways. Most of these signals are not well known. The activation of the two signaling pathways relies with the phosphorylation of Prf1, a transcription factor involved in the activation of the pheromone responsive genes.

4.2 Pheromones response induce the formation of the sexual structure

Pheromone response results in the formation of the sexual structure, the conjugative tube, and in cell cycle arrest. In *U. maydis* the mechanism that regulate the formation of the conjugative tube is poorly understood, however two important elements acting downstream the MAPK have been described to have a pivotal role in morphogenesis.

The first one is a Cdk-related kinase, called Crk1. This kinase is an Ime2-related kinase and its overexpression is able to induce polarized growth (Garrido and Perez-Martin 2003). The filamentous growth induce by Crk1 is dependent of the MAPKK Fuz7 and of the MAPK Kpp2. This kinase is a direct target of the MAPK cascade: Crk1 carries a conserved TXY in its T-loop that aligns with other MAPK and the MAPKK Fuz7 directly phosphorylates it. In addition, the MAPK Kap2 activates Crk1 through dual phosphorylation in the C-terminal domain (Garrido *et al.* 2004)Besides its role in morphogenesis, Crk1 is required for

the expression of *prf1*, which we previously observed is necessary to activate the expression of the pheromone responsive genes (Garrido *et al.* 2004) (Figure 5).

Another fundamental element controlling the polar growth in *U.maydis* is the cyclin Pcl12, a Pcl-like cyclins. This cyclin is able to interact with the essential kinase Cdk5, the homolog of Pho85 from *C.cerevisiae*. This complex was described initially to be required for the proper growth of the b-filament (Flor-Parra *et al.* 2007). Interestingly the expression of *pcl12* is induced by pheromone and cells defective in *pcl12* showed impaired formation of the conjugative tube when exposed to pheromone. (Flor-Parra *et al.* 2007).

4.3 Pheromone-induced cell cycle arrest in U. maydis

Ascomycete fungi, such as *S. cerevisae* and *S. pombe*, arrest their cell cycle in G1 in response to the pheromone (Chang and Herskowitz 1990; Davey and Nielsen 1994). Garcia-Muse and colleagues have described that in U. maydis there is a specific cell cycle arrests in G2 in response to pheromone. They demonstrated that responsive cells, treated with synthetic pheromone, were able to form the sexual structure (conjugative tube) and these cells showed a 2C DNA content. Microscope observation showed that cells had long microtubules reaching the growing region and no spindles assembled, this cytoskeleton organization is characteristic of the arrest in G2 phase in *U. maydis* (Garcia-Muse *et al.* 2003) (Figure 5).
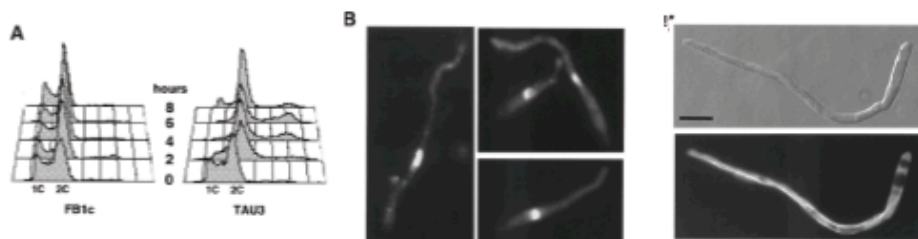
Figure 5: Pheromone-induced cell cycle arrest in G2 (Adapted from Garcia-Muse, 2003). A) FACS analysis shows that cells treated with pheromone show 2C DNA content B) Cells treated with pheromone are able to generate the conjugative tube and they show a single nucleus per cell C) Long microtubules reaching the growing region and no spindles assembled indicate an arrest in G2.

Although the reasons for such different cell cycle arrest are unknown, it is reasonable to speculate that *U. maydis* prefers to arrest cell cycle in G2 because it is the most suitable phase to support polar growth during the formation of the sexual structure. In vegetative condition, the G2 phase is characterized by the polar formation of the bud; this kind of grows requires the rearrangement of the cytoskeleton to support it. For this reason, it could be possible that a prolonged G2 phase could be the most appropriate phase for the tube formation, which needs a very strong polar growth.

4.4 G2/M transition in U.maydis

In *U. maydis* the cell cycle progression is regulated by the kinase Cdk1 in complex with specific cyclins. The complex Cdk1-Cln1 is involved in the G1/S transition, the complex Cdk1-Clb2 is specific for the G2/M and the complex Cdk1-Clb1 is required for both transitions (Garcia-Muse *et al.* 2004; Castillo-Lluva and Perez-Martin 2005). The G2/M transition is well studied in *U. maydis;* it has been described that the kinase Wee1 catalyzes the inhibitory phosphorylation of the complex Cdk1-Clb2 avoiding that cell enter into mitosis (Sgarlata and Perez-Martin 2005). The phosphatase Cdc25 removes the inhibitory phosphorylation on the Cdk1-Clb2 complex allowing the onset of mitosis (Sgarlata and Perez-Martin 2005). The repression of *wee1* elicits a decrease of the inhibitory phosphorylation of Cdk1 associated to a rapid entry into mitosis. On the other hand, the overexpression of *wee1* induces an arrest in G2 phase. The overexpression of *cdc25* determines a decrease of the inhibitory phosphorylation of Cdk1 and premature entry into mitosis. Oppositely, the repression of *cdc25* causes arrest in the progression of the cell cycle with cells showing long buds (Sgarlata and Perez-Martin 2005).

In vegetative conditions the entry into mitosis is regulated by the subcellular localization of Cdc25 (Mielnichuk and Perez-Martin 2008). Cdc25 is retained in the cytoplasm by Bmh1, a protein of the 14-3-3 family. This retention can be induced also as a response for DNA damage agents (Perez-Martin 2009). When Cdc25 is maintained outside the nucleus the

G2/M transition is delayed (Mielnichuk and Perez-Martin 2008). This kind of control has been described also in other organism such as Human and *Xenopus laevis* (Kumagai and Dunphy 1997; Graves *et al.* 2001) where Cdc25 is kept inactive in the cytoplasm by the association with the proteins of the 14-3-3 family during the normal cell cycle.

5 PHEROMONE RESPONSE AND MATING IN *S. cerevisae*

The Ascomycete fungus *S. cerevisae* is the most studied model for understands the connection between sexual development and cell cycle arrest. *S.cereviase* arrests in G1 in response to pheromone (Banuett and Herskowitz 1989) and the molecular mechanism used by pheromone to arrest the cell cycle through the MAPK cascade is well described. In other fungi the connection between pheromone, MAPK cascade and cell cycle machinery is still poorly understood.

5.1 Pheromone response pathway and cell cycle arrest in *S. cerevisae*

The budding yeast has two different mating type named **a** and α. This distinction is controlled by two no-homologous alleles called MATα and MAT**a**. To initiate the signalization, pheromone binds a G protein-coupled receptor, which leads to the release of the Gα subunit and the Gβγ subunits. This last subunit interacts with the complex Ste5-Ste11 and the kinase Ste20 (Whiteway *et al.* 1995; Leeuw *et al.* 1998). Ste5 is the scaffold protein whose recruitment to the membrane leads to the phosphorylation of the MAPKKK Ste11 by Ste20 kinase. Once activated, Ste11 phosphorylates the MAPKK Ste7, which in turns activates the MAPK Fus3, the main MAPK of this process (Herskowitz 1995; Lamson *et al.* 2006) (Figure 6A). Finally, Fus3 moves to the nucleus to activate the transcription factor Ste12 (Elion *et al.* 1993). This transcription factor controls the expression of genes involved in pheromone response and in the formation of the sexual

structure (shmoo) by binding to the Ste12 sites and PREs (pheromone response elements) sites on the promoter region.

Pheromone-induced cell cycle arrest in G1 in *S. cerevisae* is, so far, the best-understood system. Once in the nucleus the MAPK Fus3 phosphorylates the CDK inhibitor (CKI) Far1. Far1 is required for the local activation of Cdc42, the main regulator of the cellular polarization, to the site of the shmoo formation. Moreover Far1 associates in the nucleus with Cdc28/Cln1-Cln2 complex promoting its inhibition (Peter and Herskowitz 1994) (Figure 7A). In addition the MAPK Fus3 promotes the expression of the CKI Far1 and represses the expression of the cyclins CLN1 and CLN2, which are fundamental for the activation of the Cdc28. Consequently, cells arrest the cell cycle in G1. Recently it has been discovered that, not only Far1 is able to inhibit CDK activity *per se* but also it is able to bind to the docking sites of specific substrates of the Cdk/Cyclin complex disrupting the interaction (Fig. 6B). G1 cyclins recognize Cdk substrates by specific docking motif, which promote phosphorylation *in vivo;* Far1 is able to inhibit these docking sites outcompeting with the G1 cyclins (Pope *et al.* 2014).
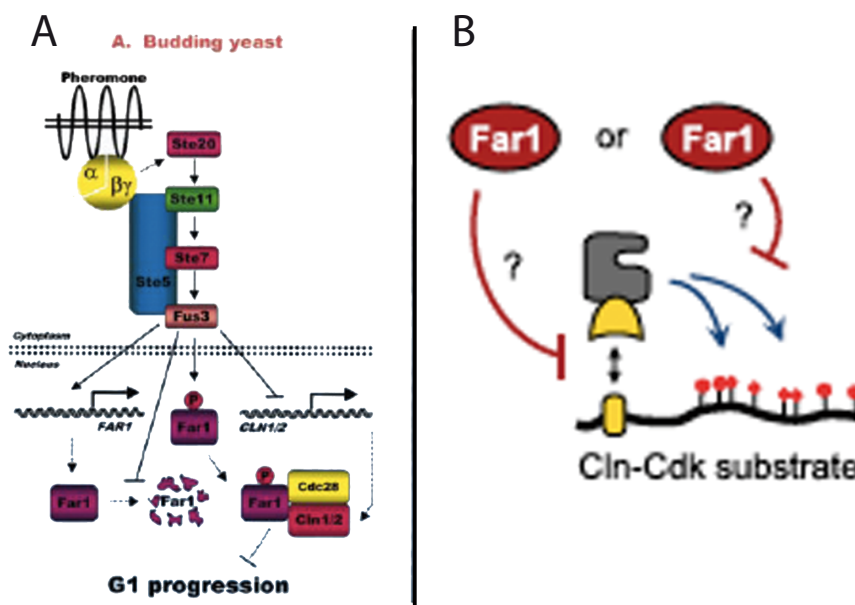
Figure 6: Pheromone-induce cell cycle arrest in G1 in *C. cerevisae* (Wilkinson and Millar 2000; Pope et al. 2014).

A) Activation of the MAPK cascade relies in the traslocation of Fus3 in the nucleus where it phosphorylates the

CDK inhibitor, Far1. The activation of Far1 inhibits the Cdk1/Cln1-2 complex avoiding the progression in mitosis. Fus3 is able also to promote the expression of *far1* and to repress the expression of *cln1-cln2*. B) Far1 is able to bind to the Cdk-cln docking sites on Cdk1/ClN1-2 complexes disrupting the interaction.

In *U. maydis*, a CKI like Far1 do not exist, at least by sequence comparison, and the only mechanism known to regulate the Cdk1-Clb2 complex, the main regulator of the onset of mitosis, is the inhibitory phosphorylation of Cdk1 performed by the kinase Wee1. For this reason, despite the activation and the elements of the MAPK cascade are conserved in *U.maydis*, the regulation of cell cycle machinery must be different in the two species. Our attempt is to study how the pheromone MAPK cascade is able to control cell cycle arrest in G2 in the phytophatogen *U.maydis*.

OBJECTIVES

OBJECTIVE

The sexual differentiation in the maize smut fungus *U.maydis* begins when two cell of the opposite mating type recognize each other through pheromone signaling. The pheromone recognition induces the activation of the MAPK cascade that control the regulation of cell cycle arrest and the formation of the sexual structure,. The objective of tis work is to understand how the pheromone MAPK cascade is able to govern the cell cycle machinery and the morphogenesis of the conjugative tube. In particular we have focused on the mechanism of regulation of cell cycle arrest.

MATERIAL & METHODS

1. STRAINS AND PLASMIDS

U. maydis strains used in this study were listed in the table 1, in which genotype, origin and reference are indicated. Recombinant plasmids, used for strains generation, were listed in the table 2, in which genotype and reference are indicated.

Table 1. *U. maydis* strains used in this study.

STRAIN	GENOTYPE	ORIGIN	REFERENCE
FB1	*a1b1*	521×518	(Banuett and Herskowitz 1989)
UMS01	*a1b1 P$_{crg1}$:fuz7^{DD} nls-gfp*	UMN4	Sonia Castanheira Dias, 2014
	a1b1 P$_{crg1}$:fuz7^{DD}	FB1	(Muller *et al.* 2003)
UMPB12	*a1b1 clb2-ha*	FB1	This study
UMPB15	*a1b1 P$_{crg1}$:fuz7^{DD} clb2-ha*	UMPB12	This study
UMS200	*a1b1 wee1-ha*	FB1	Sonia Castanheira Dias, 2014
UMS195	*a1b1 cdc25-ha*	FB1	Sonia Castanheira Dias, 2014
UMPB14	*a1b1 P$_{crg1}$:fuz7^{DD} wee1-ha*	UMS200	This study
UMPB18	*a1b1 P$_{crg1}$::fuz7^{DD} cdc25-ha*	UMS195	This study
UMPB16	*a1b1 P$_{crg1}$:fuz7^{DD} cdc25-ha pcl12Δ*	UMPB18	This study
UMPB25	*a1b1 P$_{crg1}$:fuz7^{DD} cdc25-ha crk1Δ*	UMPB18	This study
UMPB23	*a1b1 crk1-gfp*	FB1	This study
UMPB28	*a1b1 P$_{crg1}$:fuz7^{DD} crk1-gfp*	UMPB23	This study
UMPB30	*a1b1 pcl12-gfp*	FB1	This study
UMPB33	*a1b1 P$_{crg1}$:fuz7^{DD} pcl12-gfp*	UMPB30	This study
UMPB38	*a1b1 P$_{crg1}$:pcl12 nls-3gfp*	UPB30	This study
UMPB46	*a1b1 gfp-lox-cdc25*	FB1	This study
UMPB52	*a1b1 gfp-lox-cdc25 cut11-cherry*	UMPB46	This study

UMPB54	*a1b1 P$_{crg1}$:fuz7^{DD} gfp-lox-cdc25*	UMPB46	This study
UMPB62	*a1b1 P$_{crg1}$:fuz7^{DD} cdk5^{ts}cdc25-ha*	UMPB18	This study
UMPB65	*a1b1Δcrk1*	FB1	This study
UMPB70	*a1b1 P$_{crg1}$:fuz7^{DD} pcl12-cherry crk1-gfp*	UMPB23	This study
UMPB78	*a1b1 gfp-cdc25 crk1Δ*	UMPB65	This study
UMPB79	*a1b1 gfp-cdc25 crk1Δ cut11-cherry*	UMPB78	This study
UMPB80	*a1b1 P$_{crg1}$:gfp-cdc25*	FB1	This study
UMPB84	*a1b1 loxgfpΔNcdc25*	FB1	This study
UMPB86	*a1b1 P$_{crg1}$:fuz7^{DD} Kap123-ha nls-gfp*	FB1	This study
UMPB88	*a1b1 P$_{crg1}$:fuz7^{DD} loxgfpΔNcdc25*	UMPB84	This study
UMPB89	*a1b1 P$_{crg1}$:fuz7^{DD} kap123^{T867A}ha nls-3gfp*	FB1	This study
UMPB103	*a1b1 P$_{crg1}$:fuz7^{DD} cdc25-ha kap123-gfp*	UMPB18	This study
UMPB104	*a1b1 P$_{crg1}$:fuz7^{DD} cdc25-ha kap123^{T867A}gfp*	UMPB18	This study
UMPB62	*a1b1 P$_{crg1}$:fuz7^{DD} pcl12-Nvenus crk1-Cvenus*	UMPB55	This study
UMPB60	*a1b1 P$_{crg1}$:fuz7^{DD} pcl12-Nvenus*	UMPB55	This study
UMP300	*a1b1 P$_{nar1}$:srp1*	FB1	This study
UMP320	*a1b1 srp1 $^{Pnar1:}$P$_{crg1}$cdc25*	UMP300	This study
UMP303	*a1b1 kap123 ^{Pnar1} P$_{crg1}$cdc25*	UMPB29	This study
UMP299	*a1b1 P$_{nar1}$:kap123*	FB1	This study
UMP303	*a1b1 kap123 ^{Pnar1} P$_{crg1}$cdc25*	UMP299	This study
UMP317	*a1b1 P$_{crg1}$:fuz7^{DD} Kap123-ha nls-gfp crk1Δ*	UMP86	This study
UMP316	*a1b1 P$_{crg1}$:fuz7^{DD} Kap123-ha nls-gfp pcl12Δ*	UMP86	This study
UMPB320	*a1b1 P$_{crg1}$:fuz7^{DD} Kap123-ha nls-gfp kpp2Δ*	UMP86	This study
UMP321	*a1b1 P$_{crg1}$:pcl12 Kap123-ha nls-gfp*	UMP38	This study
UMP322	*a1b1 P$_{crg1}$:pcl12 kap123^{T867A}ha nls-3gfp*	UMP38	This study
UMPB325	*a1b1 P$_{crg1}$:pcl12 Kap123-ha nls-gfp crk1Δ*	UMP321	This study
UMPB326	*a1b1 P$_{crg1}$:pcl12 Kap123-ha nls-gfp fuz7Δ*	UMP321	This study
UMPB327	*a1b1 P$_{crg1}$:pcl12 Kap123-ha nls-gfp kpp2Δ*	UMP321	This study
UMPB105	*a1b1 P$_{crg1}$:fuz7^{DD} cdc25-ha $^{Pcrg1:}$*	FB1	This study

UMS12	*a1b1 P$_{crg1}$:fuz7^{DD} nls-gfp kpp2Δ*	UMS1	Sonia Castanheira Dias, 2014
UMS13	*a1b1 P$_{crg1}$:fuz7^{DD} nls-gfp prf1Δ*	UMS1	Sonia Castanheira Dias, 2014
UMS55	*a1b1 P$_{crg1}$:fuz7^{DD} nls-gfp P$_{crg1:}$cdk1-myc*	UMS51	Sonia Castanheira Dias, 2014
UMS56	*a1b1 P$_{crg1}$:fuz7^{DD} nls-gfp P$_{crg1:}$cdk1^{AF}-myc*	UMS51	Sonia Castanheira Dias, 2014
UMS15	*a1b1 P$_{crg1}$:fuz7^{DD} nls-gfp wee1^{Pnar1}*	UMS1	Sonia Castanheira Dias, 2014
UMP245	*a1b1 P$_{crg1}$:pcl12 nls-gfp crk1^{AEF}-myc*	UMPB38	This study
UMP246	*a1b1 P$_{crg1}$:pcl12 nls-gfp crk1^{AAA}-myc*	UMPB38	This study
UMS147	*a1b1 P$_{crg1}$:fuz7^{DD} cdc25-ha pcl12Δ crk1Δ*	UMS144	Sonia Castanheira Dias, 2014
UMS198	*a1b1 P$_{crg1}$:pcl12 nls-gfp P$_{crg1:}$cdk1-myc*	UMS151	Sonia Castanheira Dias, 2014
UMS199	*a1b1 P$_{crg1}$: pcl12 nls-gfp P$_{crg1:}$cdk1^{AF}-myc*	UMS151	Sonia Castanheira Dias, 2014
UMPB43	*a1b1 P$_{crg1}$.fuz7^{DD}hsl^{Ptef1}*	FB1	This study

Tabla 2: Plasmids used in this study

PLASMID	REFERENCE
pRU11	(Brachmann *et al.* 2004)
p123P$_{crg1}$:fuz7^{DD}	(Brachmann *et al.* 2004)
pClb2-HA	This study
pWee1-HA	Sonia Castanheira Dias, 2014
pCdc25-HA	Sonia Castanheira Dias, 2014
pPcl12Δ	(Flor-Parra *et al.* 2007)
pcrk1Δ	This study
pCrk1-GFP	This study
pPcl12-GFP	This study
pP$_{crg1}$:Pcl12	This study
pPcl12-cherry	This study
P$_{crg1}$:GFP-Cdc25	This study
pKap123-HA	This study
pKap123^{TA}-HA	This study

pKap123-GFP	This study
pKap123^{TA}-GFP	This study
pGFP-Cdc25	This study
pPcl12-NVenus	This study
PCrk1-CVenus	This study
pCut11-cherry	Laboratory collection
pNLS-GFP	Laboratory collection
pP$_{nar}$: Cre	Laboratory collection
pGEM-T easy	Promega
pJET1.2/blunt	Thermo Scientific
pDest (Golden Gate cloning)	Laboratory collection
pG418RΔ (Golden gate cloning)	Laboratory collection
pGFP (Golden Gate cloning)	Laboratory collection
pHA (Golden Gate cloning)	Laboratory collection
pLoxNGFP	Laboratory collection
pLoxGFP	Laboratory collection
pP$_{Nar1}$-Srp1	This study
pP$_{Nar}$-Kap123	This study
pKpp2Δ	Laboratory collection
pFuz7Δ	Laboratory collection
pPcl12Δ	(Flor-Parra *et al.* 2007)
pCrk1^{AF}-Myc	(Garrido *et al.* 2004)
pCrk1^{AAA}-Myc	(Garrido *et al.* 2004)
pCrk1^{KD}-Myc	(Garrido *et al.* 2004)
p P$_{crg1}$Cdk1^{AF}-Myc	Laboratory collection
p P$_{crg1}$Cdk1^{AAA}-Myc	Laboratory collection
pP$_{Nar}$-Wee1	(Sgarlata and Perez-Martin 2005)

2. GROW CONDITIONS AND MEDIA

2.1 General media and growth conditions

E.colli cells were grown in LB Broth-Lennox medium (LB) or on solid LB medium according to Sambrook and collegues (1989), both supplemented with 100μg/ml of ampicillin. Liquid cultures were incubated at 37° with constant shaking at 200 rpm. Solid media were incubated at 37° in aerobic conditions.

U.maydis cells were grown in yeast peptone (YP), complete medium (CM) or minimal medium with nitrate (MMNO$_3$). Appropriate carbon source was added to the media. Liquid cultures were grown at 28° with constant shaking at 250 rpm. Solid media were incubated at 28° in aerobic conditions. Cell density in liquid cultures was measured by photometer at 600nm. In order to obtain cultures in exponential phase, cells were diluted and grown to a value of OD$_{600}$= 0,5-0,8.

2.2 Protoplast regeneration and transformants selection

Protoplasts were regenerated in regeneration agar supplied with the appropriate concentration of antibiotics for transformants selection (200μg/ml Hygromycin B, 2 μg/ml Carboxin, 150μg/ml Nourseothricin, 500μg/ml G418, 5μg/ml Phleomycin). Regeneration plates were made of two layers: a bottom layer containing regeneration agar with antibiotic and a top layer of regeneration agar without antibiotic.

2.3 Inducible and conditional promoters conditions

In order to control expression of genes, the inducible promoters P$_{crg1,}$ and P$_{nar1}$ were used (Bottin *et al.* 1996; Brachmann *et al.* 2001). The first one is activated in presence of

arabinose and repressed with glucose, while P_{nar1} promoter is activated in presence of nitrate and repressed with ammonium. For induction experiments P_{crg1} was used. Cells were grown in medium containing glucose at a final concentration of 2% until a cell density of OD_{600}~0,5. Then, cells were washed three times with medium containing arabinose at a final concentration of 2%. After that, cells were continually grown in medium with arabinose as sole carbon source. To perform repression experiments P_{nar1} promoter was used. Cell were grown in $MMNO_3$ until a cell density of OD_{600}~0,5, washed three times with sterile water and then transferred to a repressive medium. For constitutive expression of genes P_{tef1} was used.

3. GENETIC METHODS

3.1 Cloning and restriction mapping

E. coli plasmid minipreparation, DNA restriction enzyme digestions, alkaline-phosphatase treatment, ligation reaction, electrophoretic analysis were performed as described by Ausubel and colleagues (1997). Restriction enzymes were purchased from New England Biolabs. Alkaline-phosphatase reactions were performed using rAPid Alkaline Phosphatase from Roche. Ligations were carried out using T4 DNA Ligase from Roche. DNA fragments purification was done according to QIAGEN QIAquick Gel Extraction Kit. *E. coli* chemically competent cells were transformed with purified plasmids or ligation mixes (Hanahan 1983)

3.2 Genomic DNA extraction from *U. maydis*

U. maydis genomic DNA was isolated by glass beads method (Hoffmann and Winston, 1997) with few modifications. 2ml of culture, grown overnight in YPD, was centrifugated at 13200 rpm for 2 min in a fastprep lysis tube. After discarding supernatant 500µl of lysis buffer (10mM Tris-HCL pH8, 1mMEDTA, 100mM NaCl, 1%SDS and 2% TRITON) and

500μL of buffered Phenol were added together with glass beads (Sigma). Cells were smashed in a Fastprep set at speed 6 for 30 sec. After centrifugation for 10 sec at 13200rpm 400μl of the aqueous phase were transferred in a new eppendorf tube and 400μl of isopropanol were added to precipitate DNA. After centrifugation for 10 sec at 13200rpm DNA was air-dried and resuspended in 50μl of distillated water by incubation at 65° with shaking for 5sec.

3.3 PCR reaction

PCR reactions were performed in a thermocycler machine. In this study two different types of DNA polymerase were used: Taq (own production) and Velocity from Bioline for high fidelity amplification. In a standard reaction for Taq polymerase of 50μl 550nM of each oligonucleotides, 10 ng DNA, 200μlM of each dNTP, 2,5μl of 10X buffer and one unit of polymerase were mixed together. Standard PCR program conditions were: initial denaturation for 2 min at 94°C, 30 cycles of 1) denaturation for 30 sec at 94°C, 2) annealing for 30 min between 55°C and 60°C according to the oligonucleotide used, 3) elongation at 72°C for 1 min to 2 min according to the length of the fragment, and final elongation time for 7 min at 72°C. PCR reactions with Velocity were performed as described in the manufacturing protocol.

3.4 *U. maydis* transformation

U. maydis transformation was performed as described by Schultz and colleagues (1990). 50ml of cell cultures at OD$_{600}$~0,7 were centrifuged at 4000rpm for 10 min and then washed once with SCS buffer (20mM sodium citrate pH5.8 1M sorbitol buffer). After that, protoplast induction was done by respuspending cells with SCS buffer supplied with NOVOZYME328 (6mg/ml). Cells were incubated at room temperature for 10-15 min with gently shaking until they lose cell wall (cells became round). The resulting protoplasts

were washed three times with STC buffer (10mM Tris-HCl pH7.5, 1M CaCl$_2$ 1M sorbitol buffer) by centrifugation at 3000rpm for 3 min. Subsequently, protoplasts were resuspended in 500μl of STC and stored in 50μl aliquots at -80°.

Trasformation was performed in ice adding to the 50μl protoplasts suspension DNA (5μl) and 1μl of heparin. After 40 min 500μl of STC containing 40% polyethylene glycol were added and the mixture was incubated for additional 30 sec in ice. Finally protoplasts were spread in two regeneration agar plates and growth at 28°C until colonies appeared.

4. GENE EXPRESSION METHODS

4.1 RNA extraction, cDNA synthesis and quantitative Real-Time PCR

Total RNA was extracted with acidic phenol solution followed by chloroform: isoamyl alcohol (24:1) solution. After the extraction, the RNA was cleaned using the High Pure RNA Isolation Kit (Roche Diagnostic GmbH) and its content quantified with a NanoVue Plus spectrophotometer (GE Healthcare). For qRT-PCR, cDNA was synthesized using the High Capacity cDNA Reverse Transcription Kit (Applied Biosystem) employing 1μg total RNA per sample. qRT-PCR was performed using the SsoAdvance Universal SYBR Green Supermix (BioRad) in a CFX96 Real-Time PCR system (BioRad). The *U. maydis tub1* gene (UMAG_01221), encoding α subunit of tubulin was used as reference. Reaction conditions were as follow: 3 min 95°C, 40 cycles of 10 sec at 95°C/ 10 sec at 60°C/ 30 sec 72°C.

5 PROTEIN METHODS

5.1 Protein extraction

Cells from 10 ml of culture were collected, washed in 10ml of sterile water and immediately resuspended in 1ml of trichloroacetic acid (TCA) 20%. After that cells were centrifuged, supernatant was removed and the pellets obtained were resuspended in 100μl of TCA

20%. After that, glass beads were added to break cells with FastPrep. Cell lysate was collected and the glass beads were washed with 200µl of TCA 5%. The whole cell lysate was collected and centrifuged for 5 min at 3000rpm. The supernatant was taken off and the pellet was resuspended in 100µl of Laemmli buffer (100mM TrisHCl pH6.8, 4% SDS, 200mM DTT, 20% glycerol and traces of bromophenol blue). Once the pellet was resuspended, 50µl of Tris 2M were added and samples were boiled at 100°C for 5 sec. Finally the samples were centrifuged at 13200rpm for 5 sec and the supernatants were collected into new tubes and frozen at -80°C.

5.2 Western blotting

Protein extracts were separated on 4-15% Mini-PROTEAN® TGX™ precast gels from Bio-Rad. Running was performed on TrisHCl/Glycine/SDS (50mM/400mM/0,02%) buffer with constant amperage. Proteins were transferred to an Inmobilon-P membrane (Millipore) using a Trans-Blot Turbo Transfer System also from Bio-Rad. The transfer was done at 0,2 mA for 30 min with transfer buffer (48mM Tris-HCl pH7.5, 39mM glycine, 0,0375%SDS and 20% methanol). The membrane was blocked for 1 hour with 10% milk in PBS-Tween. Conjugative antibody with peroxidase or primary antibody followed by a secondary antibody conjugated to peroxidase, were used and immunoreactive proteins were visualized using chemilumiscent substrate. Chemiluminescent signal was detected using film developer (Agfa CP-BU New, Carestream Biomax Xar Film).

5.3 Stripping for re-probe western blot

Primary and secondary antibodies were removed from the western blot membrane by stripping. The membrane was incubated with shaking at room temperature for 15 min in glycine 0,1M. After that, membrane was washed three times in sterile water and incubated others 15 min in SDS 0,1%. Once the SDS was removed the membrane was blocked and blotted as normal.

6. MASS SPECTOMETRY

6.1 Collection of cells for crude protein extract

For protein extraction cells, collected from 100ml liquid culture, were resuspended in 5ml of B+300 buffer (300mM NaCl, 100mM Tris pH7.5, 10% Glycerol, 1mM EDTA, 0,1% NP-40) with protease and phosphatase inhibitors (for 10ml of B+300 buffer 15µl DTT, 30µl Benzamidine, 100µl Roche protease inhibitors, 100µl phosphatase inhibitors and 100µl PMSF were added). Resuspended cells were frozen in liquid N2 and pulverized using a cryogenic mill. Pulverized cells were collected in a new 10ml falcon.

6.2 Crude protein extraction and GFP proteins purification with GFP-trap

Immunoprecipitation of GFP-tagged protein was performed using GFP-trap® beads (Chromotek). Pulverized cells were resuspended in 5ml of Buffer B300+ with protease and phosphatase inhibitors and centrifuged for 30 min at 4500rpm. Supernatant was collected and another centrifugation was repeated. In the meantime 40µl of GFP-trap® beads was equilibrated with 3ml Buffer B300+ on a rotator at 4°C for 30 min. After that, the protein-containing supernatant was added to the washed beads and incubated for 2 hours at 4°C. Following the incubation, GFP-trap® beads were washed with 5ml of B300+ buffer two times by centrifugation at 2500rpm at 4°C. Finally GFP-trap® beads were boiled for 5 min at 95° in 50µl Loading Dye buffer to elute the bound proteins. The eluted proteins were collected by centrifugation at 2500rpm for 2 min and used directly for SDS-PAGE and immunoblotting or coomassie staining and tryptic digestion.

6.3 Tryptic digestion and sample preparation for LC-MS/MS analysis

Proteins were digested with "Sequencing Grade Modified Trypsin" (Promega). Generated peptides were extracted directly from the polyacrylamide gel according to the procedure described in Shevchenko *at all.* (1996).

6.4 LC-MS/MS analysis

Peptides ere separated using reversed phase liquid chromatography with *RSLCnano Ultimate 3000* system (Thermo Scientific) followed by mass identification with *Orbitrap Velus Pro* mass spectrometer (Thermo Scientific).

7 MICROSCOPY

Images were obtained using a Nikon Eclipse 90i fluorescence microscope with a Hamamatsu Orca-ER camera and a confocal "Spinning disk" (Roper Scientific) with Olympus IX81 microscope, Yokogawa CSU-X1 confocal unit and a Photometrics Evolve camera. Microscopes and cameras were driven by Metamorph (Universal Imaging, Downington, PA). Images were further processed with Adobe Photoshop CS or ImageJ software.

7.1 Nuclei and nuclear membrane visualization

Nuclei observation was done transforming strains with plasmid that brings the *NLS-GFP* sequence. For the observation of the nuclear membrane *cut11-Cherry* endogenous fusion was introduced in the cells (Mielnichuk *et al.* 2009).

8. *U.maydis* STRAINS CONSTRUCTION

In order to generate strains, the constructs detailed below were used to transform protoplasts. Sequencing was performed by GATC Biotech and analyzed with standard bioinformatics tool (Serial Cloner 2-6-1). The integration of the constructs into the corresponding loci by homologous recombination was verified by PCR and in case of deletion also by RT-PCR. Oligonucleotides used to design the constructs are detailed in the table 3.

Table3. Oligonucleotides used in this study.

NAME	SEQUENCE (5'→3')
Cdc25-GFP1	CTGAGAGCCTTCCCGGCTTTGGTGCTTCTG
Cdc25-GFP6	AAAGTGGTGGAAATCGGTAGAGTGCACAGC
GFP-Cdc25-1	CTGAGAGCCTTCCCGGCTTTGGTGCTTCTG
GFP-Cdc25-2	CTAGGTCTCGCCTGCGTTTAAACAATCACAGAGCTGAACGCGTTTCT
GFP-Cdc25-3	CTAGGTCTCCAGGCCGATAATGAAGCGATACGGCAACGTAAG
GFP-Ccd25-4	CTAGGTCTCCGGCCCAATGGCTACTCTCCTCTCCTCACCCCTC
GFP-Cdc25-5	CTAGGTCTCGCTGCGTTTAAACATGAGGACGCGTATTGAGAGTGGTTCC
GFP-Cdc25-6	AAAGTGGTGGAAATCGGTAGAGTGCACAGC
GFP-Cdc25-P1	ATACATATGGTGAGCAAGGGCGAGGAGCTGTTCACC
GFP-Cdc25-P2	ATACAATTGTCAAGACATGTGTCGCGACAAGATGTTGCCCGTGGT
Clb2tag-1	CGAGTATGGTGGCCGAGTACTCGAATGAGA
Clb2tag-2	CTAGGTCTCGCCTGCGTTTAAACCCGAATTACATGGAGTTTCAGAGC
Clb2tag-3	CTAGGTCTCTTGGCCGGCTGACCTGCTTGAGTCGACCCTGCC
Clb2tag-4	CTAGGTCTCCGGCCCAGTAGATGCCAATGTCGGTCGCCGAA
Clb2tag-5	CTAGGTCTCGCTGCGTTTAAACAAGTTTCATTCGACTCTCTTCGCG
Clb2tag-6	TGGCTTTCGCACATCACATGGCGTACTCAC
Wee1-GFP1	GGTGGGTGCACTCGACGAACCGCGGCT
Wee1-GFP6	AAAGCCAGAAGAGGGACGAGGTTGGTTGAG
Hsl1-1	ACGTTTCAGTTTCAGTAGCACCAATAC
Hsl1-2	CTAGGTCTCGCCTGCGTTTAAACATGACGAGAAAGCTGTGCTGTTTGCAA
Hsl1-3	CTAGGTCTCCAGGCCCGAAGCTCTGCCCAAAGCTCCAGACGC
Hsl1-4	CTAGGTCTCCGGCCGATCATGTCTTCCTCGCAACGCCCCGT
Hsl1-5	CTAGGTCTCGCTGCGTTTAAACGAGAGCAAGTTGGGATGTTCGATGAGTT
Hsl1-6	AGATCTTTCGATGTCTCGTACACGTCC
Fuz7DD-check	AAGGGAAGCGACCCAGCGCCAGCTCGATGA
Crk1-1	AAATCGTGAATCGTGAAACATGAATCA

Crk1-6	TTCGGTTTCGGACGATCGGATCAAGTT
Pcl12-1	GCTTCCGCTTCTGCTGTGGACAAGTCCGC
Pcl12-GFP2	CTAGGTCTCGCCTGCGTTTAAACCAGATGGAGCGCGAGCTGTTCGGC
Pcl12-GFP3	CTAGGTCTCTTGGCCGACCTCCAGCTGTAAGGTTGCAGGTAC
Pcl12-GFP4	CTAGGTCTCCCGGCCTGCGCGCCTGAGCGTAATCATTGTCTT
Pcl12-GFP5	CTAGGTCTCGCTGCGTTTAAACGAACAGACGAAACACGGGCACG
Pcl12-6	AAGAATGACACCCAGCCGTATCGTGAATGA
Pcl12-crg1For	ACGCATATGGCTACCACCGTCGCTTCTACATAC
Pcl12-crg1Rev	CATCGCGCGCGCAATTCACGATTATTGTGAATTC
Pcl12-check	CTGCTGCTGCTGCTGCTGCCGACG
SMUT1	CGATGGCTGTGTAGAAGTACTCGCCGATAG
SMUT4	CACCACCCAATCGACGCGGAAGGCAACCCA
PHLEO1	GTGTCCGGTGCATTTCGCCTTCTCGGCG
PHLEO2	TATAAACCTCGAAAATCATTCCTACTAAGA
NAT1	TGGCTGCTGATCACAGCAAGTCAGATT
NAT2	TGTACGCATGTAACATTATACTGAAAACCT
G418-1	GCTCGGTACGGGTACATCGGATCTGCCGGC
G418-2	CTTGAGAAGGTTTTGGGACGCTCGAAGGCT
pTef	GGCGCAAGAAAATTTTTCTCTGGTTCTG
pNar1	GGTGAATAGTGAGAACAGTCTCGATCACTC
pCrg1	GAGATCACGACACCGCGAGGTTTGCGGTGA
Gfp1	ACGCTGAACTTGTGGCCGTTTACGTCG
Cherry1	CTCGCCCTCGCCCTCGATCTCGAACTCGTG
Ha/Myc	TCGCAAGACCGGCAACAGGATTCAATCTTA
N-Venus	ACGCTGAACTTGTGGCCGTTTACGTCG
C-Venus	GTCGCCGATGGGGGTGTTCTGCTGGTA
Cdc25deltaNt	ATCGAATTCATGGGCGTCGCATCCGCCAAACCGCA
Cdc25deltaN2-2	TATGGGCCCGTTTAAACCGGCAGTCGACCACTTGATAGCTGAT
Cdc25deltaN2-3	ACCGTACTCAGATTGATGGCACCGGGGATA

Kap123-1	GCAGAATCCATGGACCGCTGCGGTGGCCGA
Kap123-2	ACAGTTTAAACATTTCTCAGCTCACAATGACGTCCG
Kap123-3	TCGCCGTAGAACGGTCGCTTACAGATCGcCCGGGAGcGTAGTACTTCATGATCTGCGGCATAAA
Kap123-4	TTTATGCCGCAGATCATGAAGTACTACgCTCCCGGgCGATCTGTAAGCGACCGTTCTACGGCGA
Kap123-5	GTAGGCCGCGTTGGCCACGAGGTACTGCTGCAAACCTGCAGCC
Kap123-6	ATAGGCCTGAGTGGCCGCGCGTCGTCGACGCTTTTCCGGATC
Kap123-7	TCTGTTTAAACCCCAAATCAAGGATCACGAATCG
Kap123-8	CCATCGTGGATGTACAAGCGCGAAGCGCTT
Hsl1-1	ACGTTTCAGTTTCAGTAGCACCAATAC
Hsl1-2	CTAGGTCTCGCCTGCGTTTAAACATGACGAGAAAGCTGTGCTGTTTGCAA
Hsl1-3	CTAGGTCTCCAGGCCCGAAGCTCTGCCCAAAGCTCCAGACGC
Hsl1-4	CTAGGTCTCCGGCCGATCATGTCTTCCTCGCAACGCCCCGT
Hsl1-5	CTAGGTCTCGCTGCGTTTAAACGAGAGCAAGTTGGGATGTTCGATGAGTT
Hsl1-6	AGATCTTTCGATGTCTCGTACACGTCC
KPP2-1	AGATGCCCATCCATCCACAGCAATCCT
KPP2-6	GATTCGCTCTTCATTCGACGACCTTCG
FUZ7-1	GGGTTTCATATGCTTTCGTCCGGTGCGGATC
FUZ7-6	CCCTTAAGGGAAATGACAAGATGTGG

8.1 Generation of constructs using Golden Gate system

Constructs in figure 2 were generated using Golden Gate system (Terfruchte *et al.* 2014).

This strategy uses *BsaI*-mediated Golden Gate cloning for the generation of plasmids that

contain a gene-replacement module. Briefly, five components are mixed together in one-

pot reaction: a DNA ligase, the enzyme *Bsa*I, the storage vector carrying the gene

replacement module, the destination vector (pDest), two flanking regions homologous to

the targets locus and framed with BsaI sites with unique overhangs and. In the end of the

reaction, fragments are assembled in the destination vector harbouring the *lacZ* gene

allowing blue/white selection (Figure 1). The fragment of our interest can be linearized and transformed into *U. maydis*.
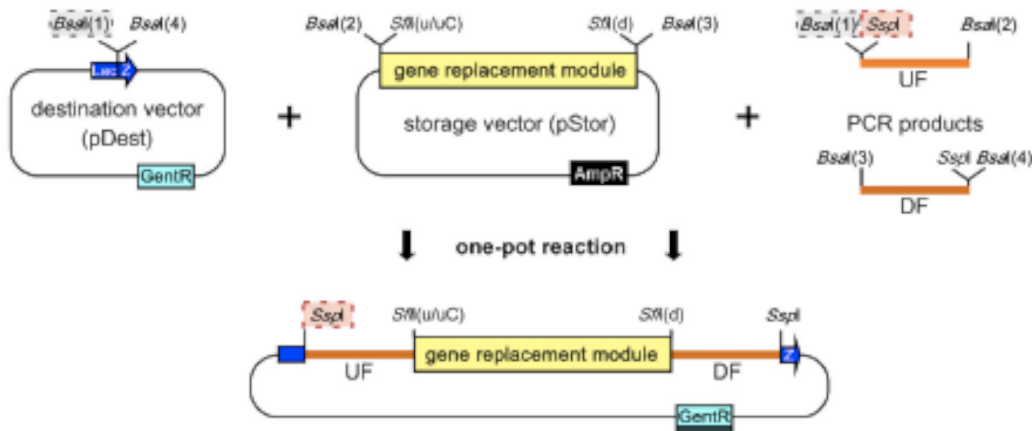
Figure 1: Schematic representation of the Golden Gate reaction

In order to generate constructs two flanking regions of about 1Kb homologous to the target locus are generated by PCR. A standard Golden Gate cloning reaction with a final volume of 15µl was set up in a PCR tube. 40ng of each purified flanks, 75ng of the storage vector carries the gene replacment cassette, 75ng of destination vector pUMa1467, 1x T4 DNA ligation buffer (Zavala-Gonzales *et al.*), 0,75µl of T4 DNA ligase (Roche, 0,75U), 0,5µl *BsaI*-HF (NEB; 10U) were mixed together. The reaction was performed in a PCR cycler machine using the following program: [37°C 2min, 16°C 5min] 50 cycles, 37°C 5 min, 50°C 5 min, 80°C 5 min.

Constructs detailed below were generated using Golden Gate system:

- **Pcl12-GFP:** Two fragments were amplified from genomic DNA. A 1Kb fragment of the C-terminal region of *pcl12* and a 1Kb fragment of the downstream region of *pcl12* were amplified using the pair of oligonucleotide PCL12-2/PCL12-3 and PCL12-4/PCL12-5. The purified fragments were mixed together in a Golden Gate standard reaction including the storage vector pGFP. The plasmid generated was linearized with *SspI* and introduced by homologous recombination to the *pcl12*

locus. The integration was checked using the pair of oligonucleotides PCL12-1/GFP1 and PCL12-6/SMUT4.
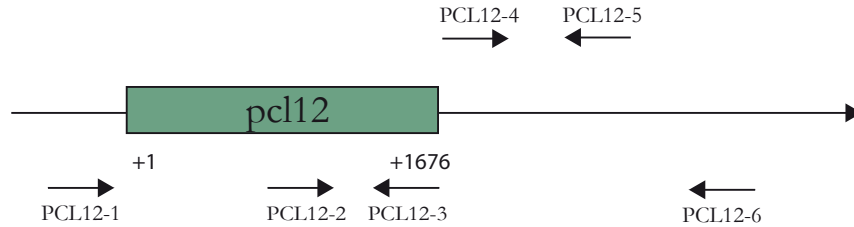
Figure 2: Schematic representation of oligonucleotides position on *pcl12* locus

- **Kap^TA123-HA:** This construction brings a punctual mutation to exchange threonine 367 with alanine in the C-terminal of the protein. Two fragments were amplified from genomic DNA. A 1Kb fragment of the C-terminal region of *kap123* was amplify using the oligonucleotides KAP123-2/KAP123-3, which are modified to exchange T367 with A, and a 1Kb fragment of the downstream region of *kap123* were amplified using the pair of oligonucleotides and KAP123-4/KAP123-5. The purified fragments were mixed together in a Golden Gate standard reaction including the storage vector pHA. The plasmid generated was linearized with *PmeI* and introduced by homologous recombination to the *kap123* locus. The integration was checked using the pair of oligonucleotides KAP123-1/GFP and KAP123-6/SMUT4. To check the point mutation, DNA of positive transformants was digested with *XmaI*.
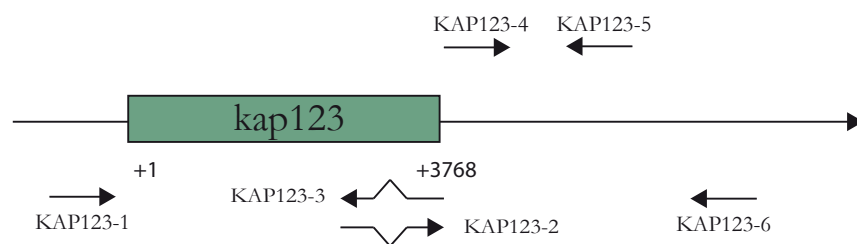
Figure 3: Schematic representation of the primers position on *kap123* locus

- **ΔCrk1-G418R:** Two fragments of about 1Kb homologous to the flanking regions of *crk1* were amplified from genomic DNA using the pairs of primers CRK1-2/CRK1-3 and CRK1-4/CRK1-5. The purified primers were mixed together in a Golden gate standard reaction including the storage vector pΔG418R. The plasmid generated was linearized with *SspI* and introduced by homologous recombination to the *crk1* locus. The insertion was checked by PCR with the pair of oligonucleotides CRK1-1/G418R1 and CRK1-6/G418R. The absence of gene expression was confirmed by RT-PCR.

Figure 4: Schematic representation of the primers position on *crk1* locus

- **P_{tef}: Hsl1:** Two fragments were amplified from genomic DNA. A 1Kb fragment of the promoter region of *hsl1* and a 1Kb fragment of the N-terminal region of *pcl12* were amplified using the pair of oligonucleotide HSL1-2/HSL1-3 and HSL1-4/HSL1-5. The purified fragments were mixed together in a Golden Gate standard reaction including the storage vector pTEF1. The plasmid generated was linearized with *SspI* and introduced by homologous recombination to the *hsl1* locus. The integration was checked using the pair of oligonucleotides HSL1-1/SMUT3 and HSL1-6/TEF1.
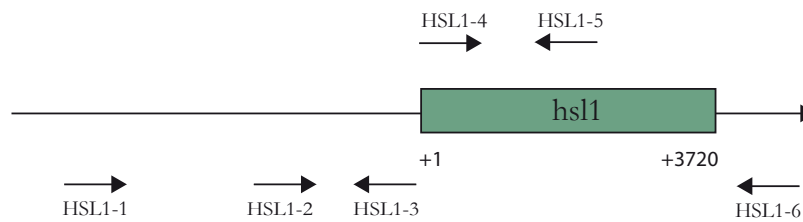
Figure 5: Schematic representation of the primers positions in *hsl1* locus

8.2 Construction of Clb2-HA

For the construction of *clb2-HA* allele two fragments were amplified from genomic DNA. A 1Kb fragment homologous to the C-terminal region of *clb2* excluding the STOP codon and a 1Kb fragment homologous to the downstream region of *clb2* were amplified using respectively the pair of primers CLB2-2/CLB2-3 and CLB2-4/CLB2-5. Both fragments were digested with *SfiI* and ligated to the linear fragment previously digested with *SfiI* from plasmid pMF5-9h. The resulted cassette *clb2-HA-hyg* was cloned into GEM-T. The resulted plasmid pClb2-HA was digested with PacI and introduced by homologous recombination in *clb2* locus. Transformants were checked by PCR using the pair of primers CLB2-1/HA and CLB2-1/SMUT4.

8.3 Construction of Crk1-GFP

For the construction of *crk1-gfp* allele two fragments were amplified from genomic DNA. A 1Kb fragment homologous to the C-terminal region of *crk1* locus excluding the STOP codon and a 1Kb fragment homologous to the downstream region of *crk1* were amplified using respectively the pair of primers CRK1-2/CRK1-3 and CRK1-4/CRK1-5. Both fragments were digested with *SfiI* and ligated to the linear fragment previously digested with *SfiI* from plasmid pMF5-3n. The resulted cassette *crk1-GFP-hyg* was cloned into pGEM-T. The plasmid pCrk1-GFP was digested with *PacI* and introduced by homologous recombination in *crk1* locus. Transformants were checked by PCR using the pair of primers CRK1-1/GFP and CRK1-6/SMUT4.

8.4 Construction of Pcl12-cherry

To generate plasmid pPcl12-cherry, plasmid pPcl12-GFP was digested with *Sfi* in order to exchange the *gfp-hyg* cassette with *cherry-G418R* cassette previously isolated with *SfI* from the plasmid pMF5-5g. Both fragments were ligated and the plasmid originated was digested with *PmeI* and transform into the *pcl12* locus. Integration was checked using the pair of primers PCL12-1/Cherry and PCL12-6/G418R.

8.5 Construction of Pcl12- NVenus, Crk1-CVenus.

To generate plasmid pPcl12-NVenus, plasmid pPcl12-GFP was digested with SfiI in order to exchange the *gfp-hyg* cassette with *N-Venus-Hyg* cassette previously isolated with SfiI from the plasmid pN-Venus-Hyg. Both fragments were ligated and the plasmid originated was digested with *PmeI* and transform into the *pcl12* locus. Integration was checked using the pair of primers PCL12-1/SMUT3 and PCL12-6/SMUT4. To generate plasmid pCrk1-C-Venus, plasmid pCrk1-GFP was digested with *SfiI* in order to exchange the *gfp-hyg* cassette with *C-Venus-G418R* cassette previously isolated with *SfiI* from the plasmid pC-Venus-G418R. Both fragments were ligated and the plasmid originated was digested with *PmeI* and transform into the *crk1* locus. Integration was checked using the pair of primers CRK1-1/C-Venus and CRK1-6/SMUT4.

For the BiFc experiments FB1 Pcl12-NVenus protoplasts were transformed with plasmid pCrk1-CVenus previously digested with *PmeI*. The integration was checked with the oligonucleotides CRK1-1/C-VENUS and CRK1-6/SMUT4.

8.6 Construction of P$_{crg1}$: Pcl12

To generate the plasmid pP$_{crg1:}$Pcl12 the entire ORF of *pcl12* was amplified from genomic DNA using primers Pcl12-OE-fwd and Pcl12-OE-rev. Purified fragment was digested with *NdeI* and *EcoRI* and ligate into the pRU11 plasmid previously digested with the same enzymes. The resulting plasmid pP$_{crg1}$: Pcl12 was digested with *SspI* and introduced by

homologous recombination into the *cbx* locus. Transformants were checked by PCR amplification with primers pCRG1 and Pcl12-check.

8.7 Construction of P_{crg1}: GFP-Cdc25

To obtain the pP_{crg1}: GFP-Cd25 plasmid the fragment GFP-CDC25 was amplified from genomic DNA of FB1 GFP-Cdc25 strain using primers GFP-Cdc25-P1 and GFP-Cdc25-P2. Purified fragment was digested with *NdeI* and *MfeI* and cloned into the pJET 1.2 ® (Thermo Fisher) and sequenced for accuracy. The generate plasmid was digested with *NdeI* and *MfeI* and ligate into the pRU11 plasmid previously digested with *NdeI* and *EcorI* (compatible with *MfeI*). The resulting plasmid pP_{crg1}: GFP-Cdc25 was digested with *SspI* and integrated by homologous recombination into the *cbx* locus. Transformants were checked with primers pCRG1 and Cdc25-GFP6.

8.8 Construction of Kap123^{TA}-GFP

To generate plasmid pKap123^{TA}-GFP, plasmid pKap^{TA}123-HA was digested with *SfiI* in order to exchange the *gfp-hyg* cassette with *ha-g418r* cassette previously isolated with *SfiI* from the plasmid pMF5-5g. Both fragments were ligated and the plasmid originated was digested with *PmeI* and transform into the *kap123* locus. Integration was checked using the pair of primers KAP123-1/GFP1 and KAP123-6/SMUT4. To checked the point mutation, DNA of positive transformants was digested with *XmaI*

8.9 Generation of the strains *a1b1 gfp-cdc25* using the CRE/Lox system

Cre/Lox system was used to generate different strains of *U.maydis* (unpublished data). Briefly, this method is based on the ability of the CRE Recombinase enzyme to recognize specific DNA sequence, called *lox* sites, and mediate recombination between pairs of these *lox* sites. In this study, genomic sequences of our interest were flanked with *lox* sites in order to promote the excision by the CRE recombinase and generate deletion of essential genes (Figure 6, A) or construction of N-terminal tagged proteins (Figure 6, B).
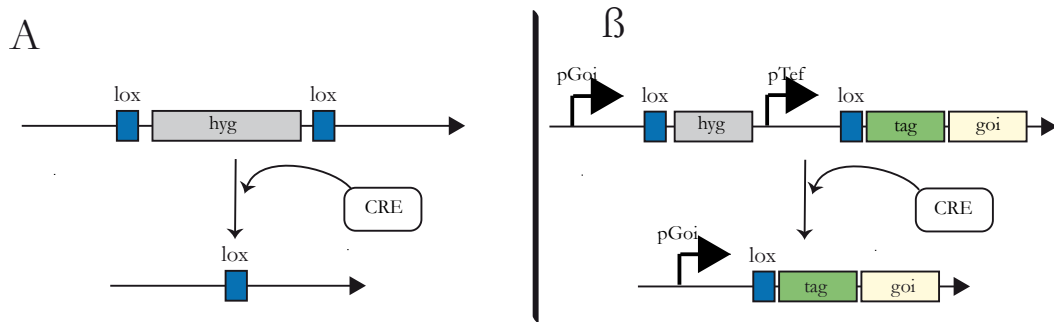
Figure 6: Shematic representation of Cre/Lox system. Gene deletion (A), N-terminal Tagging (B)

In order to generate the construction *gfp-cdc25* the Cre/Lox system was used. Primarily the plasmid pP_{tef}: Cdc25 was generated using the Golden Gate technique described above. The generated plasmid was digested with *SfiI* and cloned into the plasmid pLoxNGFP (laboratory collection) previously digested with the same enzyme. The originated plasmid $pLoxP_{tef}$:LoxNGFPCdc25 was digested with *PmeI* and integrated by homologous recombination at the *cdc25* locus. The insertion was checked with the pair of primers GFP-Cdc25-1/SMUT3 and pTEF-1/GFP-Cdc25-6. Positive clones were transformed with the plasmid pP_{crg1}:Cre and let them grow in arabinose containing plates allowing the induction of the CRE recombinase. The excision of the fragment flanked by lox sites was checked with the pairs of primers GFP-Cdc25-1/GFP-Eco2 and GFP-CDC25-6/GFP-Eco1.
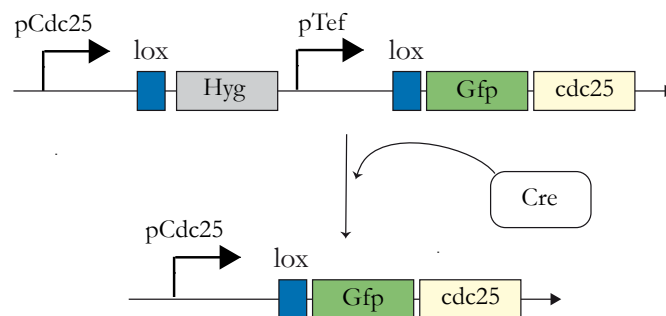
Figure 7: Schematic representation of the N-terminal tagging of Cdc25

8.10 Generation of the strains a1b1 P$_{crg1}$:fuz7^{DD}Kap123-ha nls-gfp crk1Δ, a1b1 P$_{crg1}$:fuz7^{DD} Kap123-ha nls-gfp pcl12Δ, a1b1 P$_{crg1}$:fuz7^{DD} Kap123-ha nls-gfp kpp2Δ.

To generate the strains *a1b1 P$_{crg1}$:fuz7^{DD}Kap123-ha nls-gfp crk1Δ, a1b1 P$_{crg1}$:fuz7^{DD} Kap123-ha nls-gfp pcl12Δ, a1b1 P$_{crg1}$:fuz7^{DD} Kap123-ha nls-gfp kpp2Δ,* protoplasts of *a1b1 P$_{crg1}$:fuz7^{DD} Kap123-ha nls-gfp* were generated and transformed with plasmid pCrk1Δ, pPcl12Δ and pKpp2Δ (present in the laboratory) previously digested respectively with *PacI, AflII* and *SpeI* and *PmeI*. The insertion in the endogenous locus was checked with the pair of primers Crk1-1/G4181 CRK1-6/G4182, PCL12-1/G4181 PCL12-6/ G4182 and Kpp2-1/ G4181 Kpp2-6/ G4182.

8.11 Generation of the strains a1b1 P$_{crg1}$:pcl12 Kap123-ha nls-gfp crk1Δ, a1b1 P$_{crg1}$:pcl12 Kap123-ha nls-gfp pcl12Δ, a1b1 P$_{crg1}$:pcl12 Kap123-ha nls-gfp kpp2Δ.

To generate the strains *a1b1 P$_{crg1}$:pcl12 Kap123-ha nls-gfp crk1Δ, a1b1 P$_{crg1}$:pcl12 Kap123-ha nls-gfp pcl12Δ, a1b1 P$_{crg1}$:pcl12 Kap123-ha nls-gfp kpp2Δ,* protoplasts of *a1b1 P$_{crg1}$:pcl12 Kap123-ha nls-gfp* were generated and transformed with plasmid pCrk1Δ, pFuz7Δ and pKpp2Δ (present in the laboratory) previously digested respectively with *PacI* and *PmeI*. The insertion in the endogenous locus was checked with the pair of primers Crk1-1/G4181 CRK1-6/G4182, FUZ7-1/G4181 FUZ7-6/ G4182 and Kpp2-1/ G4181 Kpp2-6/ G4182.

8.12 Generation of the strains a1b1 P$_{crg1:}$ pcl12 nls-gfp crk1^{AEF}-myc and a1b1 P$_{crg1:}$ pcl12 nls-gfp crk1^{AAA}-myc.

To generate *a1b1 P$_{crg1:}$ pcl12 nls-gfp crk1^{AEF}-myc* and *a1b1 P$_{crg1:}$ pcl12 nls-gfp crk1^{AAA}-myc,* protoplast of *a1b1 P$_{crg1:}$ pcl12 nls-gfp* were done and transform with plasmids pCrk1^{AF} and pCrk1^{AAA} previously digested with *AhdI* and *PacI*. The insertion in the endogenous locus was checked with CRK1-6/SMUT4 and CRK1-1/SMUT3. PCR products obtained from the left border were digested with *EcoRI* to check the AF point mutation. PCR products

from the left border were digested with *SacII* and *XhoI* to check the AAA point mutation.

Transformants that did not harbour the point mutations were selected as control

RESULTS

1. INDUCTION OF THE PHEROMONE MAPK CASCADE CAUSES A G2 CELL-CYCLE ARREST

The pheromone response in *U.maydis* resulted on the cell cycle arrest in G2 (Garcia-Muse *et al.* 2003) and in the formation of the sexual structure, the conjugative tube. This response does not depend only of pheromones but involves the integration of environmental and internal cellular signals, most of which are not well known (Feldbrugge *et al.* 2004). Since we are interested in understand how the pheromone-dependent MAPK cascade is able to induce cell cycle arrest, we decided to overcome the problem of the unknown signaling network by using an activated allele of the MAPKK Fuz7. This allele, called *fuz7^{DD}*, carries two point mutations, resulting in S259D and T263D that mimic an active allele of Fuz7 (Muller *et al.* 2003) (Fig.1A, B). The inducible promoter P*crg1*, which is active in arabinose containing medium and repressed in presence of glucose, controls its expression. (Fig. 1C). The induction of the allele *fuz7^{DD}* resulted in the formation of the conjugative tube indistinguishable from the one resulting from the pheromone activation of the MAPK cascade (Fig. 1 D) (Muller *et al.* 2003).
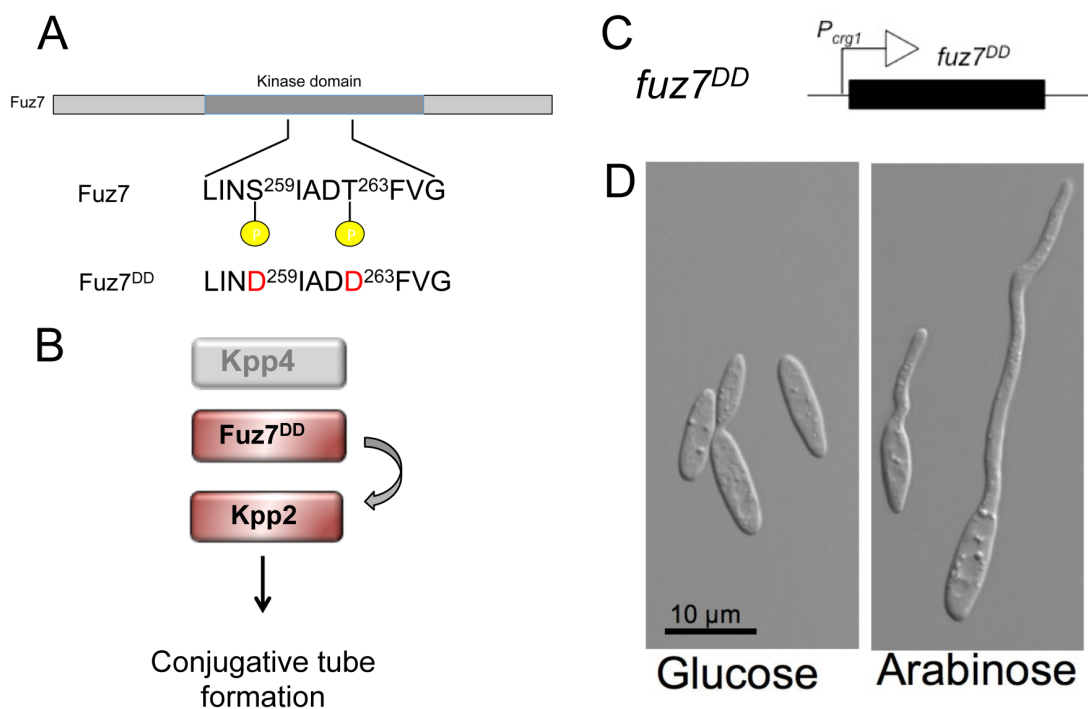
Figure1: The induction of an activated allele of the MAPKK Fuz7 results with the formation of the conjugative tube. A) The allele *fuz7^{DD}* carries two point mutations resulting in S259D and T263D, which mimic an active kinase **B)** The induction of *fuz7^{DD}* allele results in the formation of the conjugative tube. **C)** The expression of *fuz7^{DD}* allele is controlled by an inducible promoter, P$_{crg1}$, which is active in presence of arabinose and repressed in presence of glucose **D)** Cells grown in arabinose-containing medium for 4 hours showed the conjugative tube.

To prove that the expression of *fuz7^{DD}* induces a G2 cell cycle arrest, the DNA content was analyzed by flow cytometry. Wild-type control and a strain carrying the *fuz7^{DD}* were analyzed in CMD and after 2, 4, 6 hours of induction of the *fuz7^{DD}* allele (CMA). We observed that *fuz7^{DD}* cells growing in arabinose-containing medium accumulated 2C DNA content. (Fig.2)

Figure2: Cells expressing the *fuz7^{DD}* allele are cell cycle arrested. For FACS analysis, samples of wild type cells and cells carrying the *fuz7^{DD}* allele were taken after 2,4 and 6 hours of induction in arabinose-containing

medium. Cells carrying the *fuz7^{DD}* allele showed an accumulation of 2C DNA content indicating arrest in cell cycle progression in G2 or in mitosis

To discriminate whether this 2C DNA content corresponds to the G2 phase or mitosis, we analyzed the nuclei content as well as the integrity of nuclear membrane since in *U. maydis* the 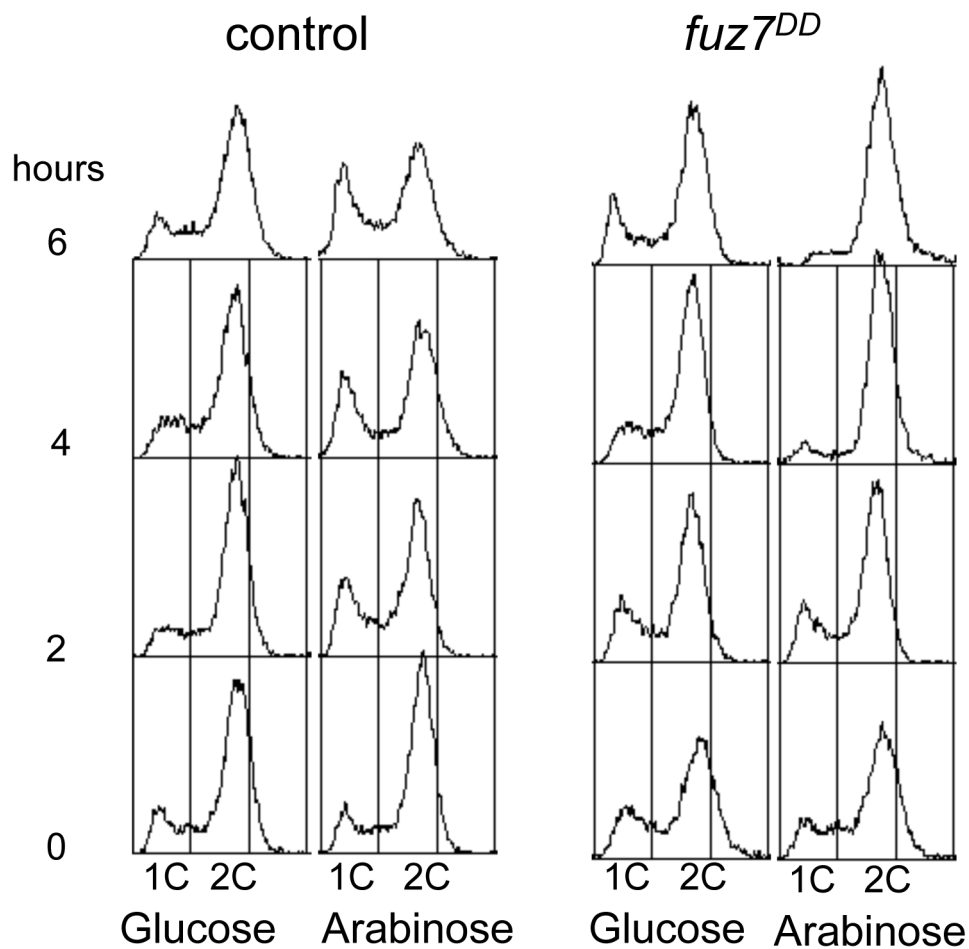nuclear envelope disassembles in mitosis (Straube *et al.* 2003) (Fig.3A, B). To perform this experiment, a strain carrying the *fuz7^{DD}*, the Cut11-cherry fusion protein (Cut11 is a component of the nuclear membrane) and NLS-GFP fusion protein was generated. When *fuz7^{DD}* allele was induced, cells showed one single nucleus per cell with an intact nuclear membrane surrounding the nucleus (Fig. 3C). Therefore, we could conclude that cells expressing *fuz7^{DD}* were arrested in G2. This arrest in G2 is equivalent to the arrest observed upon addition of pheromone (Garcia-Muse *et al.* 2003).
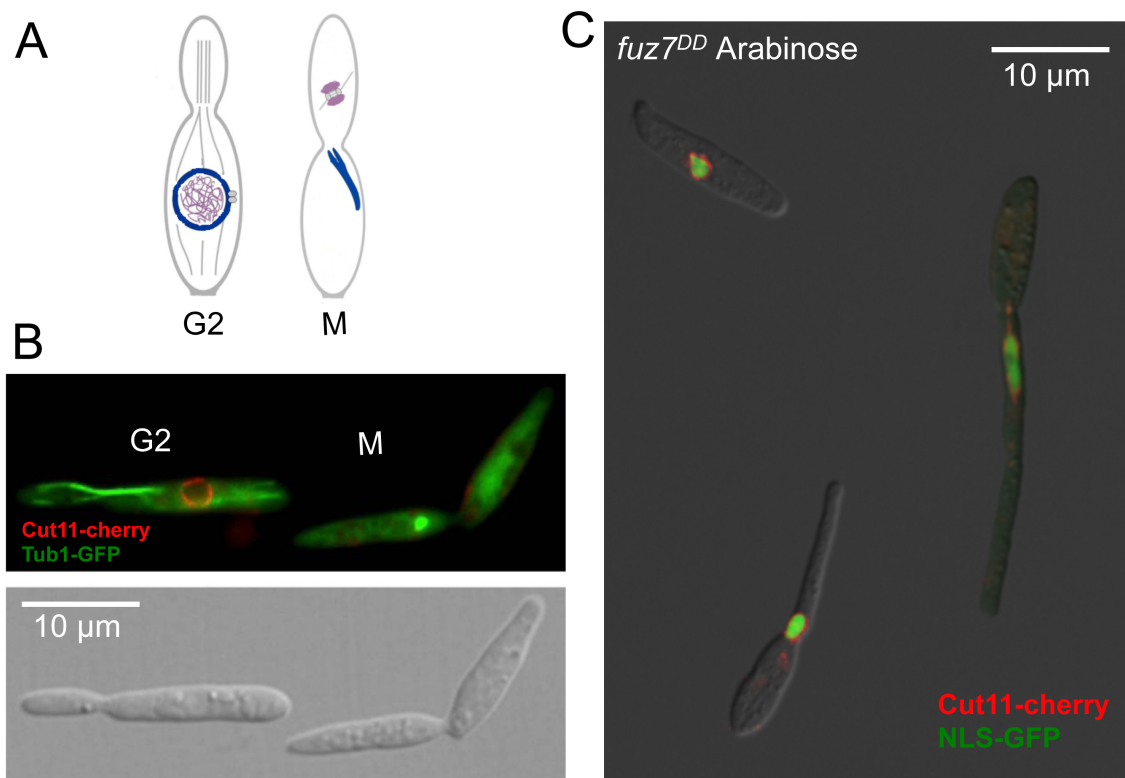
Figure3: Cells expressing the *fuz7^{DD}* allele are arrested in G2 A) In *U.maydis* G2 and M phase are well distinguishable: in G2 phase the nuclear envelope is intact and surrounds the nucleus in the mother cell; in mitosis the nuclear membrane disassembles and accumulates in the mother cell, while the nuclear content pass to the daughter cell. B) The integrity of the nuclear envelope can be observed by fluorescence microscopy using

the fusion protein Cut11-cherry. In G2 phase we can detect the nuclear envelope around the nucleus while in mitosis disappears. C) Cells growing in inducing conditions of the *fuz7^DD*allele and carrying the fusion proteins Cut11-Cherry and NLS-GFP showed an intact nuclear membrane surrounding the nucleus indicating that the cell cycle was arrested in G2 phase.

To further validate our experimental system we checked that the G2 cell cycle arrest induced by *fuz7^DD* was dependent by the downstream targets of the MAPKK Fuz7. In *U. maydis* the pheromone signal is transmitted via a MAPK module formed by the Kpp4, Fuz7 kinase and Kpp2 kinase. It has been described that the transcription factor Prf1, a HMG transcription factor, is acting downstream the MAPK and it is necessary for the transcription of the *a* and *b* mating type genes (Hartmann *et al.* 1996) but not it is not required for the formation of the conjugative tube as well as the cell cycle arrest (Muller *et al.* 2003) In order to analyze whether Kpp2 and Prf1 were required for cell cycle arrest induced by *fuz7^DD* expression, deletions of *kpp2* and *prf1* genes were performed in strain carrying the *fuz7^DD* allele and the DNA content was analyzed by flow cytometry. Deletion of *kpp2* leads to cells that were unable to arrest the cell cycle while the deletion of *prf1* did not affect the cell cycle arrest (Fig. 4). These data showed that Kpp2 was required for the *fuz7^DD* – induced cell cycle arrest whereas Prf1 does not affected this cell cycle regulation

All these results demonstrated that the expression of *fuz7^DD* faithfully reproduces the G2 cell cycle arrest induced by pheromone.
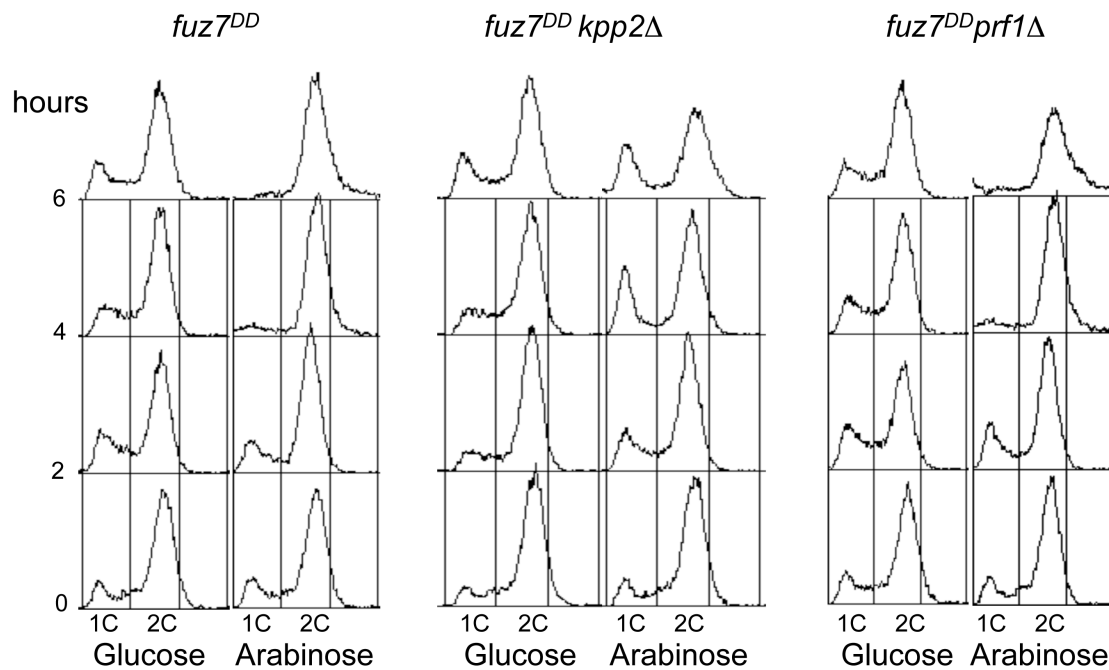
Figure 4: Cell cycle arrest induced by *fuz7^{DD}* allele is dependent of the MAPK Kpp2. For FACS analysis, samples of cells carrying the *fuz7^{DD}* allele and lacking *kpp2* and *prf1* were taken after 2,4 and 6 hours of induction in arabinose-containing medium. As control a strain expressing the *fuz7^{DD}* allele was used. FACS analysis of the mutant *kpp2* showed cells with 1C and 2C DNA content. Cells defective in *prf1* showed an accumulation of 2C DNA content.

2. WEE1-DEPENDENT INHIBITORY PHOSPHORYLATION OF CDK1 REQUIRED FOR THE *fuz7^{DD}* –DEPENDENT CELL CYCLE ARREST

The G2/M transition in *U.maydis* is controlled by the inhibitory phosphorylation on the Y15 residue of Cdk1 mediated by the kinase Wee1 (Sgarlata and Perez-Martin 2005). Using a specific antibody against the inhibitory phosphorylation of Cdk1 we observed that upon the induction of *fuz7^{DD}* allele, the level of the Y15 phosphorylation increased suggesting that this mechanism could be the responsible of the G2 cell cycle arrest (Fig. 5A, B).

A

control   *fuz7DD*

Time of induction (h)   0   1   2   3   4   0   1   2   3   4

Cdk5 ▷
Cdk1 ▷

Cdk1Y^{15}P ▷

B

Cdk1Y15P Signal Normalized to Cdk1Signal (A.U.)

■ control
□ *fuz7DD*

n=2 exp.

Time after *fuz7DD*-induction (h)
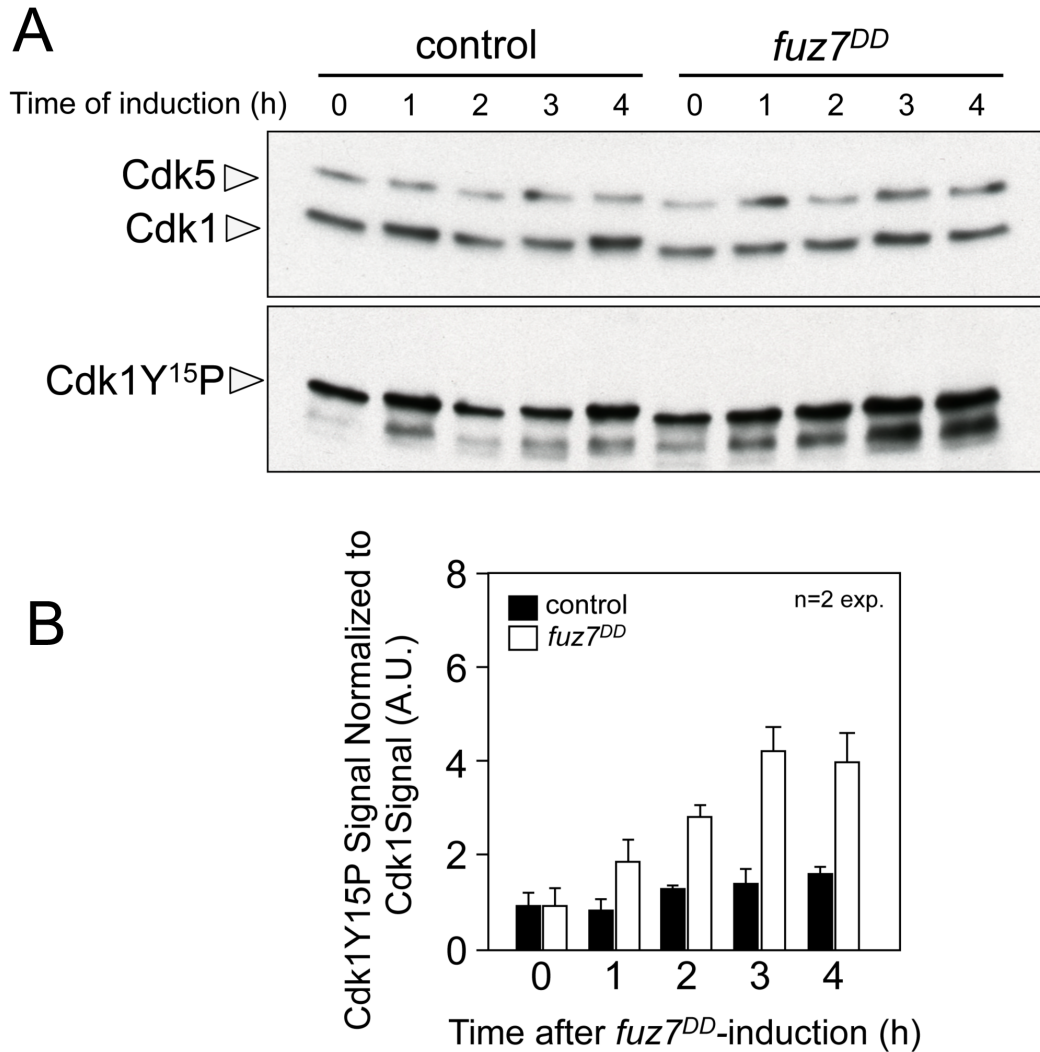
Figure5: Inhibitory phosphorylation of Cdk1 increases upon induction of the *fuz7DD* allele. A) Western analysis of the phosphorylated form of Cdk1. Protein extracts from wild type and from cells expressing the *fuz7DD* allele grown in inducing conditions were taken at the times indicated. B) The phosphorylation signal, from two different expositions, of the Cdk1 phosphorylated form was normalized to the Cdk1 signal and plot in function of the induction time. Wild type cells were used as control.

In order to study the effect of the inhibitory phosphorylation on the G2 cell cycle arrest we decided to construct a mutant allele of *cdk1*, called *cdk1^AF*, in which the conserved site of the phosphorylation was replaced with residues that cannot be phosphorylated, *cdk1^AF*. Since the expression of this allele is lethal (Sgarlata and Perez-Martin 2005), the inducible promoter P*crg1* controlled the expression of an ectopic copy of this allele. The construct generated was introduced in a strain carrying the *fuz7DD*, and in this way we could

simultaneously express both alleles by growing cells in CMA. As control we introduced an ectopic copy of the *cdk1* also under the *crg1* promoter in a strain carrying *fuz7DD* allele (Fig.6A). The ectopic alleles of *cdk1* were tagged with Myc to follow the protein production and to distinguish from the protein produced by the endogenous allele (Fig.6 B). Cells expressing the additional copy of the wild type *cdk1* were able to form a conjugative tube cell-cycle arrested as those of cells expressing the *fuz7DD* allele, while cells carrying the *cdk1* allele refractory to the inhibitory phosphorylation resulted in filaments carrying several nuclei indicating that cells were not cell cycle arrested (Fig.6 C, D). This result indicated that the inhibitory phosphorylation of Cdk1 is required for the G2 cell cycle arrest.
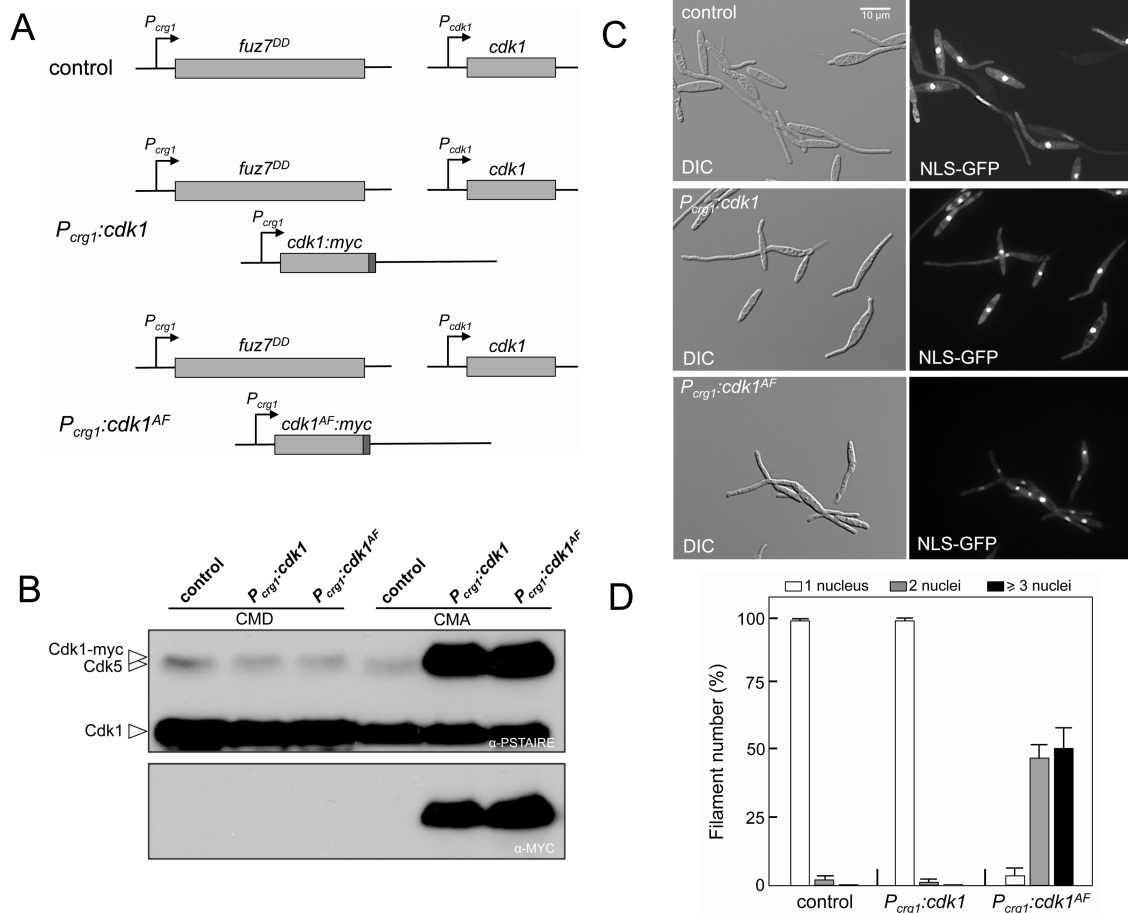
Figure 6: The inhibitory phosphorylation of Cdk1 is required for cell cycle arrest induced by the *fuz7DD* allele. A) Schematic representation of the strains used. The alleles *cdk1* and *cdk1AF* under the regulation of the *Pcrg1* were introduced ectopically in a strain carrying the *fuz7DD* allele and the endogenous copy of *cdk1*. B) Expression of the ectopically myc-tagged allele of Cdk1. Protein extracts from wild type cells and from cells expressing the *cdk1* and *cdk1AF* alleles were immunoblotted using anti P-STAIRE and anti-myc antibody. C)

Nuclei content of cells expressing the *cdk1* and *cdk1^AF* alleles. Control cells bringing the fusion protein NLS-GFP and the *fuz7^DD* allele and cells expressing the *cdk1/cdk1^AF* alleles, the fusion protein NLS-GFP and the *fuz7^DD* allele were grown in arabinose containing medium for 4 hours. The left panel part show DIC images and the right part images taken with the GFP channel. Scale bar 10 μm D) Nuclei content in control and mutant cells. The number of nuclei per filament was count upon the induction. The percentage of filaments having one, two or more than three nuclei was plotted for control cells, cells expressing the *cdk1* and *cdk1^AF* alleles.

To address whether Wee1 activity was necessary for the *fuz7^DD*-induced cell cycle arrest we exchanged the endogenous promoter of *wee1* with the inducible promoter *nar1* (Fig.7A). This promoter allows the expression of *wee1* in minimal medium containing nitrate as nitrogen-source (MM-NO$_3$) and it is repressed in complete medium. Cells were grown in CMA to repress this allele at the same time the *fuz7^DD* allele was induced. The down regulation of *wee1* resulted in cells multinucleated with more then three nuclei per cell demonstrating that Wee1 was necessary for the cell cycle arrest induced by *fuz7^DD* (Fig. 7 B,C)
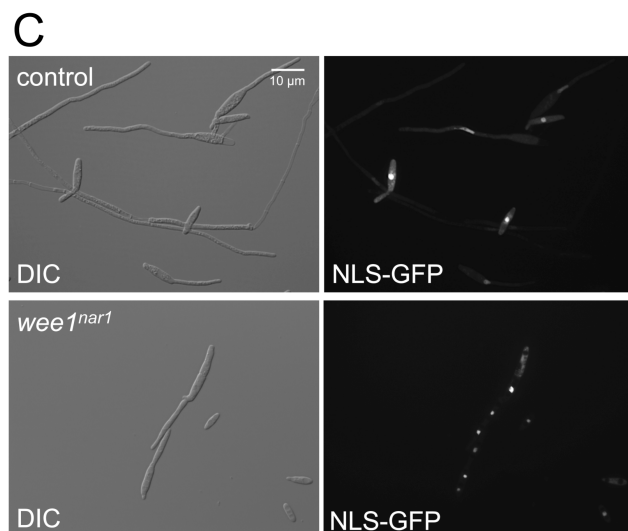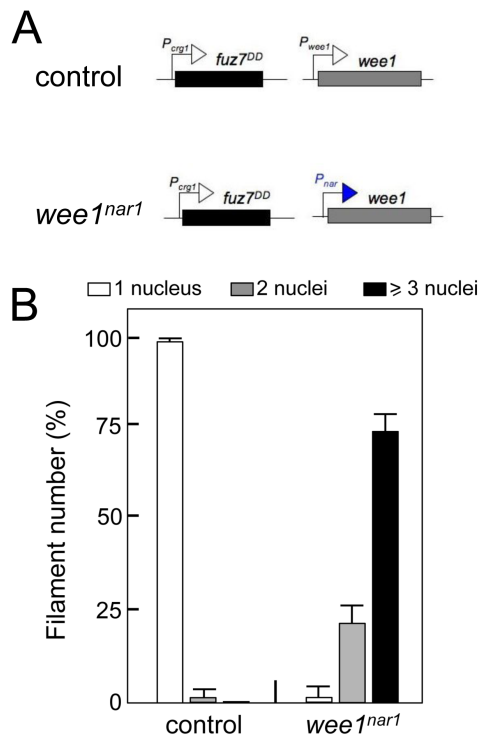
Figure 7: The kinase Wee1 is required for cell cycle arrest induced by the _fuz7^DD_ allele. A) Schematic representation of the strain used. The endogenous promoter of _wee1_ was exchanged with the _P~nar1~_ .**B)** Nuclei content of control and mutant cells. The number of nuclei per filament was count upon the induction of the _fuz7^DD_ allele and _wee1^nar1_ allele. The percentage of filaments having one, two or more than three nuclei was plotted for control cells and cells down regulating _wee1_. **C)** Nuclei content of cells expressing the _wee1^nar1_ allele. Control cells carrying the fusion protein NLS-GFP and the _fuz7^DD_ allele and cells expressing the _wee1^nar1_ allele, the fusion protein NLS-GFP and the _fuz7^DD_ allele were grown in inductive medium (CMA) for 4 hours. The left panel part shows DIC images and the in right part images taken with the GFP channel. Scale bar 10 μm.

3. PHEROMONE AND B-FACTOR USE DIFFERENT MECHANISM TO ARREST THE CELL CYCLE.

Since the pheromone response triggers the activation of a complex transcriptional program (Zarnack _et al._ 2008), we wondered whether the activation of the MAPK cascade could modify the expression of some of the described G2/M transition regulating genes. We checked levels of the cyclin Clb2 anc Clb1, that in complex with Cdk1 drive the transition into mitosis (Garcia-Muse _et al._ 2004), the phosphatase Cdc25 and the kinase Wee1, which are regulators of the Cdk1 activity (Sgarlata and Perez-Martin 2005; Sgarlata and Perez-Martin 2005). In addition, we included the genes encoding the kinase Hsl1 and the 14-3-3 protein Bmh1, involved in the control of Wee1 and Cdc25 (Mielnichuk and Perez-Martin 2008; Castanheira _et al._ 2014). Analysis of the gene expression of these described regulators of the G2/M transition was performed upon the activation of _fuz7^DD_. However, it is very crucial to discriminate whether the changes in expression of these genes is a consequence or a cause of an arrested cell cycle progression. To discriminate carefully genes whose expression was specifically altered by _fuz7^DD_ activation regardless the cell-cycle arrest, a strain carrying the ectopic allele refractory to the inhibitory phosphorylation, _cdk1^AF_, was included in the analysis. In this way, despite the activation of _fuz7^DD_ cell cycle is not arrested.

Transcriptional analysis reveals that only *hsl1* dramatically decreased in a cell-cycle arrest independent way (Fig.8).
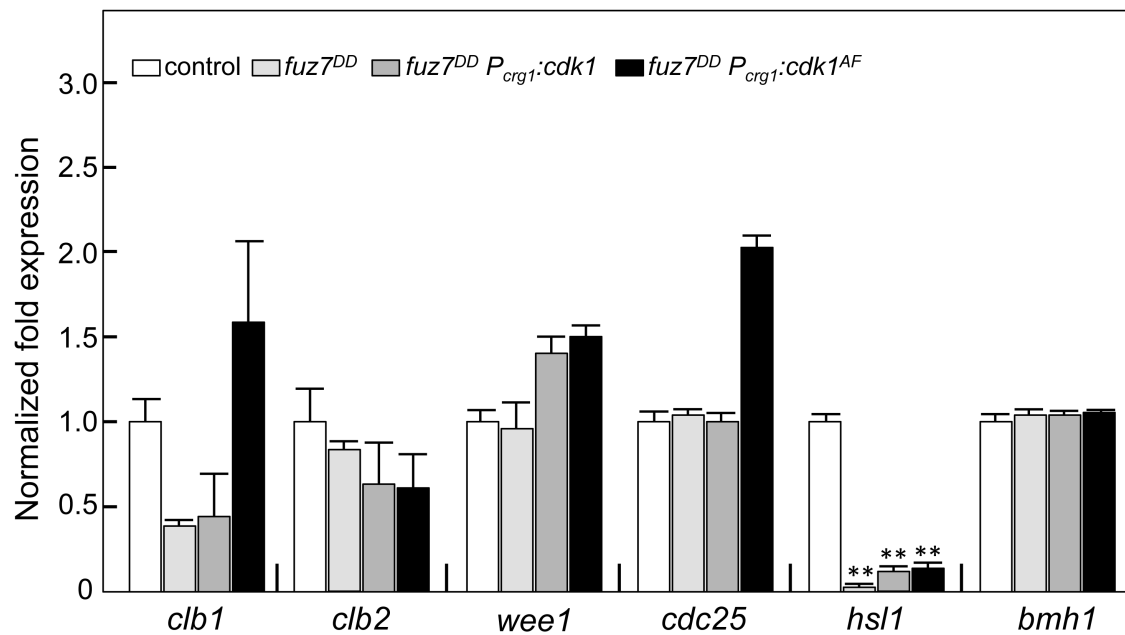
Figure 8: *hsl1* **decreases upon the induction of** *fuz7^{DD}* **allele. Quantitative real-time PCR of G2/M regulators. RNA was isolated after 6 hours of induction. As internal control the expression of** *tub1* **(tubulin α) was used. Values are referred to the expression of each gene in wild type cells. Each column represents the mean value of four independent biological replicates.**

It has been shown that the cell cycle arrest induced by b-factor is sustained by two different mechanisms: one requires the kinase Chk1, which phosphorylates Cdc25 promoting its recruitment in the cytoplasm (Mielnichuk and Perez-Martin 2008), and the other one involves the kinase Hsl1, which mRNA levels decreases upon the induction of the b-factor, promoting an increase of the Wee1 activity (Castanheira *et al.* 2014). The decrease in the mRNA levels of *hsl1* observed when *fuz7^{DD}* is induced, prompted us to wonder whether the cell cycle arrest induced by *fuz7^{DD}* could be also mediated by the same mechanism. To analyze this hypothesis, we deleted in a strain carrying the *fuz7^{DD}* allele, the *chk1* gene and we introduced the *hsl1^{tef1}* allele. In this allele the constitutive promoter (*tef1*) controls *hsl1* expression, bypassing its down regulation during the activation of *fuz7^{DD}*. In this strain when *fuz7^{DD}* was induced cells were able to observe that in conjugative tube cell cycle was

arrested (Fig. 9). This result contrasts with the reported b-dependent cell cycle arrest (Castanheira *et al.* 2014) and therefore indicates that pheromone and b-factor use different mechanisms to arrest the cell cycle.

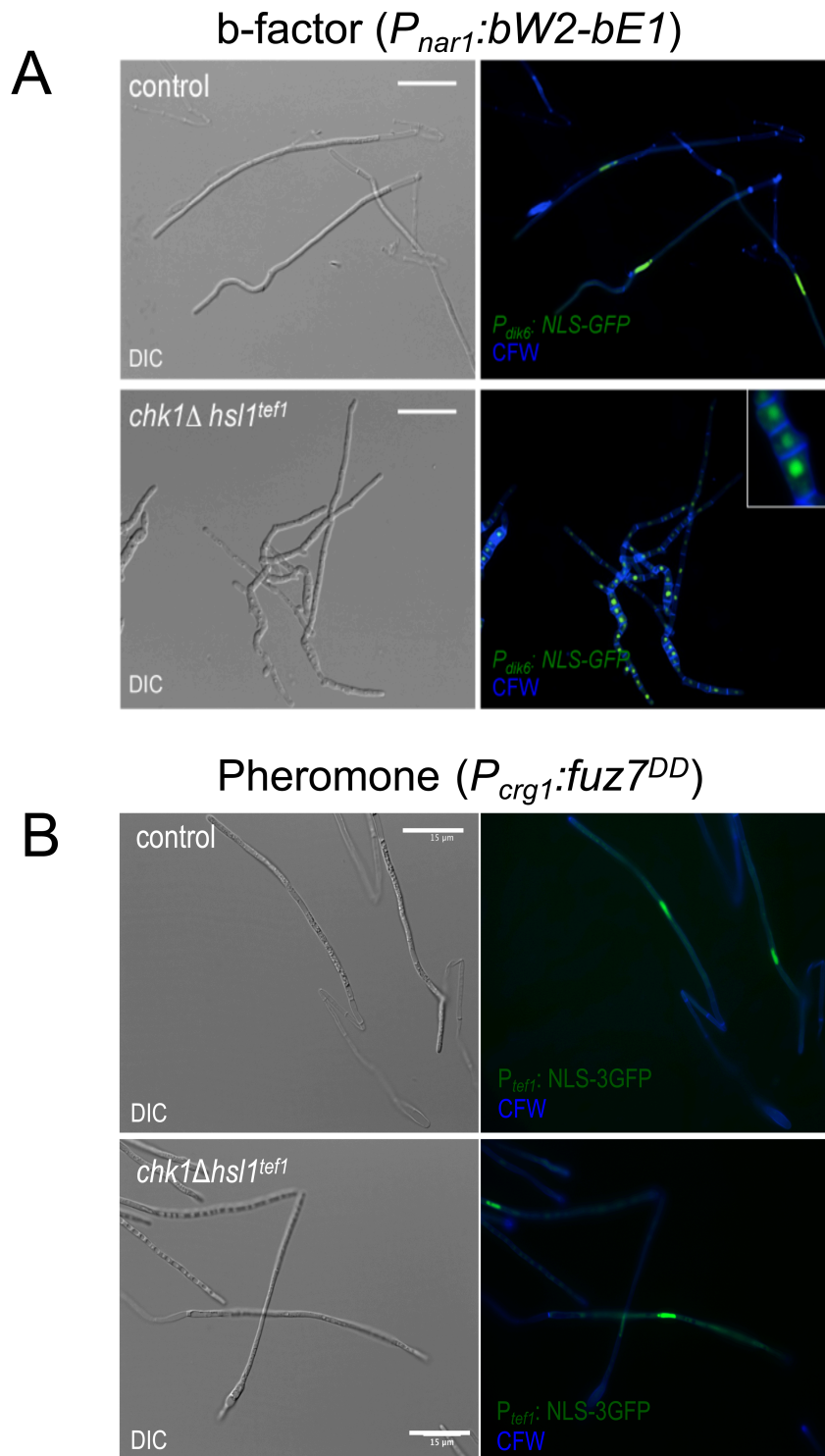**Figure 9 : Pheromone and b-factor use different mechanism to arrest the cell cycle. Cell carrying the deletion of *chk1*, the hsl1tefl and expressing the b-factor and cells carrying the deletion of *chk1*, the hsl1tefl and the fuz7DD**

Beside its role in cell cycle, Hsl1 has a role also in morphogenesis. In *S. cerevisiae,* Hsl1 not only regulates the Wee1-like kinase Swe1 but it is also involved in the organization of the septin ring in the neck during bud formation (Barral *et al.* 1999). This constriction formed by the septin ring is fundamental for cell separation during cell cycle. Also in *U. maydis* Hsl1 localized in the neck of budded cells, consistent with the role already observed in *S. cerevisiae*, and it has been described also a role in the formation of the infective filament (Castanheira *et al.* 2014). In this case, the down regulation of Hsl1 is required for the correct formation of the neck connecting the mother cell and the filament. In wild-type cells no constriction in the neck of the filament is formed but when the expression of *hsl1* is up regulated a clear constriction similar to the one formed during the budding cycle is generated (Castanheira and Perez-Martin 2015). We generated a strain carrying the *fuz7^{DD}* and the *hsl^{tef1}* allele and we have observed a constriction in the filament neck characteristic of the bud morphology but not of the wild-type conjugative tube (Fig. 10). This observation suggests that the down-regulation of *hsl*1 upon the *fuz7^{DD}* induction is most probably related to the role of Hsl1 in morphology than to the cell cycle arrest.
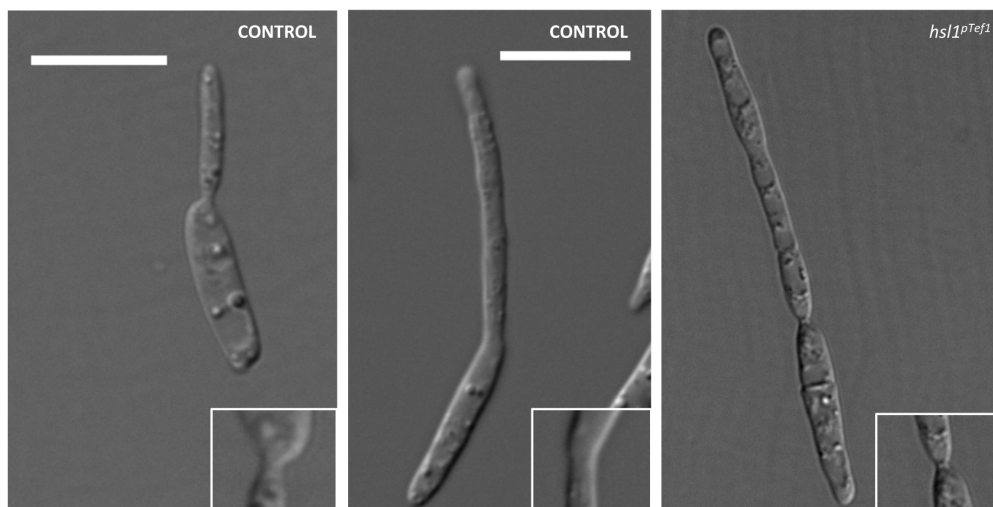
Figure 10: Down regulation of *hsl1* controls the filament constriction. Cells carrying the *hsl^{tef1}* allele and the *fuz7^{DD}* allele were grown in inducing conditions and were observed by DIC light microscopy. The panel shows

a cell in vegetative growth, a filament induced by *fuz7DD* allele and a filament of a cell carrying the *hslᵗᵉᶠ¹* and the *fuz7DD* alleles.

4. CDC25 PROTEIN LEVEL DECREASES UPON THE INDUCTION OF *fuz7dd*.

Since we do not observed changes in gene expression of the master regulator of the G2/M transition upon the activation of *fuz7DD*, we decided to analyze protein levels. For that we generated three strains harbouring the *fuz7DD* allele and the fusion proteins Cdc25-HA, Wee1-HA and Clb2-HA. All these HA-tagged alleles generate proteins that were fully functional. As control we used strains carrying the fusion proteins Cdc25-HA, Wee1-HA and Clb2-HA without the *fuz7DD* allele. We observed that, upon the induction of *fuz7DD* allele, there was a decrease of the phosphatase Cdc25 levels while we did not observed significative changes in Wee1 and Clb2 levels (Fig. 11). This result pointed to the decrease of Cdc25 levels upon the activation of *fuz7DD* allele as the most probably cause of the G2 cell cycle arrest.
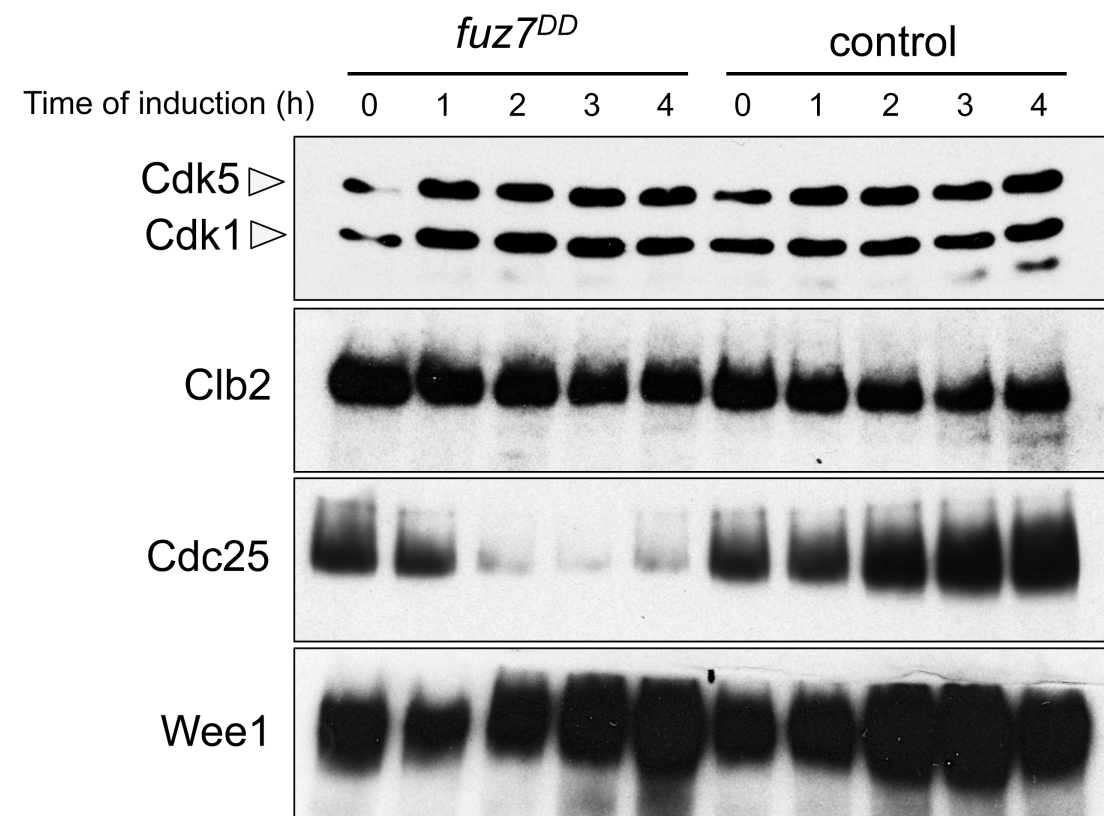
Figure 11 : Cdc25 decrease upon the activation of the *fuz7^DD* allele. Protein level of G2/M transition regulators. Protein extracts from cells carrying the HA-tagged alleles and from cells carrying the *fuz7^DD* allele growing in inducing conditions, were collected at the indicated times. Equivalent amount of protein was loaded in each case.

Since the down regulation of Cdc25 could be the cause of the cell cycle arrest induced by the *fuz7^DD* allele, we wonder if the overexpression of *cdc25* could release this cell cycle arrest. To address this question we introduced an ectopically copy of *cdc25* gene under the control of the *crg1* promoter in a strain carrying the *fuz7^DD* allele and the fusion protein NLS-GFP. The ectopic allele of Cdc25 was tagged with HA to analyze the protein production. Since the *crg1* promoter regulated the expression of both alleles, we could induce the expression at the same time. Cells growing in inducing conditions (CMA) were able to arrest the cell cycle (Fig. 12B). and we also observed that Cdc25 protein production increased upon the induction of the *fuz7^DD* allele (Fig.12A). These results illustrated that the down regulation of Cdc25 levels was not the cause of cell cycle arrest induced by the *fuz7^DD* allele, or at least not the only cause

A

B
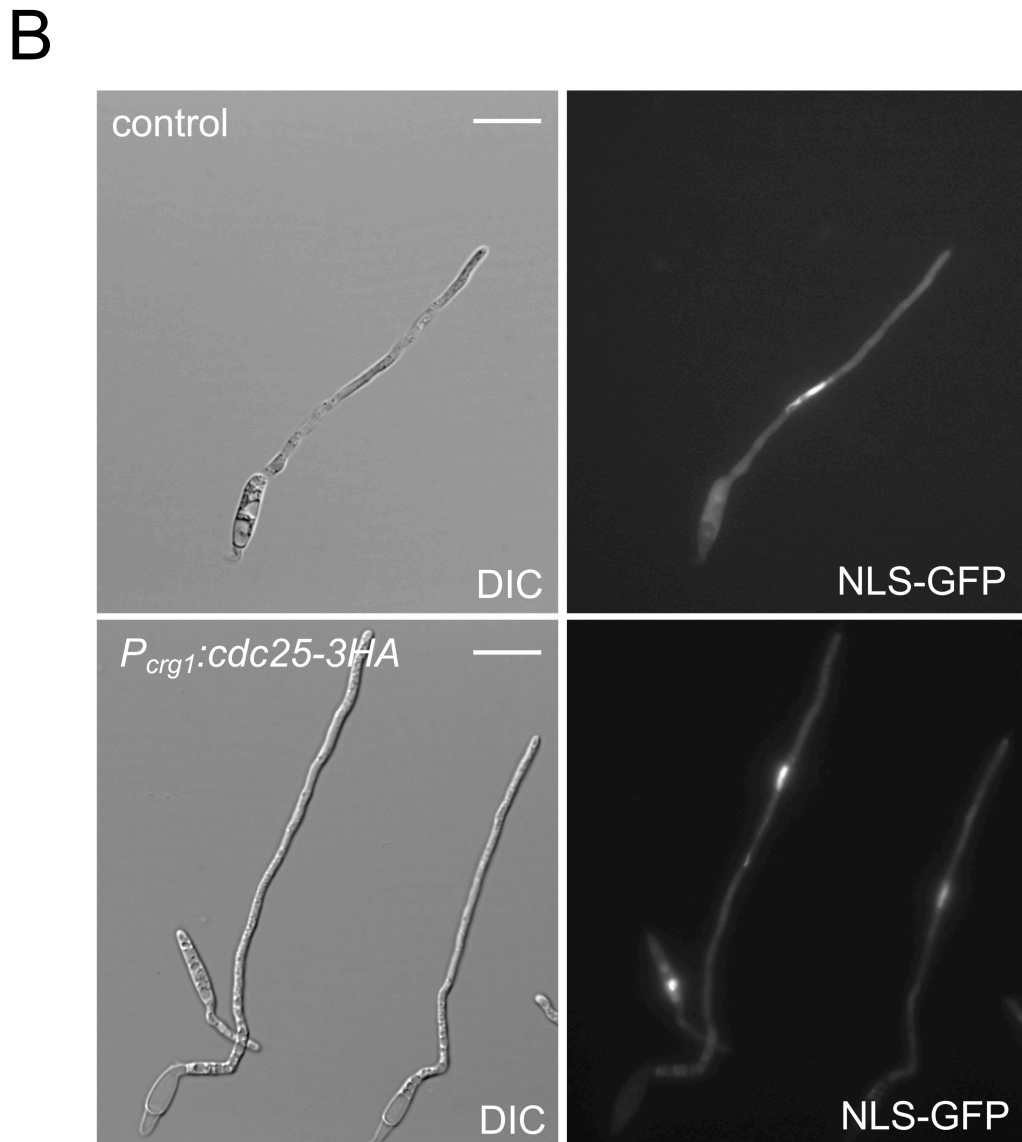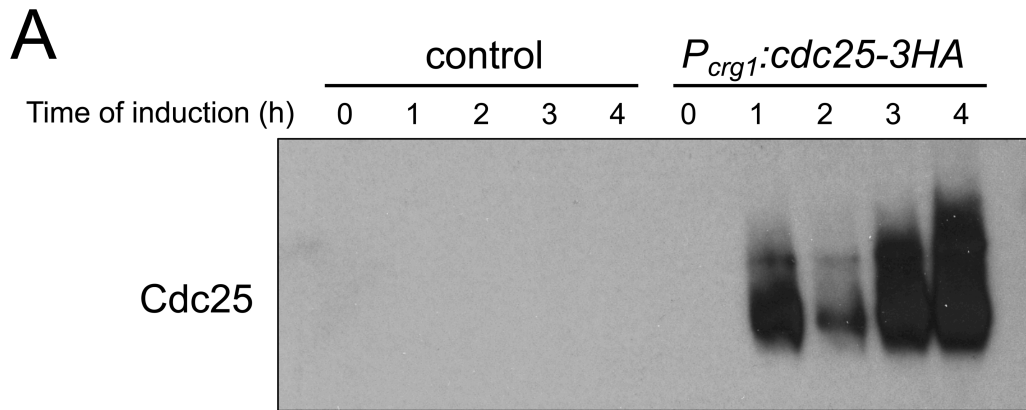
Figure12: The overexpression of Cdc25 does not release cell cycle arrest. A) Overexpression of Cdc25. Extract from cells carrying the fuz7^{DD} allele and the P$_{crg1}$: Cdc25 allele were collected at the indicated time. B) Control cells expressing the fuz7^{DD} allele and cells carrying the P$_{crg1}$: Cdc25 allele and the fuz7^{DD} allele were observed with fluorescence microscopy to detect GFP signal. Note that cell cycle is arrested. Scale bar 15 μm

5. PCL12 IS REQUIRED FOR THE DECREASE OF CDC25 LEVELS AS WELL AS G2 CELL CYCLE ARREST.

Previous results from our laboratory (Flor-Parra *et al.* 2007) showed that the cyclin Pcl12, a Pcl-like cyclin, was required for the proper polar growth of the conjugative tube and that the expression of this gene was induced by pheromone. More important, preliminary data also suggested that Pcl12 could be required in the *fuz7*^{DD} dependent cell cycle arrest. Therefore, we decided to analyze in more detail the role of Pcl12 in the cell cycle arrest induced by *fuz7*^{DD}. We generated a strain carrying a deletion of *pcl12*, the allele *fuz7*^{DD} and the fusion protein NLS-GFP. We observed that in the absence of Pcl12, once the *fuz7*^{DD} is induced, the filaments produced showed more than one nucleus per cell indicating that Pcl12 was required for cell cycle arrest induced by *fuz7*^{DD} (Fig.13A)

We also analyzed the level of Cdc25 in cell lacking *pcl12* and expressing *fuz7*^{DD}. As control, we used the strain carrying the *fuz7*^{DD} and the fusion protein Cdc25-HA. We found that Cdc25 levels does not decrease upon the activation of *fuz7*^{DD} suggesting the Pcl12 could be also required for the down regulation of Cdc25 (Fig. 13B).
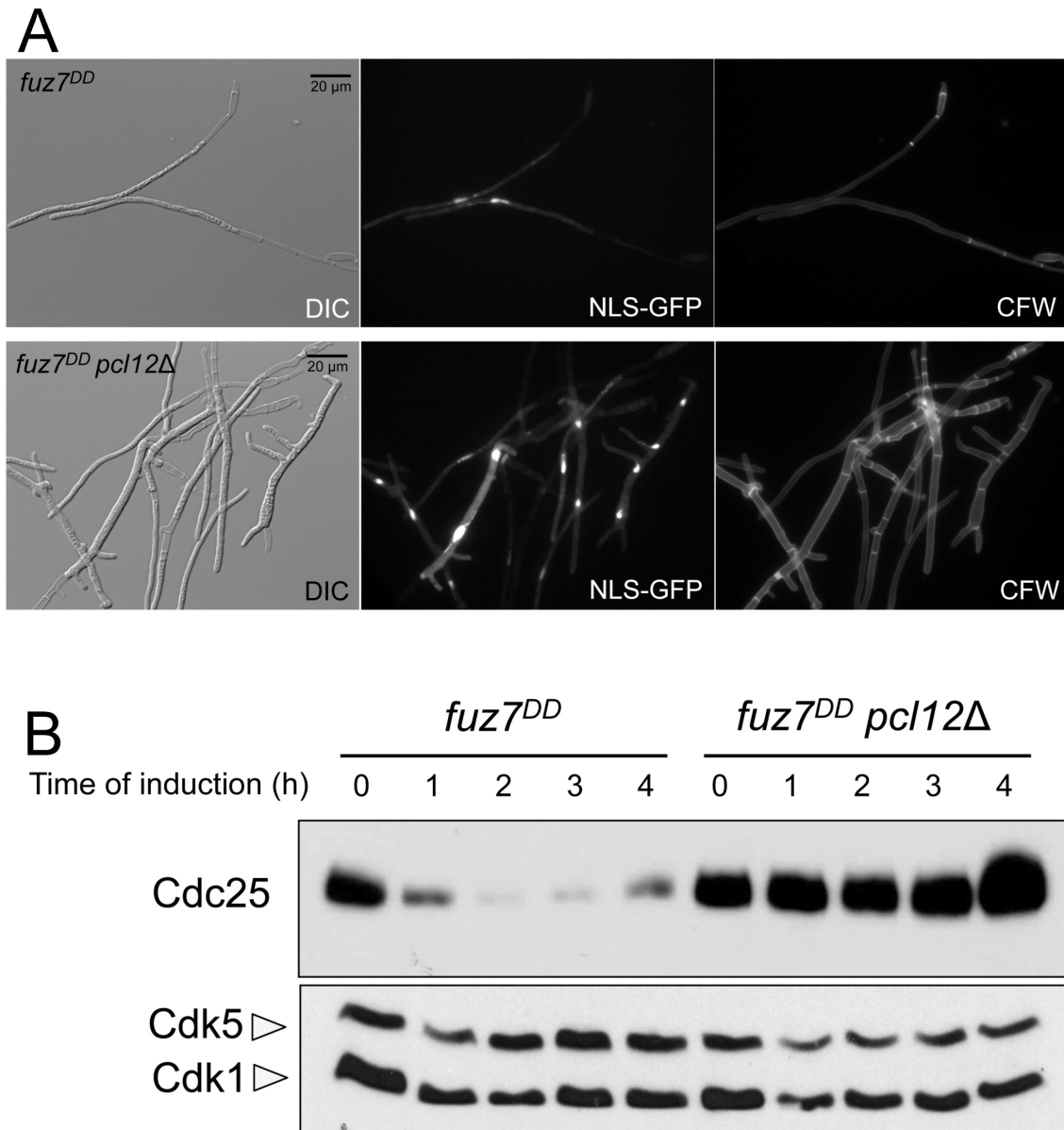
Figura 13: Pcl12 is required for cell cycle arrest induced by the *fuz7^DD* allele and for the decrease of Cdc25 levels. A) Nuclei content in cells carrying *fuz7^DD* allele, the fusion protein NLS-GFP and lacking *pcl12*. Cells carrying the *fuz7^DD* allele and the fusion protein NLS-GFP were used as control. The upper part of the panel shows images of control cells. Cells were assayed by DIC light microscopy and by fluorescence microscopy to visualize GFP signal and calcofluor staining. Scale bar 20 μm. **B)** Cdc25 protein levels in cells defective for *pcl12*. Protein extracts from cells carrying the *fuz7^DD* allele and from cells carrying the *fuz7^DD* allele and the deletion of *pcl12*, growing in inducing conditions, were collected at the indicated times.

Pcl12 interacts specifically with Cdk5, an essential CDK catalytic subunit with role in morphogenesis (Castillo-Lluva *et al.* 2007; Alvarez-Tabares and Perez-Martin 2008). The

Cdk5-Pcl12 complex is required for the proper polar growth of both infective filament and the conjugative tube (Flor-Parra *et al.* 2007).

Since the absence of Pcl12 affects the ability to arrest cell cycle upon the induction of the *fuz7*^{DD} allele, we wondered if the associated kinase Cdk5 had also a role in *fuz7*^{DD}–induced cell cycle arrest. Since Cdk5 is essential, a temperature-sensitive allele was used (Castillo-Lluva *et al.* 2007). Cells at permissive temperature (22°C) are able to grow while at restrictive temperature (34°C) were not. An intermediate temperature of 32°C allows a residual growth although the Cdk5 function was severely affected (Castillo-Lluva *et al.* 2007). Strain carrying the *cdk5*^{ts} and the *fuz7*^{DD} alleles were grown in CMD at permissive temperature and then shifted to 32°C in CMA. The filament growth of these cells was affected in agreement with the described role of Cdk5 in morphogenesis, but when we analyzed the nuclear content we observed that these cells showed one nucleus per cell indicating that Cdk5 was not involved in the cell cycle arrest induced by *fuz7*^{DD} (Fig.14A). We also checked Cdc25 levels upon the activation of *fuz7*^{DD} in *cdk5*^{ts} mutant cells. As control, we used the strain carrying the *fuz7*^{DD} and the tagged Cdc25-HA. We found that Cdc25 levels in the termosensitive mutant were similar to the Cdc25 levels observed in the control cells supporting the idea that Cdk5 was not required for *fuz7*^{DD} –dependent cell cycle regulation (fig.14B). In summary, all these data suggest that cell cycle arrest induced by *fuz7*^{DD} requires Pcl12 but not Cdk5.
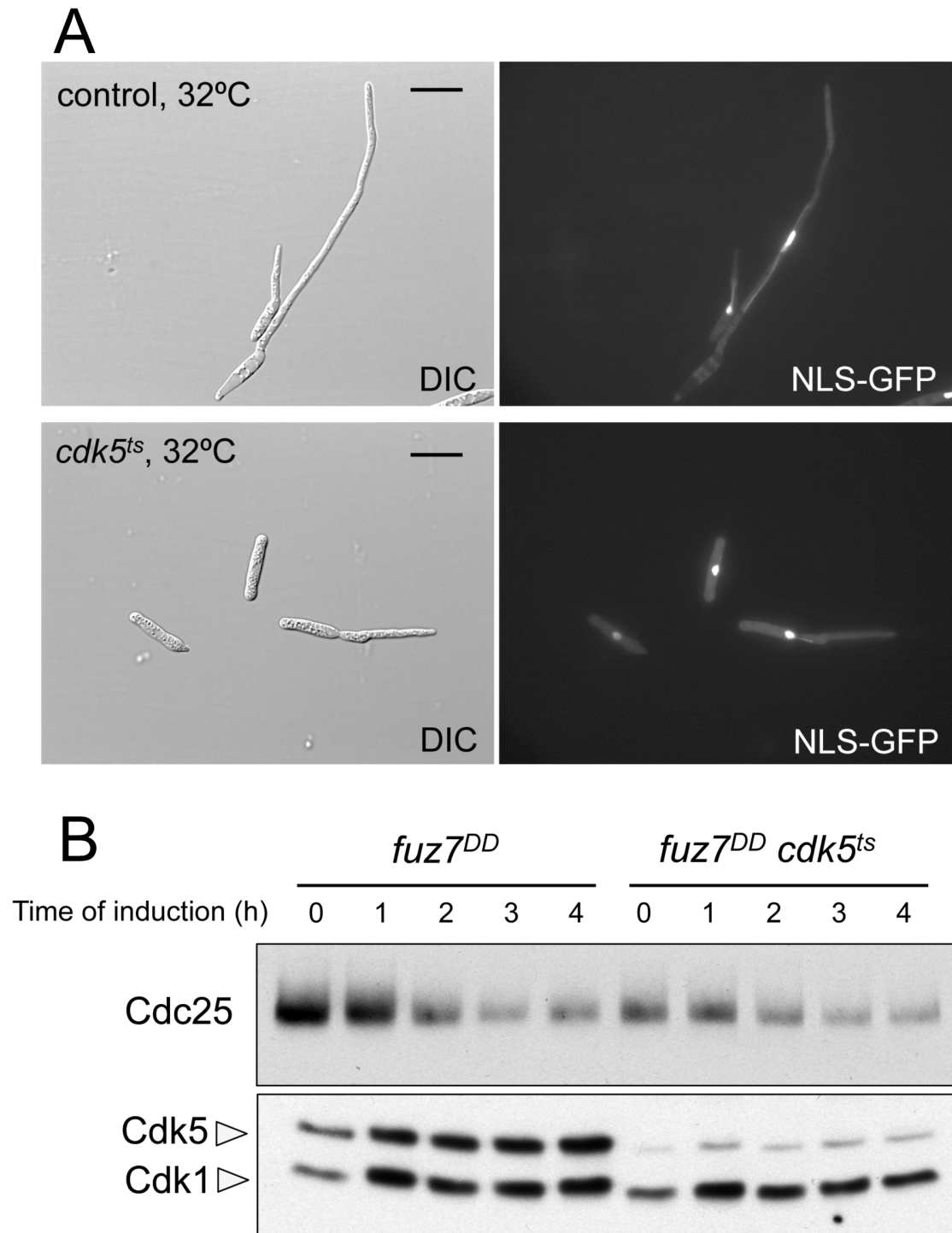
Figure 14: Cdk5 was not involved in cell cycle arrest induced by *fuz7DD* allele. A) Nuclei content in cells harbouring Cdk5ts allele, the *fuz7DD* allele and carrying the fusion protein NLS-GFP. The upper part of the panel shows images of control cells while the bottom part of the panel shows images of the termosensitive mutant. Cells were observed by DIC light microscopy and by fluorescence microscopy. Cells were grown in inducing condition at 32°C. **B)** Cdc25 protein level in cells defective of *cdk5*. Protein extracts from cells carrying the *fuz7DD* allele and from cells carrying the *Cdk5ts* and *fuz7DD* alleles, growing in inducing conditions, were collected at the indicated times.

6. CRK1 IS REQUIRED FOR THE DECREASE OF CDC25 LEVELS AS WELL AS G2 CELL CYCLE ARREST.

Since Pcl12 is a cyclin and Cdk5 was not required for cell cycle arrest, we decided to look for additional interactors of Pcl12 that might have a role in cell cycle arrest induced by the *fuz7^{DD}* allele. To look for putative targets we performed Mass Spectrometry experiments in collaboration with Prof. Gerhard Braus from the University of Goettingen (Germany). We created a strain carrying the fusion protein Pcl12-GFP and the allele *fuz7^{DD}*. This strain seems to behave like a no-tagged strain with respect to conjugative tube formation. After 3 hours of *fuz7^{DD}* induction, we immunoprecipitated Pcl12 by using GFP-TRAP beads. Interactors of Pcl12 were then identified by LC-MS (Fig. 14A). Between the specific targets identified, there was the kinase Cdk5, described as a specific CDK of Pcl12, important players of the cell cycle as Bmh1 or Septins and regulators of cellular transport like Kap123, a βimportin. Interestingly, one of the most represented targets was the Cdk-related kinase Crk1, an Ime2-like kinase (Fig. 14B) (Garrido and Perez-Martin 2003).
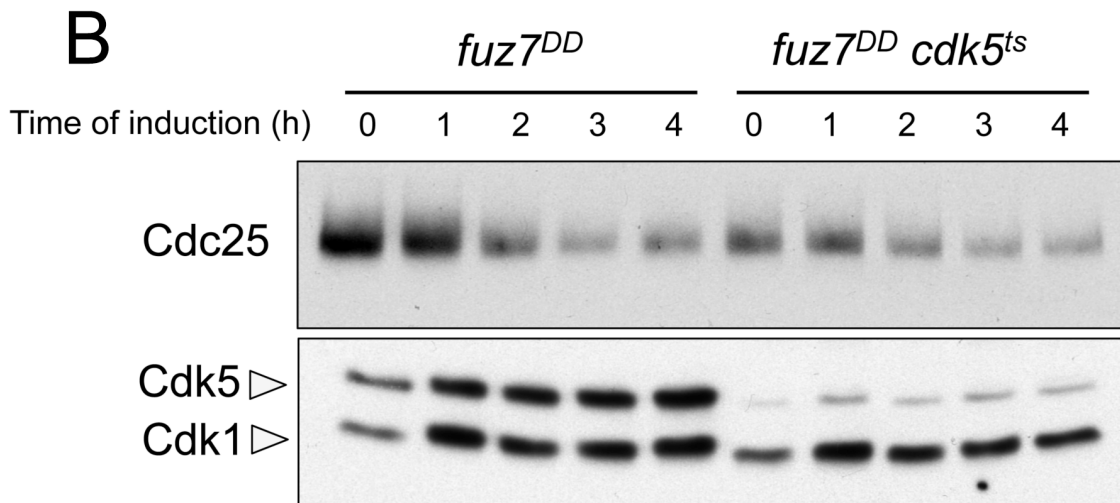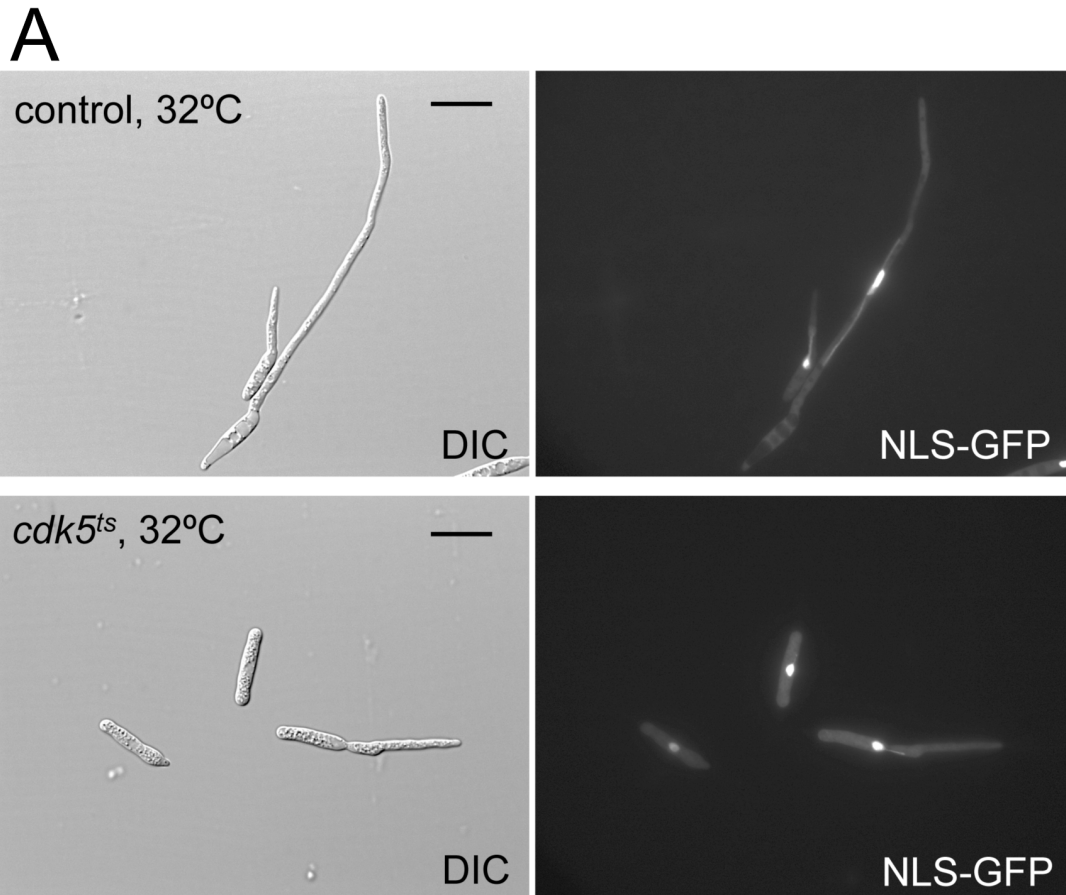
Figure 15 : The kinase Crk1 interacts with Pcl12. A) Schematic representation of Mass Spectrometry experiments. Native protein extract from carrying the *fuz7DD* allele and the fusion protein Pcl12-GFP cell growing in inducing condition was used. Pcl12 was immunoprecipited using GFP-TRAP beads. Interactors were eluted by boiling and digested with trypsin directly from gel. The generated peptides were identified by LC-MS/MS analysis. **B)** Table of Pcl12 interactors. In the table targets and number of unique peptides identifying the proteins were listed.

Interestingly, the Cdk-related kinase Crk1 is a direct downstream target of the MAPK cascade. This kinase has a role in polar growth but no function in regulation of the cell cycle has been described so far (Garrido *et al.* 2004). To investigate the possibility of a role of Crk1 in the regulation of the cell cycle, we generated the deletion of *crk1* in a strain carrying the *fuz7*^{DD} allele and the fusion protein NLS-GFP. Upon the induction of the *fuz7*^{DD}, the filament produced showed several nuclei per cell indicating that cell cycle was not arrested (Fig.16A); of note, the filaments observed in Crk1 mutants were morphologically distinct from those observed in Pcl12 mutants (see below for further clarifications). Consequently, we also analyzed Cdc25 protein levels. We found that upon the activation of *fuz7*^{DD} Cdc25 levels do not decrease in absence of *crk1* (Fig. 16B). These findings indicated that the kinase Crk1, as the cyclin Pcl12, was required for cell cycle arrest induced by *fuz7*^{DD} as well as for the down regulation of Cdc25 level.

A

B
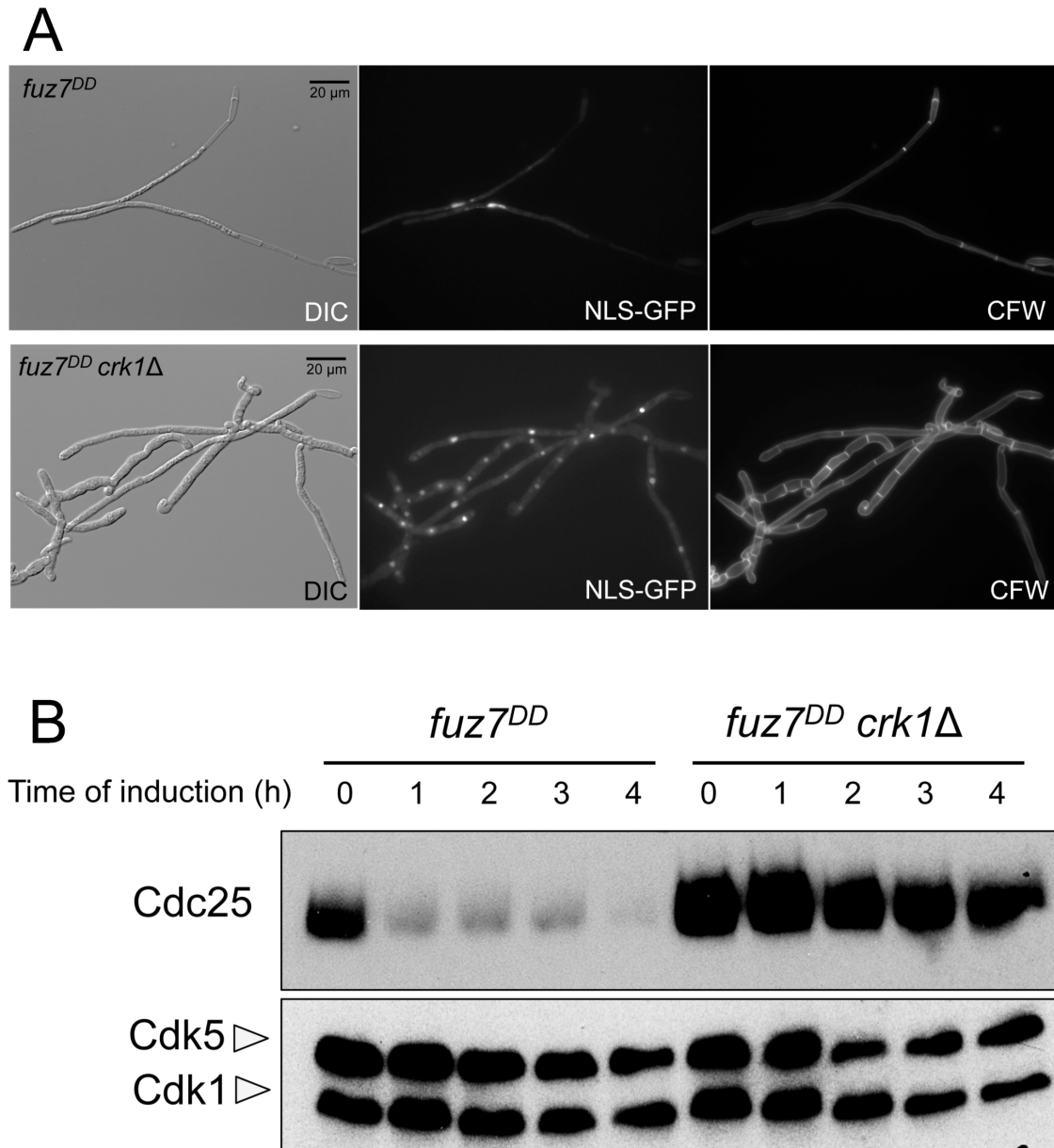
Figure 16: Crk1 is required for cell cycle arrest induced by the *fuz7DD* allele and for the decrease of Cdc25. A) Nuclei content in cells carrying *fuz7DD* allele, the fusion protein NLS-GFP and lacking *crk1*. As control cells carrying the *fuz7DD* allele and the fusion protein NLS-GFP were used. The upper part of the panel shows images of control cells while the bottom part of the panel shows images of the mutant. Cells were assayed by DIC light microscopy and by fluorescence microscopy to visualize GFP signal and calcofluor staining. Scale bar 20 μm. B) Cdc25 protein level in cells defective of *crk1*. Protein extracts from cells carrying the *fuz7DD* allele and from cells carrying the *fuz7DD* allele and the deletion of *crk1*, growing in inducing conditions, were collected at the indicated times.

7. PCL12 AND CRK1 INTERACT IN THE CYTOPLASM

The results above suggested that Crk1 and Pcl12 could be interactors involved in control of the *fuz7^DD*-dependent cell cycle arrest. To better understand where this interaction takes place we investigated the subcellular localization of such interaction. Previous results showed that Crk1 localizes in the nucleus as well in the cytoplasm in the infective filament (Bielska *et al.* 2014) while Pcl12 localizes only in the cytoplasm (Flor-Parra *et al.* 2007). A strain carrying the fusion proteins Crk1-GFP, Pcl12-Cherry and the allele *fuz7^DD* was generated. Once the *fuz7^DD* was induced, we observed that Crk1 localizes in the nucleus and along the conjugative tube. Pcl12 localizes along the conjugative tube and we did not detect signal in the nucleus as it was described for the infective hyphae. Finally, when we merged the two signals we were able sometimes to co localize Crk1 and Pcl12 in dots along the filament but we were able to detect also the single signals of Crk1 and Pcl12, suggesting that distinct complexes co-exist in the cytoplasm of the conjugative tubes (Fig.17).
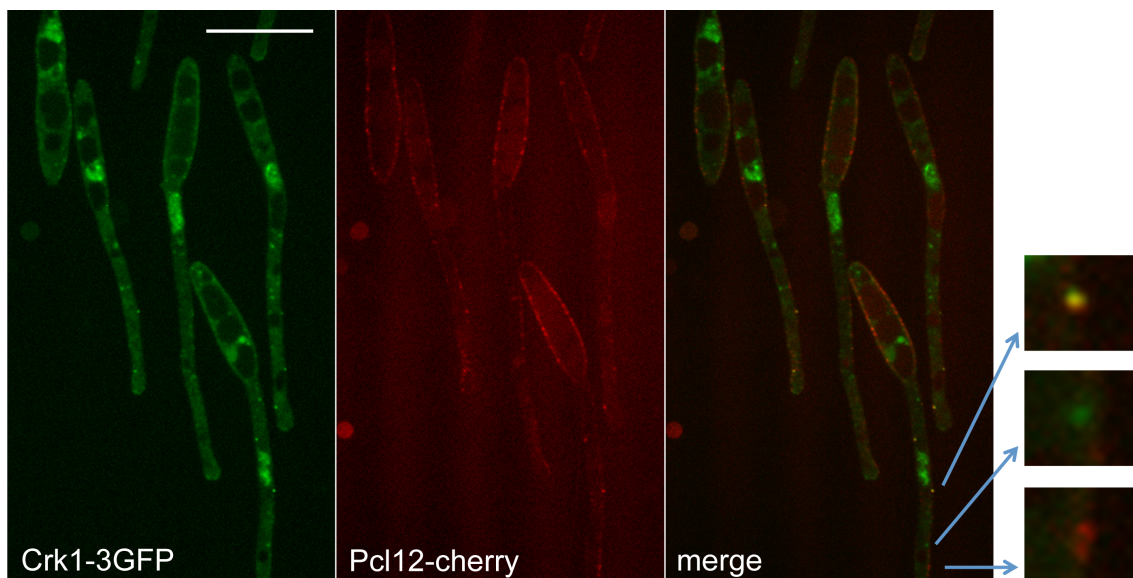
Figure 17: Crk1 and Pcl12 co-localize in the cytoplasm. Cells carrying the fusion proteins PCL12-Cherry and CRK1- GFP and expressing the *fuz7^DD* allele were grown in inducing conditions. Cells were assayed by fluorescent microscopy using the GFP and the Cherry channels. The panel shows the localization of Crk1-GFP, in the middle the localization of Pcl12-cherry and the last one the merge between the two signals.

In order to verify that Crk1 and Pcl12 interact in the cytoplasm, we performed BiFC experiments. This technique allows detecting protein interaction *in vivo* using microscopy (Kerppola 2008; Miller *et al.* 2015). It is based on the association between two no-fluorescent fragments of a fluorescent protein (Fig.18A). These fragments are fused with the two putative interactors. When they are interacting, the fluorescent protein is formed and we can detect signal in the cell. Besides that, the fluorochrome formation stabilizes also the complex formed by two proteins, in this way also transitory interaction can be detect. We generated a strain carrying the allele *fuz7*[DD] and the fusion proteins Pcl12 and Crk1 with the two no-fluorescence fragments of Venus. When cells are forming the filament upon the activation of *fuz7*[DD], we observed signal along the conjugative tube confirming that the interaction between Pcl12 and Crk1 occurs in the cytoplasm (Fig.18B, C).
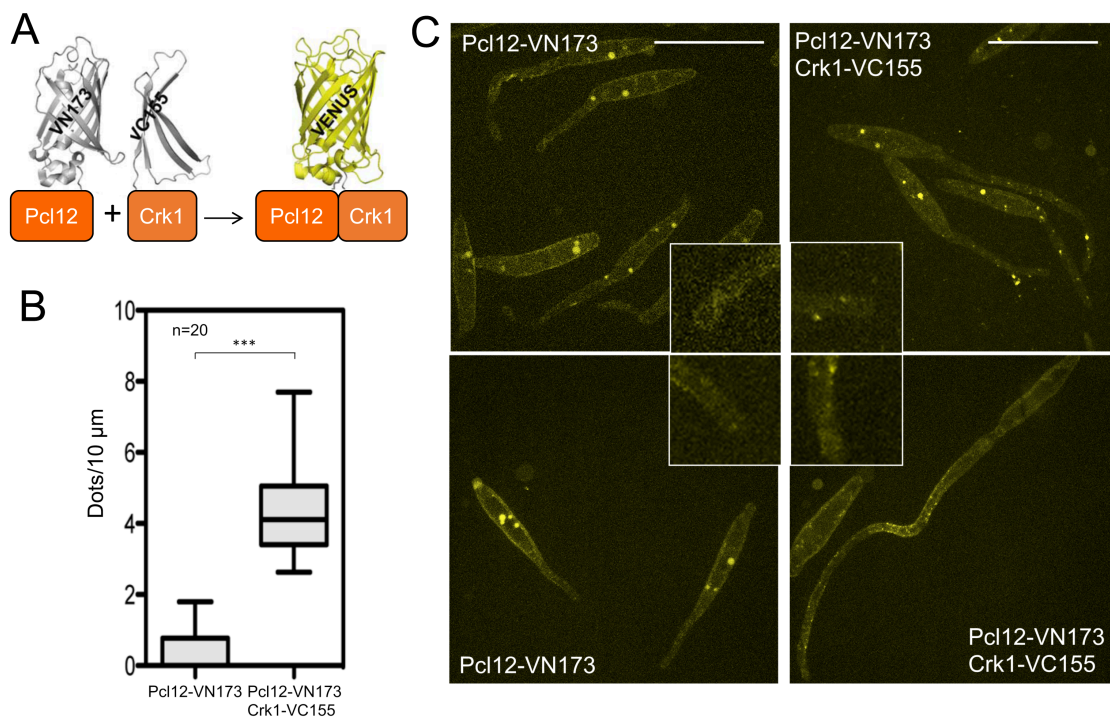
Figure 18: Crk1 and Pcl12 interact in the cytoplasm. A) Schematic representation of the BiFC experiments. Pcl12 and Crk1 were fused with two no-fluorescent fragments of the fluorochrome Venus that can complement: Pcl12-VN173 and Crk1-VC155. When the two proteins interacts also the fluorescent protein Venus is formed and we can detect signal. B) Dots number in the filaments. The number of dots related to the filament length was plotted for control cells and cells carrying the two no-fluorescent fragments. C) Crk1 and Pcl12 interaction. The left part of panel shows cells carrying only the fusion protein Pcl12-VN173 (not fluorescent) while the right part

of the panel show cells carrying both fusion proteins. Cells were grown in inducing conditions and visualized with the YFP channel. Notice that signal in the cell body was no specific.

8. OVEREXPRESSION OF PCL12 IS ABLE TO INDUCE CELL CYCLE ARREST.

During the characterization of Pcl12 and its role in governing the infective filament formation, it was described how the overexpression of *pcl12* was sufficient to induce strong polar growth and to arrest the cell cycle in G2 (Flor-Parra *et al.* 2007). Taking in consideration that Crk1 and Pcl12 are interacting and both are required for cell cycle arrest, we wondered if Crk1 was involved in cell cycle arrest induced by overexpressing *pcl12*. (fig.19) To address this question, we deleted a gene in a strain carrying the ectopic overexpression of *pcl12* under the control of the *crg1*promoter and fusion protein NLS-GFP. Upon the induction of the *pcl12* overexpression, cells lacking Crk1 did not arrest cell cycle indicating that Crk1 was necessary for the cell cycle arrest induced by Pcl12. Moreover, to discriminate whether the cell cycle arrest induced by Pcl12 was dependent of the MAPKK Fuz7 or of the downstream MAPK Kpp2, strain lacking both genes and overexpressing *pcl12* were generated. Interestingly, cell cycle was arrested in these cells indicating that Fuz7 and Kpp2 were not necessary for the cell cycle arrest induced by Pcl12 (Fig. 20).
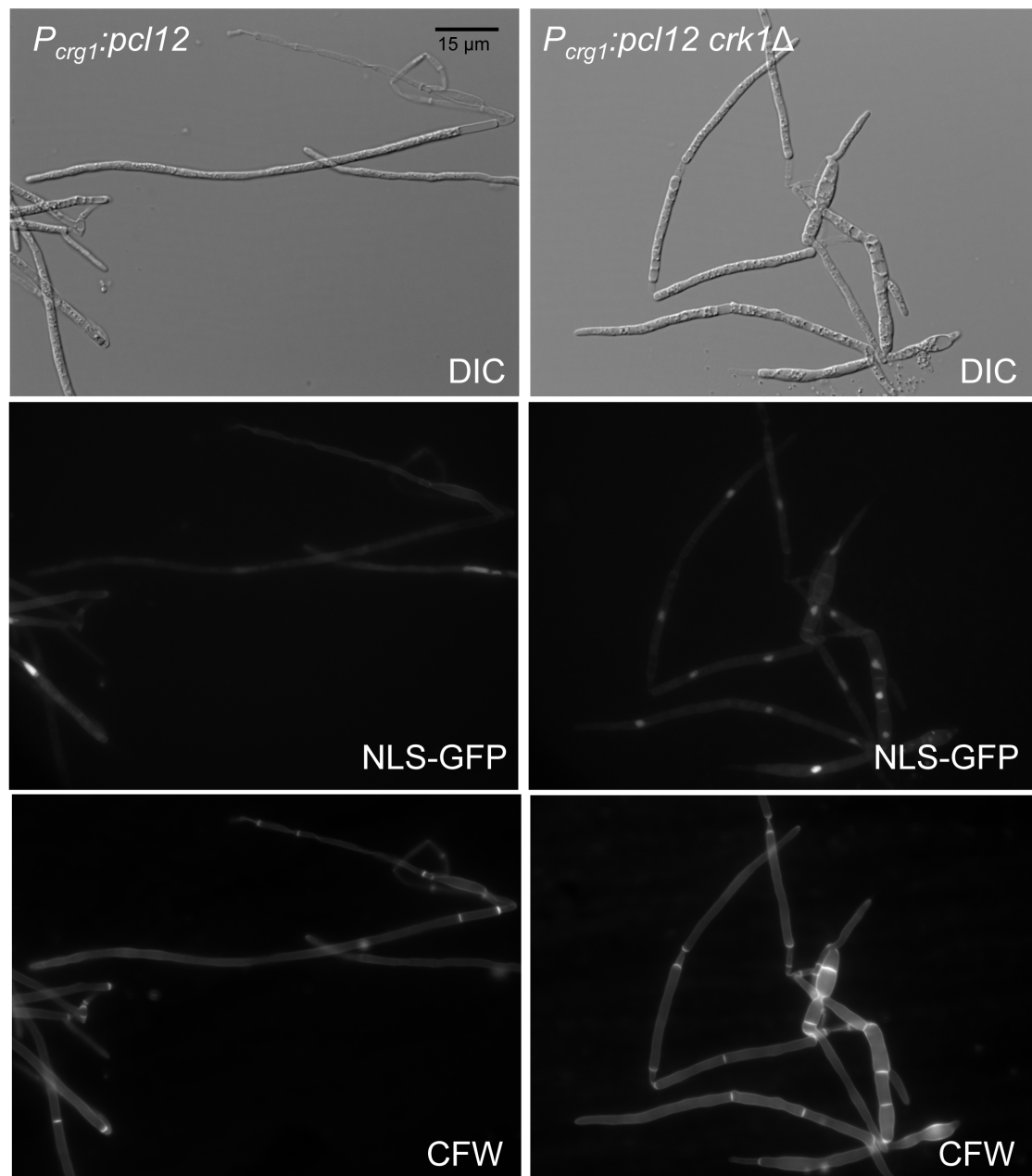
Figure 19: Crk1 is required for Pcl12-induced cell cycle arrest. Nuclei content of cells overexpressing *pcl12* **and lacking** *crk1*. **Cells were grown in inducing conditions over night and observed by light microscopy and fluorescence microscopy to observe GFP. Notice that cells showed more than one nucleus. Scale bar 15 μm.**
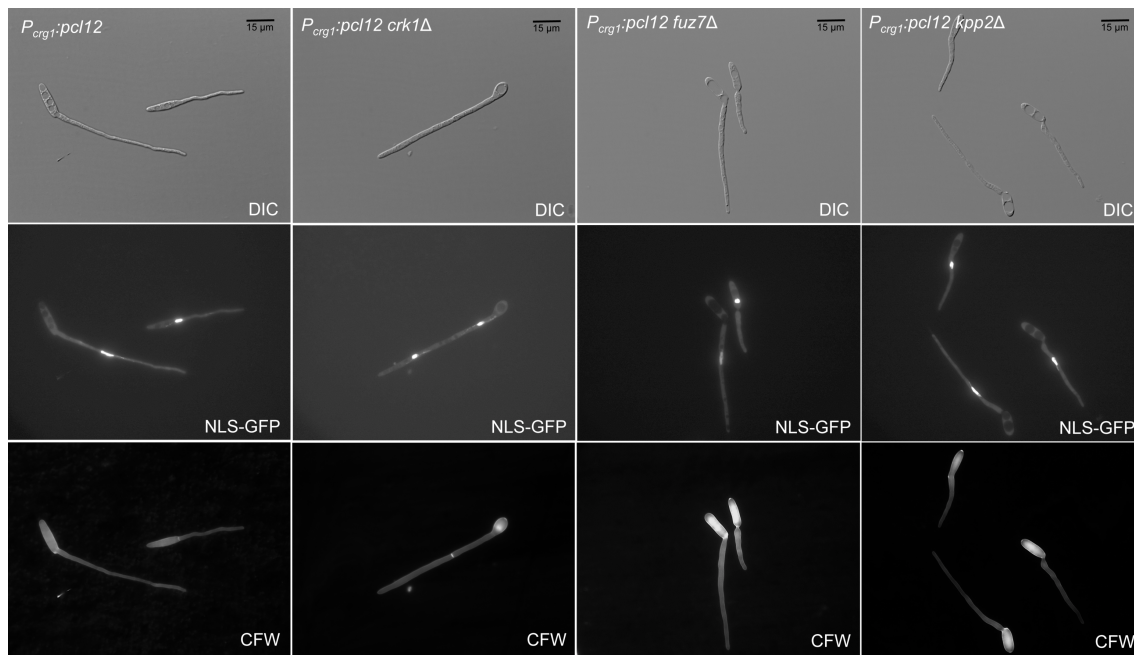
Figura 20: The overexpression of *pcl12* induces cell cycle arrest. Nuclei content observation. **Cells overexpressing *pcl12* and cells overexpressing *pcl12* and lacking *crk1*, *fuz7* and *kpp2* were grown in inducing conditions and assayed by DIC light microscopy and by fluorescent microscopy using the GFP and DAPI channels. The panel shows in the upper part DIC images, in the bottom part fluorescent images. Notice that in cells lacking *fuz7* and *kpp2* we could detect just one nucleus. Scale bar 15 μm.**

In was described that the ability of Crk1 to promote polar growth was dependent of the MAPKK Fuz7 and the MAPK Kpp2 (Garrido *et al.* 2004). Fuz7 was able to phosphorylate Crk1 in its Thr and Tyr residues on the T-loop, while Kpp2 interacts on the C-terminal where the kinase Crk1 possesses the MAPK consensus sites (Garrido *et al.* 2004). Because in this study we observed that neither Fuz7 nor Kpp2 were required for cell cycle arrest induced by Pcl12, we wondered if the phosphorylations performed by Fuz7 and Kpp2 on Crk1 were necessary for cell cycle arrest. To answer this question we generated strains carrying the allele overexpressing *pcl12* and an allele of Crk1 unable to be phosphorylated in its TEY motif, *crk1^{AEF}*, and an allele of *crk1* with point mutations that disrupt the MAPK consensus sites in the C-terminal domain, c*rk1^{AAA}*. In both cases, filaments showed one nucleus per cell indicating that cell cycle was arrested and the phosphorylation of Fuz7 and Kpp2 was not required for the cell cycle arrest. All these results indicate that Crk1 was

required for cell cycle arrest, but unlike occurs for morphogenesis, the activity of Crk1 did not depend of Fuz7 and Kpp2 (Fig.21). Since it was described that TEY phosphorylation was required for Crk1 activity, we wonder if the kinase activity of Crk1 was required for cell cycle arrest. To address this question an allele of *crk1* without kinase activity (kinase-dead) was introduced in a strain carrying the allele overexpressing *pcl12*. Cells were not able to arrest cell cycle supporting that Crk1 kinase activity was important for cell cycle arrest (Fig.21).
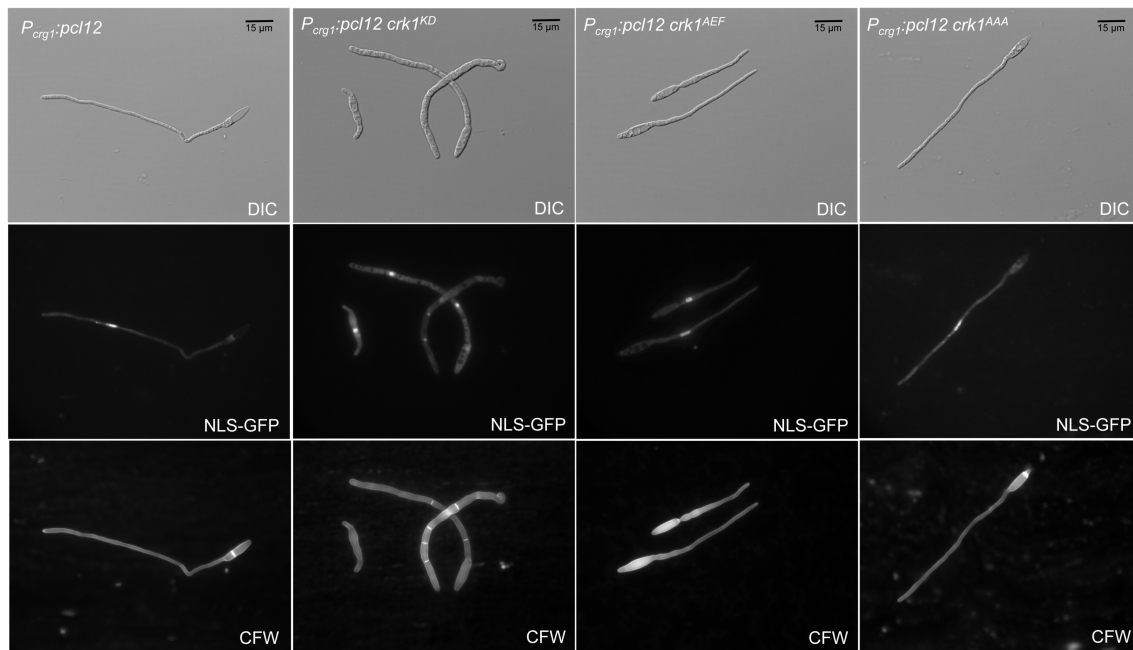
Figure 21: Cell cycle arrest induced by Pcl12 is independent of the MAPKK Fuz7 and the MAPK Kpp2. Nuclei content of cells overexpressing Pcl12 and carrying the *crk1KD*, *crk1AEF*, *crk1AAA* alleles. Cells were observed by light microscopy and fluorescence microscopy to check the nuclei content. Notice that the allele of Crk1 without kinase activity did not cause the arrest of the cell cycle but the filament was still formed. Scale bar 15 μm.

9. *pcl12-* INDUCED CELL CYCLE ARREST REQUIRES CDK1 INHIBITORY PHOSPHORYLATION

We analyzed Cdc25 protein levels in cells overexpressing *pcl12*. We observed that Cdc25 levels do not decrease upon the overexpression of *pcl12* (Fig.22A). Since we already knew that the down regulation of Cdc25 correlates with cell cycle arrest but it seems not to be the ultimate cause of it, we wondered if cell cycle arrest induced by *pcl12* does not require the inhibitory phosphorylation of Cdk1 as we observed for the cell cycle arrest induced by *fuz7^{DD}*. To investigate this hypothesis the allele *cdk1^{AF}*, refractory to phosphorylation, controlled by the *crg1* promoter was transformed ectopically in a strain overexpressing pcl12. The overexpression of *pcl12* is controlled also by the *crg1* promoter, in this way we could induce at the same time both allele by growing cells in CMA. As control, in a strain overexpressing *pcl12*, the wild type copy of *cdk1* under the control of the *crg1* promoter was introduced ectopically. Cells carrying the wild type copy of Cdk1 were arrested, whereas cells expressing the allele refractory to the inhibitory phosphorylation show more that one nucleus per cell (Fig.22A). This finding indicates that the inhibitory phosphorylation of Cdk1 was also the primary mechanism operating in cell cycle arrest induced by Pcl12.

A

P_{crg1}:pcl12 P_{crg1}:cdk1

P_{crg1} pcl12

P_{cdk1} cdk1

P_{crg1} cdk1:myc

P_{crg1}:pcl12 P_{crg1}:cdk1^{AF}

P_{crg1} fuz7^{DD}

P_{cdk1} cdk1

P_{crg1} cdk1^{AF}:myc

B

P_{crg1}:pcl12 P_{crg1}:cdk1   15 μm

P_{crg1}:pcl12 P_{crg1}:cdk1^{AF}

DIC   DIC

NLS-GFP   NLS-GFP

CFW   CFW
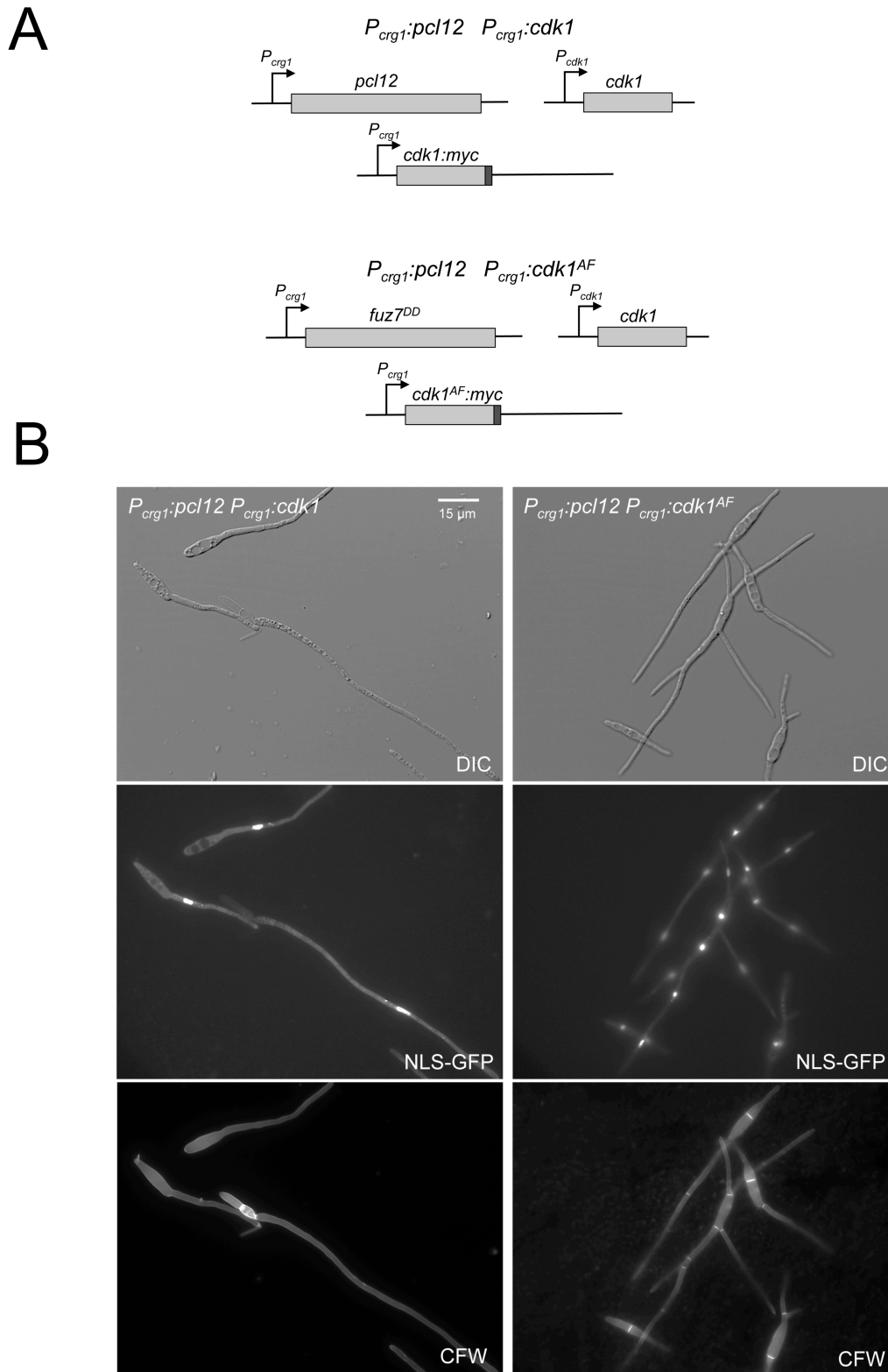
Figure 22: Schematic representation of the strains used. The cdk1 and cdk1^{AF} alleles were introduced ectopically in a strain carrying the *Pcrg1:Pcl12* allele and the endogenous copy of *cdk1*. C) Nuclei content of the strain used. Cells were grown in inducing conditions and observed with light microscopy and fluorescent microscopy to detect nuclear signal and septa. Scale bar 15 μm
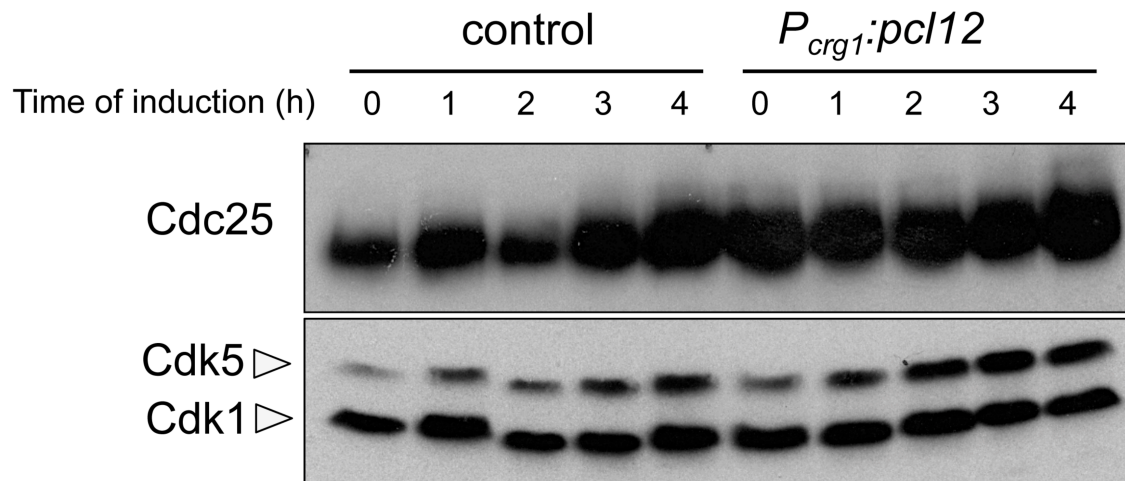
Figura 23: Cell cycle arrest induced by Pcl12 requires the inhibitory phosphorylation of Cdk1. A) Cdc25 protein level. Protein extracts from wild type and from cells overexpressing Pcl12 growing in inducing condition were collected at the indicated times.

10. CRK1 AND PCL12 INTERACT TO CONTROL CELL CYCLE ARREST BUT NOT TO CONTROL THE CONJUGATIVE TUBE FORMATION.

The findings that Crk1 and Pcl12 were physically interacting and that Crk1 was required for cell cycle arrest induced by Pcl12 supported the notion that Crk1 and Pcl12 were partners to regulate cell cycle arrest. During this study, we also noticed that the deletion of *pcl12* or *crk1* in cells carrying the *fuz7DD* allele affected the morphology of the conjugative tube. However, when we generated the double mutant in a strain carrying the *fuz7DD* allele, we observed that the morphology of the filament was impaired more severely than the single mutants, suggesting that Crk1 and Pcl12 could be acting in two different pathways to control filament morphology (Fig. 24). Is important to keep in mind, that Pcl12 acts in complex with the kinase Cdk5 to control polar growth of the conjugative tube induced by the *fuz7DD* allele (Castillo-Lluva *et al.* 2007; Flor-Parra *et al.* 2007). In the same way, the kinase Crk1 requires the activation of the MAPKK Fuz7 to control morphogenesis (Garrido *et al.* 2004). We believe that, Crk1 could be differentially regulated by the MAPKK Fuz7 to operate in morphogenesis and by Pcl12 to control cell cycle arrest, while

Pcl12 could be acting in complex with Cdk5 to control the morphogenesis and in complex with Crk1 to control cell cycle arrest (Fig.25).
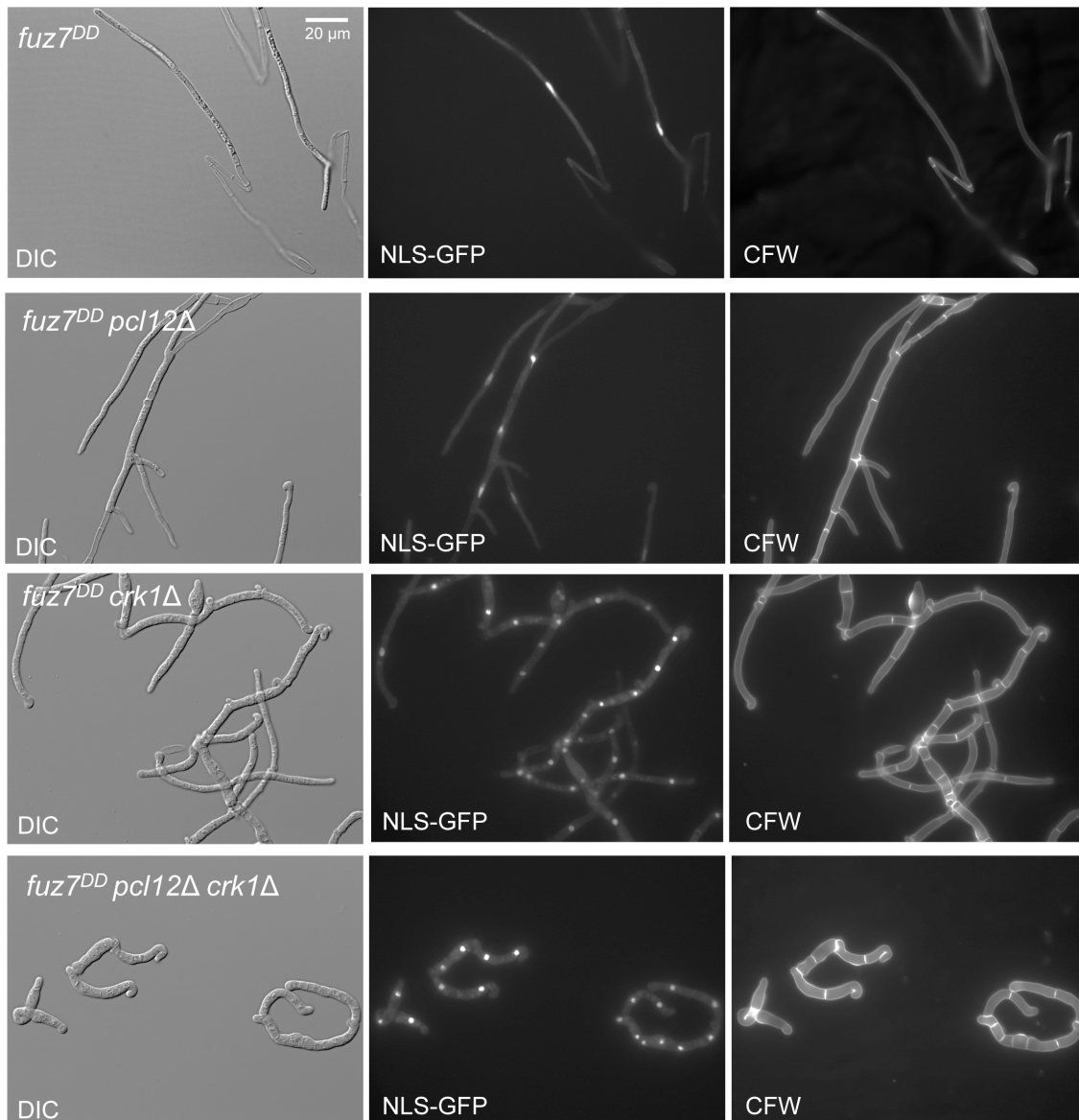
Figura 24: Crk1 and Pcl12 are acting in two separate pathways to control morphogenesis. Morphology of the filament induced by the *fuz7DD* allele in absence of *pcl12* and *crk1*. Cells were grown in inducing condition of the *fuz7DD* allele and cells were assayed by light microscopy and fluorescence microscopy. The panel shows the images of control cells, the single mutants and the double mutant. Notice that the morphology of the double mutant is more affected than the single mutants. Scale bar 20 μm.

A Morphogenesis — Cell cycle arrest

Morphogenesis table:

o/e	wt	pcl12Δ	crk1Δ	pcl12Δ crk1Δ
fuz7[DD]	+++	++	++	+
[1]pcl12	+++	n.a.	+++	n.a.
[2]crk1	+++*	n.a.	n.a.	n.a.

Cell cycle arrest table:

o/e	wt	pcl12Δ	crk1Δ	pcl12Δ crk1Δ
fuz7[DD]	+	-	-	-
pcl12	+	n.a.	-	n.a.
[2]crk1	-*	n.a.	n.a.	n.a.
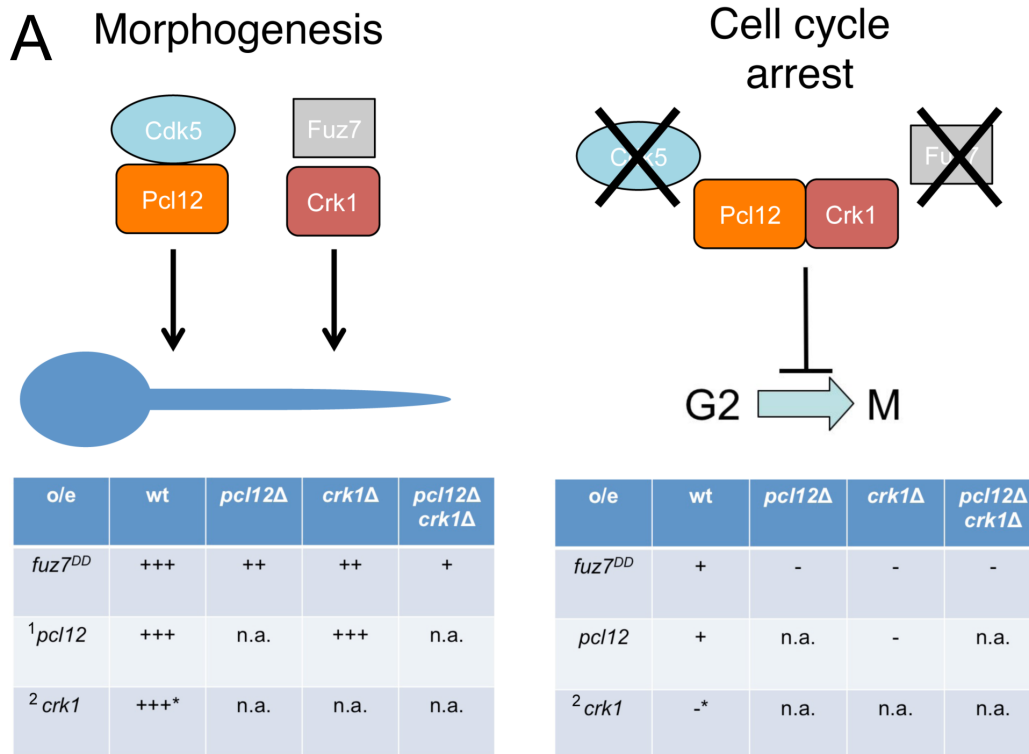
* *pcl12* is not being expressed in this condition

[1] **Flor-Parra *et al.* (2007)** *Plant Cell* **19**, 3280

[2] **Garrido *et al.* (2004)** *Genes Dev.* **18**, 3117

B

Cell cycle arrest

Pcl12

Activation Loop

Catalytic Loop

Crk1

^{253}TEY^{255}

^{190}FHRDMK

P+1 Loop

WYRAPE^{265}

Fuz7
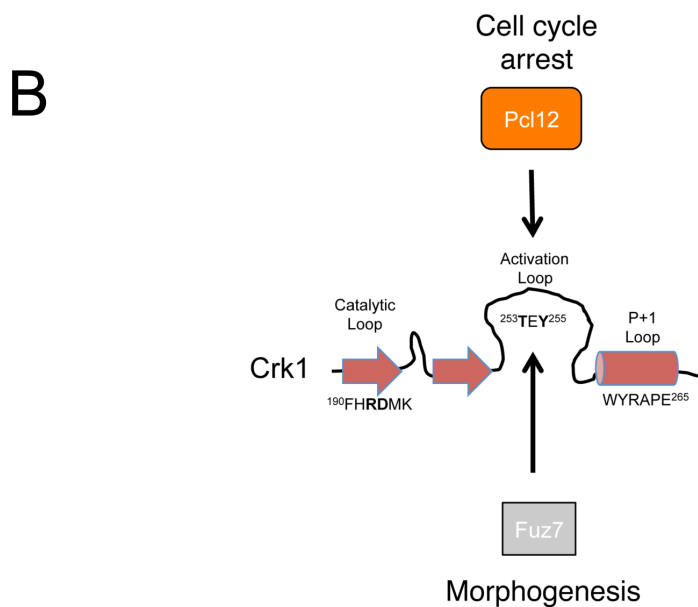
Morphogenesis

Figure 25: Crk1 and Pcl12 are interacting to control cell cycle arrest but not to control morphogenesis. A) Schematic representation of morphogenesis and cell cycle arrest regulation by Crk1 and Pcl12. Morphogenesis of the conjugative tube is controlled by the complex Cdk5-Pcl12 and by Crk1 that is activated by the MAPKK Fuz7. On the other hand the cell cycle arrest is regulate by the complex Crk1-Pcl12 and the kinase Cdk5 or the MAPKK Fuz7 are not required. Genetic data support this relationship between Crk1 and Pcl12. B) Crk1 is able to interact with Fuz7,that phosphorylates the TEY motif in the T-loop, and with the cyclin Pcl12.

11. CDC25 DOES NOT DECREASE WHEN IT LOCALIZES IN THE NUCLEUS.

It has been demonstrated that in *U. maydis* the sequestration of Cdc25 in the cytoplasm is a mechanism that inhibits the G2/M transition (Mielnichuk *et al.* 2009). Since the decrease of Cdc25 levels was not the cause of cell cycle arrest induced by *fuz7DD* allele but there was a correlation between these two events, we hypothesized that the retention of Cdc25 in the cytoplasm could lead to cell cycle arrest and later on to its degradation. To test this hypothesis, we sought to alter the nucleus/cytoplasm traffic in order to retain Cdc25 into the nucleus. For that, we first checked whether the treatment of cells carrying the fusion protein GFP-CDC25 with Leptomycin B (LMB), a drug that inhibits nuclear exports by targeting Exportin 1 (Crm1), keeps Cdc25 in the nucleus in budding cells (fig. 26). After 30 minutes of treatment with Leptomycin B (100ng/ml) (LMB), we were able to detect Cdc25 signal in the nucleus. Interestingly, when we added LMB and we induced *fuz7DD* allele, we did not observe decrease in Cdc25 protein levels suggesting that when Cdc25 localized in the nucleus it was not down regulated (Fig.27A). These cells treated with LMB showed conjugative tube formation indicating that the *fuz7DD* allele was correctly induced and the MAPK cascade was activated (Fig. 27B).
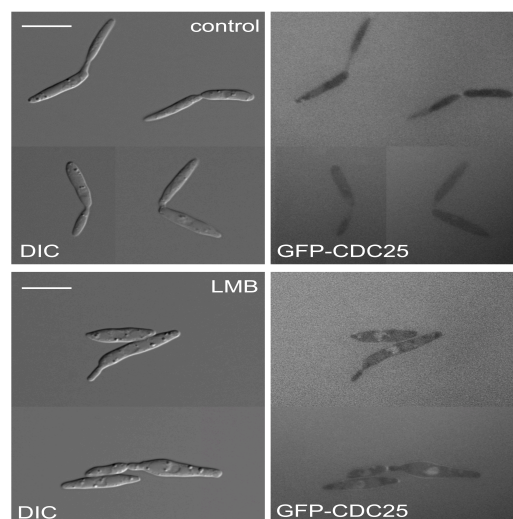
Figure 26: Accumulation of Cdc25 in the nucleus. A) Cells carrying the *fuz7DD* allele and the fusion protein GFP-Cdc25 were treaded with LMB (100ng/ml). Ethanol (LMB is soluble in ethanol) was added to the control culture. Cells were observed with GFP to detect FP signal. Note the accumulation of GFP in the nucleus.
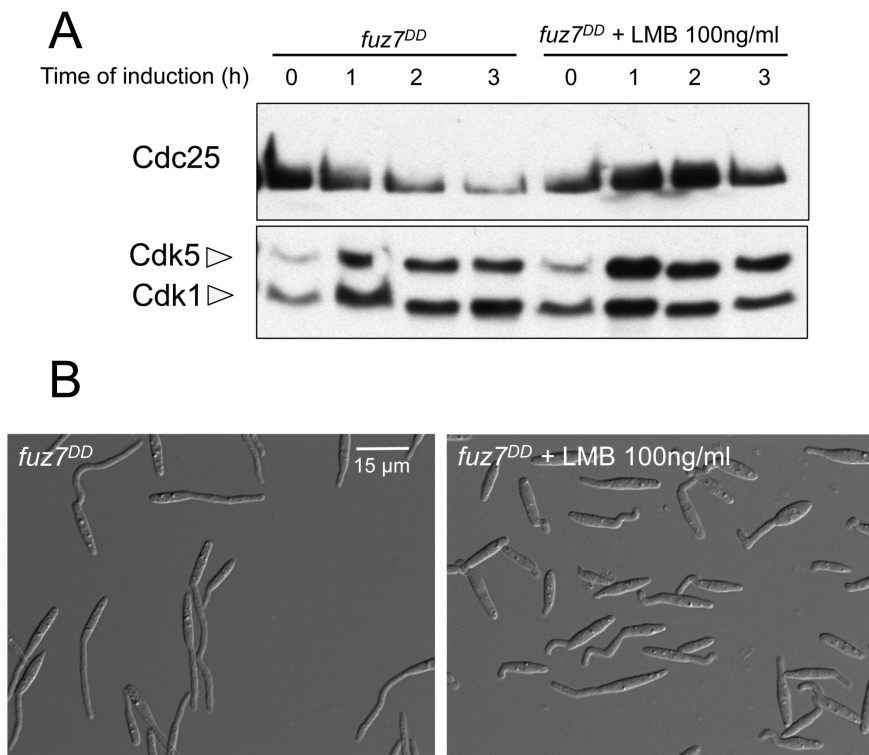
Figure 27: Accumulation of Cdc25 in the nucleus shields its down regulation. A) Cdc25 protein level. Protein extracts from control cells carrying the *fuz7DD* allele and from cells carrying and treaded with LMB (100ng/ml) were collected at the indicated times. Cells were grown at inducing conditions and ethanol (LMB is soluble in ethanol) was added to the control culture. **B)** Filament induction of cells treated with LMB. The panel shows DIC images of the control cells and of cells treated with LMB. Notice that the filamentation was induced. Scale bar 15 μm.

12. THE IMPORTIN β KAP123 IS RESPONSIBLE OF CDC25 LOCALIZATION.

One of the putative interactors of Pcl12, sorted by the Mass Spectrometry analysis, was an importin β of the subfamily IMB4, that we called Kap123 (UMAG_15014) because of the sequence similarity to the correspondent *S.cerevisiae* protein. The fact that Pcl12 interacted with an importin called our attention, taking in account that Pcl12 is a cytoplasmatic protein. Importin are divided into two families, α and β. The β importins can bind and transport cargos by themselves or form a heterodimer with α Importin. In this case, α Importin interacts with the cargo protein whereas the β Importin with the nuclear pore. In

U. maydis there are seven β importins and just one α importin, called Srp1. The β importin Kap123 (UMAG_15014) belongs to the subfamily IMB4 (Fig.28A). No members of the subfamily IMB3 are found in *U. maydis*. However, it has been demonstrated that in *C. cerevisiae* IMB4 importin can substitute the function of the IMB3 (Rout *et al.* 1997) (Fig.28A). This is important because in *S. pombe* it has been described that the nuclear import of Cdc25 is regulated by an importin of the subfamily IMB3 called Sal3 (Chua *et al.* 2002). Interestingly, in *U. maydis* Kap123 is the most similar importin to Sal3. For all these reasons we asked if Kap123 could have a role in the regulation of Cdc25 localization.

Since we failed to obtain the single mutants *Δkap123* and *Δsrp1*, we generated conditional mutants exchanging the promoter of *kap123* and *srp1* with *Pnar1*, which is repressed in rich medium (YPD). The down regulation of *kap123* and *srp1* support the notion that these genes were essential (Fig.28B). To study if Kap123 and Srp1 were involved in Cdc25 localization we introduced ectopically the *GFP-Cdc25* allele controlled by the *crg1* promoter in the conditional strains (endogenous allele can barely be detectable). Cells were grown in YPA in order to repress the *kap123* and *srp1* and to up regulate *cdc25* expression. As control we used a strain overexpressing *cdc25*. We observed that when we down regulated *srp1*, Cdc25 was able to localized in the nucleus like in the control cells. (Fig. 28C) Contrary, when the expression of *kap123* was repressed, we were not able to observe Cdc25-GFP accumulation in the nucleus indicating that Kap123 was involved in the transport of Cdc25 to the nucleus (Fig. 28C). Moreover the fact that Srp1 was not required for Cdc25 localization suggested that Kap123 did not need the α importin to traslocate Cdc25 in the nucleus, as it has been described for other targets of β Importin (Harel and Forbes 2004; Flores and Seger 2013)
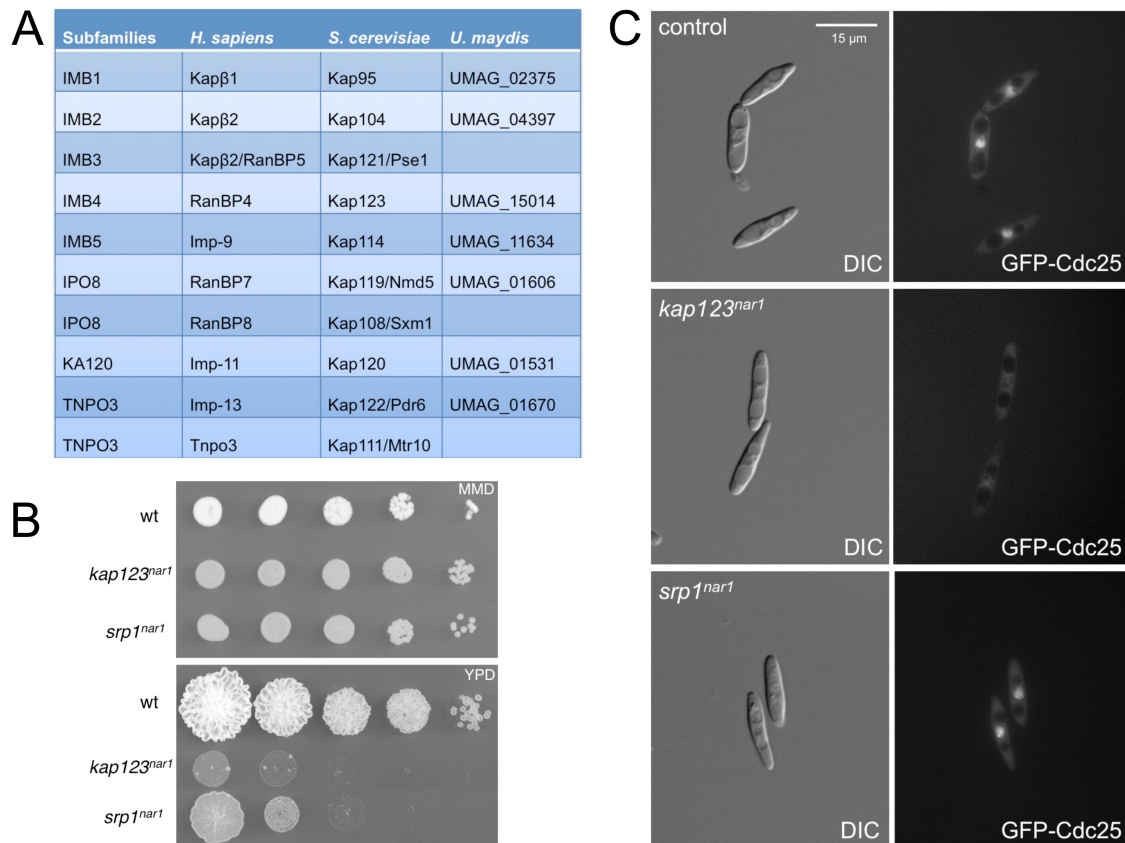
Figure 28: Importinβ Kap123 is involved in Cdc25 localization. A) List of β Importin. The table shows the β Importins present in *Homo sapiens, S. cerevisiae* and *U. maydis*. **B)** Conditional mutants of the β Importin Kap123 and the α Importin Srp1. The two conditionals strains and a control (WT) were grown in repressive condition of nar1 promoter. In exponential phase, cultures were spotted in serial dilutions in no repressive conditions (MMD) and in repressive conditions (YPD). Notice that both importins were essential. **C)** Cdc25 localization in conditional mutants. FB1 cells and conditional cells overexpressing the fusion protein GFP-Cdc25, growing in YPA, were observed with fluorescence microscopy using the GFP channel. The panel shows in the upper part images of control cells, in the middle images of Kap123 conditional mutants and in the bottom part Srp1 conditional mutant. The overexpression of *cdc25* resulted with the Cdc25 nuclear localization; notice that Cdc25 did not localize in the nucleus when the importin Kap123 was down regulated. Scale bar 15 μm.

13. IMPORTIN KAP123 COULD BE A TARGET PF PCL12/CRK1 COMPLEX

One interesting possibility was that Kap123 was a target of Crk1-Pcl12 complex and that the phosphorylation could interfere with the ability of the β importin to translocate Cdc25 to the nucleus. To address this hypothesis we first checked whether we can observed any change in the protein mobility upon the induction of the *fuz7^{DD}* allele. We generated a strain

carrying the fusion protein Kap123-HA, that was functional, and the $fuz7^{DD}$ allele. We observed that upon the activation of $fuz7^{DD}$ allele there was a shift in the electrophoretic mobility of Kap123 suggesting a phosphorylation upon the activation of the $fuz7^{DD}$ allele (Fig.29A). We checked whether this change in Kap123 electrophoretic mobility was depending of *crk1* or *pcl12*. We originated two strains lacking *pcl12* and *crk1* and carrying the $fuz7^{DD}$ allele. After four hours of growth in inducing conditions protein extracts from *crk1* or *pcl12* mutants discarded a change in Kap123 mobility supporting the notion that Crk1 and Pcl12 were required for the Kap123 shift when $fuz7^{DD}$ allele is induced (Fig. 29B). Moreover we checked if this change in mobility of Kap123 was dependent of the MAPK Kpp2. To address this question we generated a strain carrying the deletion of *kpp2* and the $fuz7^{DD}$ allele. In inducing condition, no change in Kap123 mobility was detected illustrating that the phosphorylation was also dependent of Kpp2 (Fig. 29B).

We analyzed also change in Kap123 electrophoretic mobility in cells overexpressing *pcl12*. In agreement to our hypothesis, the overexpression of *pcl12* induced a molecular shift of Kap123 (Fig.29 C). To prove that Pcl12 needed to be associated with the kinase Crk1 to induce the mobility shift of Kap123, we constructed a strain carrying the $fuz7^{DD}$ allele the deletion of *crk1* and the fusion protein Kap123-HA; no change in Kap123 mobility was detected indicating that Pcl12 and Crk1 likely phosphorylated Kap123 (Fig.29D).. Furthermore we analyzed if the shift induced by Pcl12 was dependent of the MAPKK Fuz7 and of the MAPK Kpp2. We generated two strains carrying the fusion protein Kap123-HA, the $fuz7^{DD}$ allele and the deletion of *fuz7* and *kpp2*. After induction of *pcl12,* we detected a shift assessing that this change in electrophoretic mobility was independent of the MAPK cascade, provided that Pcl12 has been expressed in an independent way (Fig.29D).
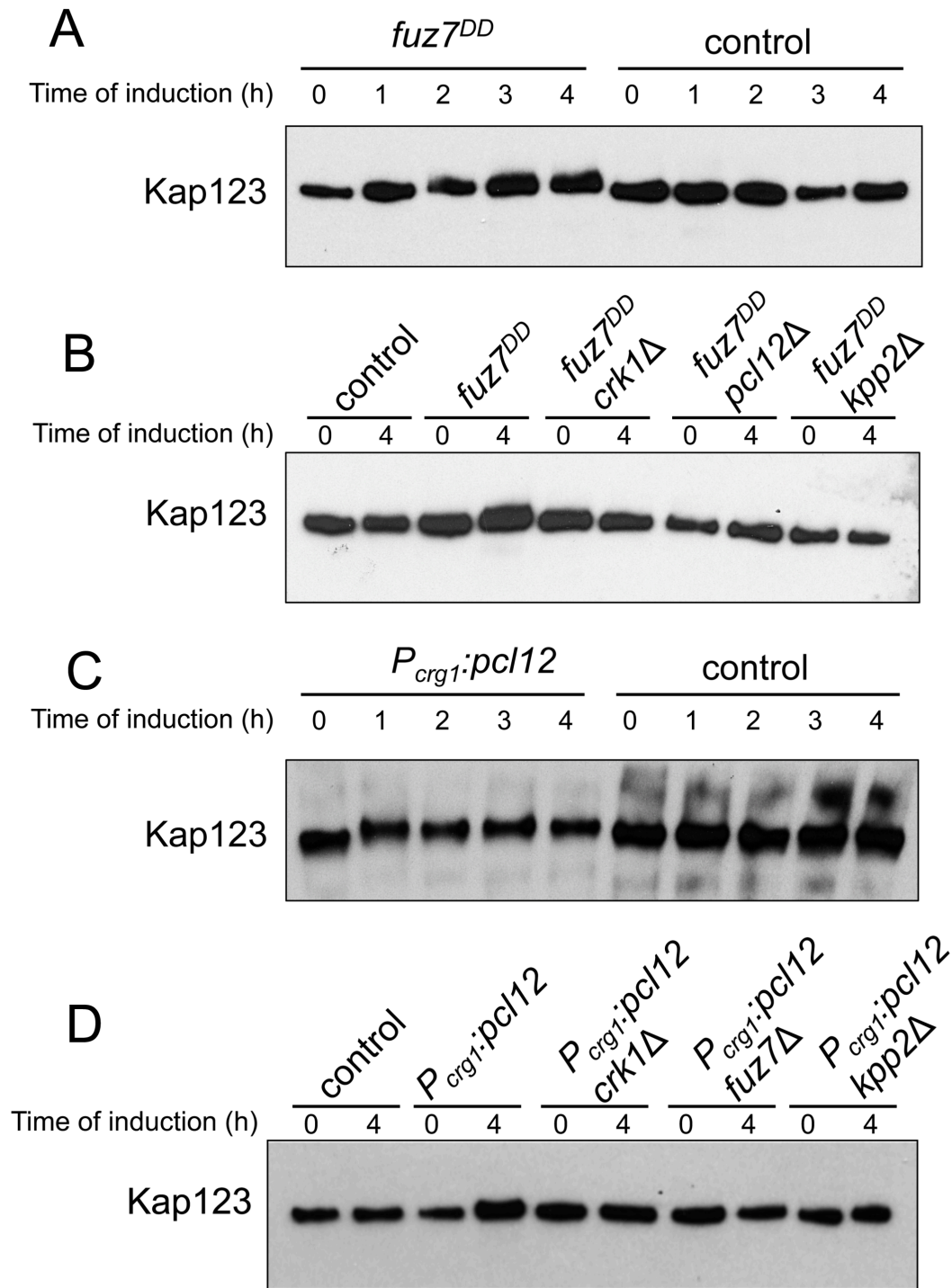
Figure 29: Phosphorylation of Kap123 is performed by the complex Crk1-Pcl12. A) Phosphorylation of Kap123 upon the induction of the *fuz7DD* allele. Protein extracts from cells expressing the *fuz7DD* allele, the fusion protein Kap123-HA and growing in inducing conditions were collected at the indicated times. Kap123 shifts upon the induction of the *fuz7DD* allele. **B)** Pcl12 and Crk1 are required for the electrophoretic shift of Kap123. Protein extracts from cells expressing the *fuz7DD* allele and the deletion of crk1 and pcl12 were growing in inducing conditions. Protein extracts were collected at the indicating times. Kap123 did not shift in absence of pcl12 and Crk1. Protein extracts from cells carrying the *fuz7DD* allele and the deletion of kpp2 growing in

inducing conditions were collected at the indicated times. C) Phosphorylation of Kap123 upon the overexpression of pcl12. Cells overexpressing pcl12 and cells carrying the fusion protein Kap123-HA were grown in inducing conditions. Protein extracts were collected at the indicated times. D) Crk1 is required for the phosphorylation of Kap123 upon the overexpression of Pcl12. Cells overexpressing pcl12 and lacking kpp2 and fuz7 were grown in inducing conditions. Protein extracts were collected at the indicated times. The phosphorylation was independent by the MAPK cascade.

14. THE KAP123 UNABLE TO BE PHOSPHORYLATED IS UNABLE TO ARREST CELL CYCLE

Because the complex Crk1-Pcl12 seems to be able to phosphorylate the importin Kap123 we looked for putative CDK sites on Kap123 amino acid sequence. We found two putative sites, ^{324}DEDSPSR^{330} and ^{864}KYYTPGR^{870}, that we decided to mutate in order to generate two alleles of *kap123* refractory to phosphorylation. We were able to exchange the threonine in position 867 with alanine, allele *kap123^{T867A}*, but we failed to obtain the other mutation (fig. 30A). Interestingly, the prediction of the Kap123 showed that the CDK site we mutated was located on protein surface, a suitable position to interact with cargo proteins (fig. 30B). To check if the cell cycle arrest induced by the *fuz7^{DD}* allele was affected by this mutation, we generated a strain carrying the *fuz7^{DD}* allele and the refractory allele *kap123^{T867A}*, as control a strain carrying the fusion protein Kap123-HA and the *fuz7^{DD}* allele. Interestingly, we observed that when *fuz7^{DD}* allele was induced, cells were not able to arrest cell cycle illustrating that the Kap123 phosphorylation was required to control *fuz7^{DD}* -induced cell cycle arrest. (Fig. 30D). Moreover we checked if the mutation T867A affected the electrophoretic mobility of Kap123 upon the induction of the *fuz7^{DD}* allele. We observed that there was no shift in Kap123^{T867A} mobility suggesting that importin was most likely phosphorylated in this CDK site when the *fuz7^{DD}* allele was active (Fig.30C). Taking in consideration that Kap123 affected Cdc25 localization, we checked Cdc25 levels in cells carrying the allele refractory to phosphorylation *kap123^{T867A}* and the *fuz7^{DD}* allele. Upon the

induction of *fuz7^{DD}* allele, Cdc25 levels did not decrease suggesting that the phosphorylation of Kap123 was required for Cdc25 degradation (Fig. 30C).
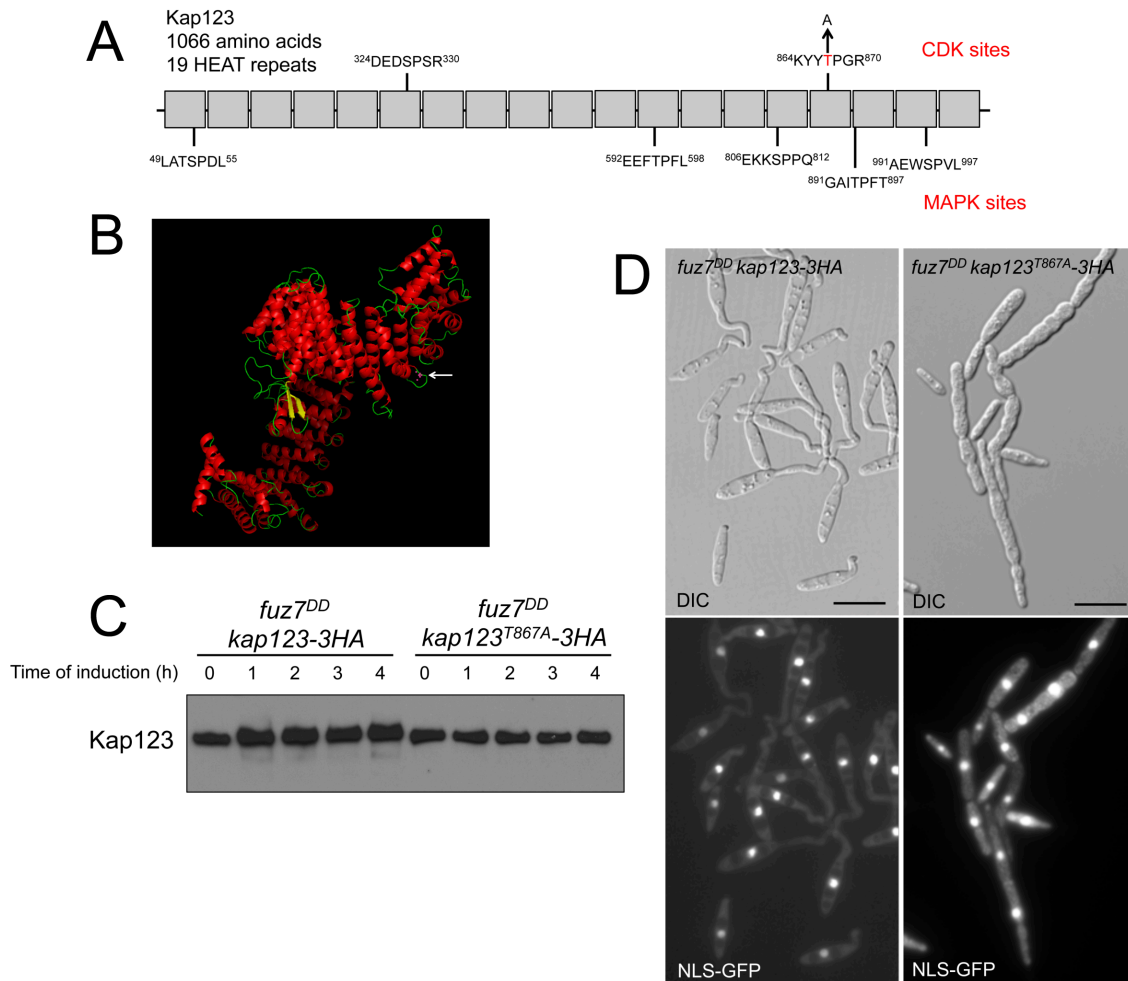
Figure 30: Point mutation in CDK sites results in cell cycle arrest. A) Schematic representation of the amino acidic sequence of the Importin Kap123. The protein is composed of 1066 amino acids organized in 19 HEAT repeats. The sequence brings five putative MAPK sites and two CDK sites. B) Putative 3D Importin conformation. Notice that the position of the mutated CDK site is on the protein surface (white arrow). C) Kap123 changes in mobility upon the induction of the *fuz7^{DD}* allele. Cells expressing the *fuz7^{DD}* allele and the fusion protein kap123-3HA (used as control) and from cells expressing the *fuz7^{DD}* allele and the mutated version of the fusion protein kap123^{T867A}-3HA were grown in inducing conditions. Proteins extracts from these cultures were collected at the indicated times. D) Nuclei content of cells carrying the mutated version of the Kap123^{T867A}. These cells, that expressed also the fusion protein NLS-GFP, were observed with fluorescence microscopy to visualize GFP signal. The panel shows on the left the control cells which bring the wild type copy of the importin Kap123 tagged with HA and on the right cells carrying the mutated version.

DISCUSSION

In this work we have investigated cell cycle arrest induced by pheromone in the phytopathogenic fungus *U.maydis.* The virulence in this fungus is strictly connected with the sexual development and the beginning of the pathogenic program starts when two compatible no-pathogenic cells mate in response to pheromone. This signal is perceived by receptors located on the plasma membrane and transmitted in the cell through the MAPK pathway. This cascade is able to modulate two fundamental events for mating: the formation of the conjugative tube and the cell cycle arrest. In this study we have focused on the mechanism of cell cycle arrest and how the MAPK cascade is able to govern it. The most important findings will be discussed in the following section.

1.PHEROMONES INDUCE G2 CELL CYCLE ARREST IN *U. maydis*

In most of fungi able to reproduce sexually, pheromone-dependent cell cycle arrest allows two compatible cells to synchronize their cell cycle in the same phase before mating. It has been described that *U. maydis* arrests cell cycle in G2 in response to pheromone (Garcia-Muse *et al.* 2003) while in others fungi, such as *S. cerevisiae* or *S. pombe,* cell cycle arrests in G1 (Chang and Herskowitz 1990; Davey 1998). In these fungi, in which plasmogamy is followed by karyogamy, it makes sense to synchronize cell cycle before S phase in such a way that karyogamy resulted in a diploid nucleus. However, for a plethora of fungi, such as basidiomycetes, karyogamy is delayed later on during the life cycle and therefore plasmogamy results in a dikaryotic cell with two distinct nuclei. In these cases a G1 cell cycle arrest is not mandatory. Moreover, since compatible cells need to form the sexual structure by enhancing polar growth, it makes sense to arrest the cell cycle in the phase where the polar growth will be the most suitable. In the case of *U.maydis* this cell cycle phase is G2, in which bud formation occurs during axenic growth. In this phase, the

cytoskeleton machinery is promoted to sustain strong polar growth such as the required for bud formation or for the formation of the conjugative tube.

2. PHEROMONE CELL CYCLE ARREST DEPENDS OF CRK1 AND PCL12

The response to pheromone relies in two major events: one is the cell cycle arrest and the other one is the formation of the conjugative tube. In this study we have described the role that the Cdk-related kinase, Crk1, and the Pcl-like cyclin, Pcl12, play in these two mechanisms. It was previously described that Pcl12 and Crk1 were required for morphogenesis. Pcl12, which expression is induced by pheromone, acts in complex with Cdk5 to control the proper formation of both infective filament and conjugative tube (Flor-Parra *et al.* 2007). The overexpression of Crk1 is able to induce polarized growth (Garrido and Perez-Martin 2003) and its ability to promote polar growth depends of the phosphorylation by the MAPKK Fuz7 on the T-loop and the MAPK Kpp2 on the C-terminal (Garrido *et al.* 2004). However, their role in cell cycle arrest was not described yet. In this study we assessed that Crk1 and Pcl12 are required to sustain cell cycle arrest induced by the pheromone MAPK cascade. Moreover we found that this cell cycle arrest was independent of Crk1 activation by the MAPK cascade, even if we demonstrated that the its kinase activity was required for cell cycle arrest. Therefore, we believe that the interaction between Crk1 and Pcl12 is able to activate Crk1 to control cell cycle arrest. The double activation of Crk1 done by the MAPKK Fuz7 and by the cyclin Pcl12 is possible because Crk1 is a kinase belonging to the RD-kinase family. These kinases are characterized by a conserved arginine preceding the conserve catalytic aspartate in the activation segment in the catalytic loop (Johnson *et al.* 1996). These kinases are activated by the T-loop. The primary mechanism to regulate the kinase activity is the phosphorylation on one or more residues on the T-loop that counteract to the positive charges of the arginine allowing the T-loop to refold and in this conformation the kinases is able to

interact with substrate; otherwise RD kinases can be activated by interaction with a cyclin. This binding force the T-loop to refold and to activate the kinase (Nolen *et al.* 2004). Crk1 is a RD kinase that seems to be activated by two indepenet manners: in one side it is phosphorylated in the TEY motif in T-loop by the MAPKK Fuz7, and it is also able to interact with the cyclin Pcl12. This apparent flexibility for activation allows this kinase to play specific roles during morphogenesis (interacting with the MAPK cascade) as well as during the control the cell cycle arrest, interacting with Pcl12 (Figure 1).

In this study we assessed how the formation of the sexual structure and cell cycle arrest are regulate by the same elements, Crk1 and Pcl12, but their activation is different. For what concern the morphogenesis Crk1 need to be phosphorylated by the MAPKK Fuz7 and the MAPK Kpp2, whereas Pcl12 acts in complex with the kinase Cdk5. Interestingly we found that either Cdk5 or the phosphorylations performed by Fuz7 and Kpp2 on Crk1 kinase are not required for cell cycle arrest. In this case Crk1 and Pcl12 are acting as partners to control cell cycle arrest. We believe that in *U. maydis* during the response to pheromone, there are two different populations of Pcl12: one is acting in complex with Crk1 and another one is acting in complex with the kinase Cdk5. The same occurs for Crk1 that interacts with Pcl12 to control cell cycle arrest but not for control morphogenesis. This dual role played by Pcl12 and Crk1 in cell cycle arrest regulation and in control of the morphology of the sexual structure is played also by Far1 in *S. cerevisiae*. Indeed Far1 is able to interact with the G1-Cdk1 complexes to arrest the cell cycle in G1 (Peter and Herskowitz 1994) but it is also able to control the polar growth during shmoo formation interacting with the guanine-nucleotide exchange factor Cdc24, the activator of GTPases Cdc42, a regulator of cell polarity (Nern and Arkowitz 1999; Shimada *et al.* 2000)
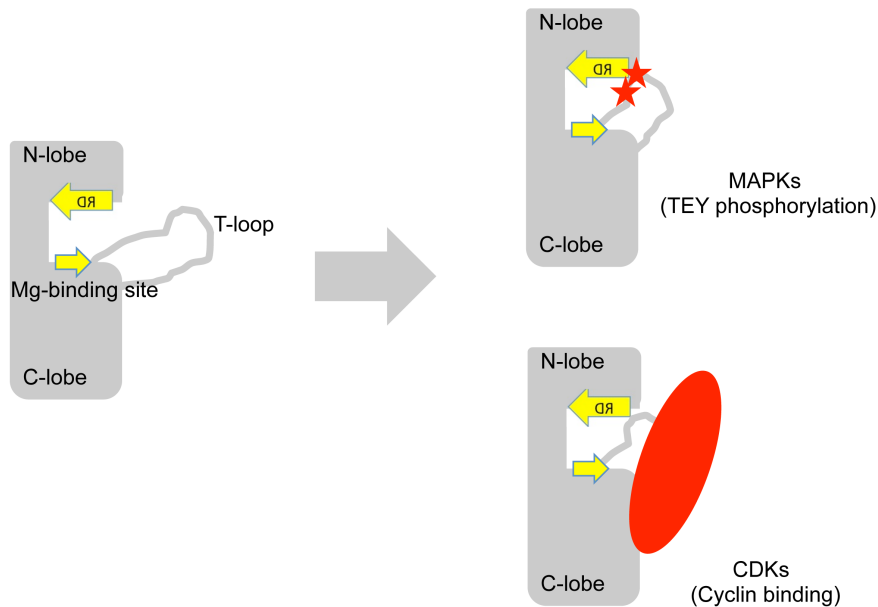
Figure 1: Schematic representation of the two modality of activation of the kinase Crk1.

3.MECHANISM OF PHEROMONE-INDUCED CELL CYCLE ARREST

Unlike *S. cerevisae*, *U.maydis* does not mate spontaneously but the mating program starts when cells are in starvation. To bypass this nutritional signaling we used an activated allele of the MAPK Fuz7, *fuz7^{DD}*, regulated by an inducible promoter (Muller *et al.* 2003). In this way we were able to activate the MAPK pathway without adding pheromone or growing cells in special media conditions. After validation of the G2 cell cycle arrest when the *fuz7^{DD}* allele is active, we assessed that the inhibitory phosphorylation of Cdk1 is part of the mechanism of cell cycle arrest induced by pheromone. This reaction is catalyzed by the kinase Wee1 which activity is fundamental for pheromone cell cycle arrest. These arguments are in agreement with the mechanism operating during the G2/M transition in which the level of the phosphorylated form of Cdk1 determines the progression in mitosis or a delay in G2 phase (Sgarlata and Perez-Martin 2005). When we analyzed protein levels of G2/M master regulators in presence of an active MAPK cascade, we observed a decrease in the phosphatase Cdc25 protein levels. Cdc25 is required to remove the inhibitory phosphorylation of Cdk1 and promote the entry into mitosis (Sgarlata and

Perez-Martin 2005). Paradoxically when we overexpressed Cdc25, assuming that cells were able to re-entry the cell cycle, we observed that cell cycle was still arrested and no decrease in Cdc25 levels was detected. This finding led us to think that another mechanism was involved in cell cycle arrest and the down regulation of Cdc25 was associated with it but not the only cause. Previous result that the cytoplasmatic recruitment of Cdc25 leads to an increase of the inhibitory phosphorylation of Cdk1 associated with a delay in G2/M transition (Mielnichuk and Perez-Martin 2008) and our observation that Cdc25 nuclear localization avoids its down regulation, indicated that a regulation in mechanism of Cdc25 cytoplasmatic traffic could operate in cell cycle arrest induced by pheromone. The finding that importin Kap123, an interactor of Pcl12 sorted by Mass Spectometry, was involved in Cdc25 localization supported this hypothesis. When we found that Kap123 electrophoretic mobility changed upon the activation of the MAPK cascade and this shift was dependent of Crk1 and Pcl12 we considered the hypothesis that the complex Crk1-Pcl12 could phosphorylate the importin Kap123 and affect the ability to transport Cdc25 in the nucleus. The observation that Kap123 [T867A] form refractory to CDK phosphorylation did not change in electrophoretic mobility upon the activation of the MAPK cascade and cells carrying the Kap123 [T867A] protein were not arrested sustained our hypothesis. Furthermore we demonstrated that Cdc25 levels do not decrease in presence of Kap123 [T867A]. Following these results, we propose a model where upon the activation of the MAPK cascade the complex Crk1-Pcl12 is formed. This complex phosphorylates the importin Kap123 avoiding the entrance into the nucleus of Cdc25. The retention of Cdc25 in the cytoplasm avoids the progression in mitosis and promote G2 cell cycle arrest due to the increase of the inhibitory phosphorylation of Cdk1. Consequently, Cdc25 accumulated in the cytoplasm where is down regulated (Fig.2)
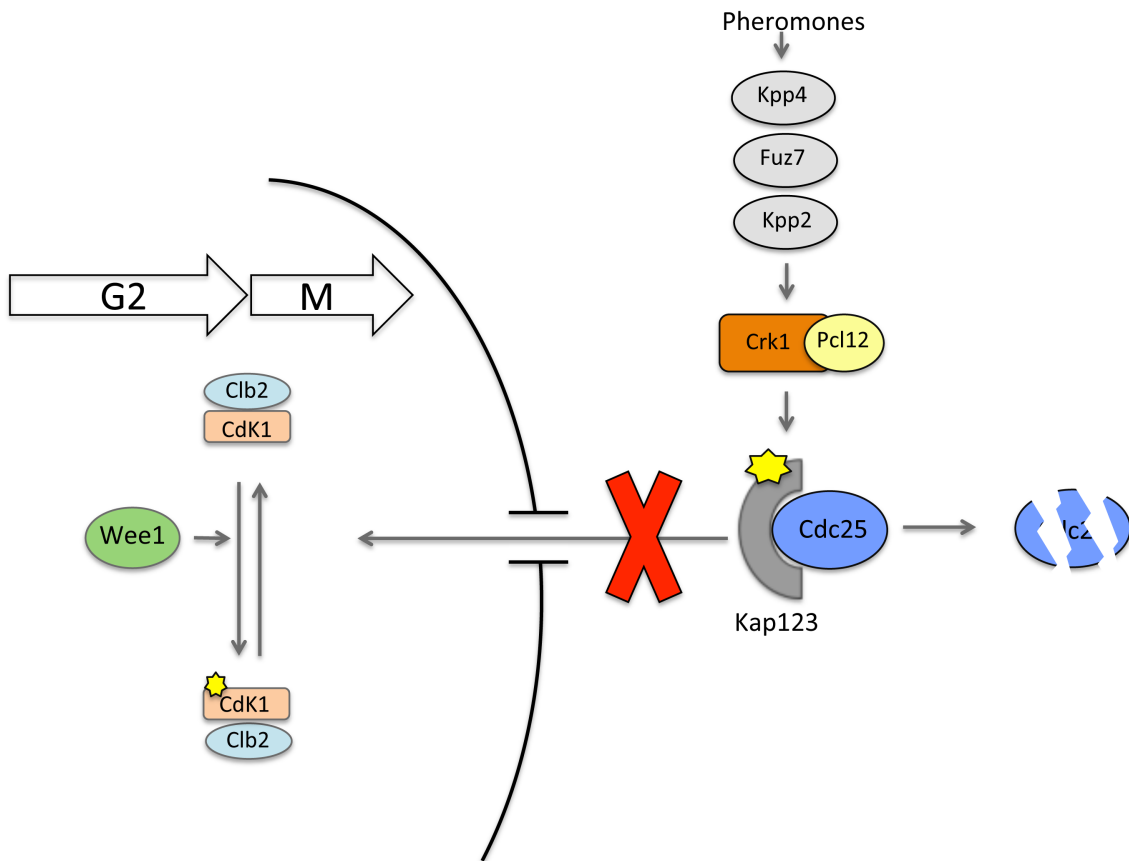
Figure 2: Model of the pheromone cell cycle arrest. The activation of the MAPK cascade by pheromones leads with the formation of the Crk1-Pcl12 complex. This complex is able to phosphorylate the Importin Kap123 affecting its ability to traslocate in the nucleus to dephosphorylate Cdk1 an dpromote the entry into mitosis. Once Cdc25 acumulates in the cytoplasm is degraded.

The decrease of Cdc25 level is associated with the activation of the MAPK cascade. Therefore when we overexpressed *pcl12* alone without the induction of the MAPK cascade we did not observe decrease in Cdc25 levels. We believe that the MAPK cascade triggers the Cdc25 degradation. Although we have no clue about which mechanisms are involved in this degradation, we can envisioned at least two non-exclusive ways. The first one is that the MAPK cascade could activate some E3 ubiquitin ligase, able to recognize and target Cdc25 for degradation by proteasome. We already investigated the role of the APC (Anaphase promoting complex) (Castillo-Lluva *et al.* 2004) and SCF (Skp, cullin, F-box) complexes, which are involved in degradation of important cell cycle regulators, however our results indicated that these complexes were not involved in the Cdc25 levels decrease

observed upon FuzDD activation. Nowadays, we are currently working on a HECT-E3 ubiquitin ligase that we called Tom1 upon its sequence similarity to Tom1 from S. cerevisiae. In *S.cerevisae*, Tom1 targets for degradation Cdc6, an essential regulator of DNA replication, but also several ribosomal protein and histones (Kim and Koepp 2012; Singh *et al.* 2012; Sung *et al.* 2016). We observed that in *U. maydis* Tom1 is essential and using a conditional mutant we found that the decrease of Cdc25 levels upon fuz7DD activation was prevented.

The other hypothesis is that the MAPK cascade or other effector kinases are directly able to phosphorylate Cdc25 tagging for its degradation. U. maydis Cdc25 is characterized by a long N-terminal region that is not conserved in other fungi (Carbo and Perez-Martin 2010). We noticed that in this region there are three putative MAPK phosphorylation sites. It could be well that the phosphorylation of Cdc25 in its N-terminal region could direct the protein for its degradation. It has been reported that in *Xenopus leavis* Cdc25A can be targeted for the degradation by the ERK pathway causing a cell cycle arrest (Isoda *et al.* 2009). To address this question, we are performing a deletion assay of the N-terminal region trying to link the presence of this domain with the observed decrease in the Cdc25 protein levels.

4.PHEROMONE CELL CYCLE ARREST AND b-CELL CYCLE ARREST

We consider that the regulation of Cdc25 localization is the firstly mechanism operating in cell cycle arrest induced by pheromone. The decision could be explained by the fact that, in *U. maydis* the mating process is not an irreversible decision: after fusion, two cells to continue the sexual development and generate the infective filament need to form the b-factor. The proper formation of the b-factor occurs when two partners are compatible also for the b-factor, otherwise the sexual development arrests and the two cells need to release the cell cycle and go back to their vegetative form. For this reason, keeping Cdc25 in the

cytoplasm and avoiding the entrance in the nucleus is the most suitable choice in case the cell needs to re-entry cell cycle. Following this hypothesis, only when the sexual development successfully progress Cdc25 is degraded. We believe that we observed Cdc25 down regulation because we used conditions where the MAPK cascade is over activated due to the induction of the *fuz7^{DD}* allele. This MAPK condition of over activation is characteristic of a successful mating development. Indeed, the fact that the pheromone MAPK pathway output reflects a graded input it has been demonstrated in *C. cerevisae* (Conlon *et al.* 2016). It is reasonable to speculate that *U. maydis* needs to degrade Cdc25 to prepare the proper condition for the formation of the infective filament. Indeed the G2 cell cycle arrest in the infective filament is due to two mechanisms: the down regulation of *hsl1*, a negative regulator of Wee1, and the cytoplasmic recruitment of Cdc25 by Bmh1, a 14-3-3 protein (Mielnichuk *et al.* 2009; Castanheira *et al.* 2014). We consider that U. maydis needs to down regulate Cdc25 levels to avoid Cdc25 accumulation in the cytoplasm that cannot be completely recruited by Bmh1 when the infective filament is formed. The failure of Bmh1 to recruit Cdc25 in the cytoplasm might lead to the formation of an infective filament that is not arrested in cell cycle. Indeed, it has been observed that impairing the binding between 14-3-3 and Cdc25 or overexpressing Cdc25 resulted in a filament that was not arrested in cell cycle (Mielnichuk *et al.* 2009).

CONCLUSION

CONCLUSION

- In *U.maydis* pheromone signal induces G2 cell cycle

- G2 cell cycle arrest induced by pheromone requires the inhibitory phosphorylation of Cdk1

- Cdc25 down regulation depends of the activation of the MAPK cascade

- The Cdk-related kinase Crk1 acts in complex with the cyclin Pcl12 to arrest cell cycle in response to pheromone

- Crk1 is activated by the MAPK Fuz7 to control morphogenesis and by the cyclin Pcl12 to control pheromone cell cycle arrest

- The β-importin, Kap123, is required for Cdc25 localization

- The β-importin, Kap123 is phosphorylated by the Crk1-Pcl12 complex

- The allele *kap123^{T867A}* refractory to phosphorylation avoids pheromone cell cycle arrest and Cdc25 down regulation.

BIBLIOGRAPHY

Alvarez-Tabares, I. and J. Perez-Martin (2008). "Cdk5 kinase regulates the association between adaptor protein Bem1 and GEF Cdc24 in the fungus Ustilago maydis." Journal of cell science **121**(Pt 17): 2824-2832.

Banuett, F. (1995). "Genetics of Ustilago maydis, a fungal pathogen that induces tumors in maize." Annual review of genetics **29**: 179-208.

Banuett, F. and I. Herskowitz (1989). "Different a alleles of Ustilago maydis are necessary for maintenance of filamentous growth but not for meiosis." Proceedings of the National Academy of Sciences of the United States of America **86**(15): 5878-5882.

Banuett, F. and I. Herskowitz (1989). "Different a alleles of Ustilago maydis are necessary for maintenance of filamentous growth but not for meiosis." Proc Natl Acad Sci U S A **86**(15): 5878-5882.

Barral, Y., *et al.* (1999). "Nim1-related kinases coordinate cell cycle progression with the organization of the peripheral cytoskeleton in yeast." Genes & development **13**(2): 176-187.

Bielska, E., *et al.* (2014). "Long-distance endosome trafficking drives fungal effector production during plant infection." Nature communications **5**: 5097.

Bolker, M. (2001). "Ustilago maydis--a valuable model system for the study of fungal dimorphism and virulence." Microbiology **147**(Pt 6): 1395-1401.

Bolker, M. and R. Kahmann (1993). "Sexual pheromones and mating responses in fungi." The Plant cell **5**(10): 1461-1469.

Bottin, A., *et al.* (1996). "Isolation of a carbon source-regulated gene from Ustilago maydis." Mol Gen Genet **253**(3): 342-352.

Brachmann, A., *et al.* (2004). "A reverse genetic approach for generating gene replacement mutants in Ustilago maydis." Mol Genet Genomics **272**(2): 216-226.

Brachmann, A., *et al.* (2001). "Identification of genes in the bW/bE regulatory cascade in Ustilago maydis." <u>Mol Microbiol</u> **42**(4): 1047-1063.

Carbo, N. and J. Perez-Martin (2010). "Activation of the cell wall integrity pathway promotes escape from G2 in the fungus Ustilago maydis." <u>PLoS Genet</u> **6**(7): e1001009.

Castanheira, S., *et al.* (2014). "Programmed cell cycle arrest is required for infection of corn plants by the fungus Ustilago maydis." <u>Development</u> **141**(24): 4817-4826.

Castanheira, S. and J. Perez-Martin (2015). "Appressorium formation in the corn smut fungus Ustilago maydis requires a G2 cell cycle arrest." <u>Plant signaling & behavior</u> **10**(4): e1001227.

Castanheiro, T., *et al.* (2014). "Cyclocarbopalladation/cross-coupling cascade reactions in sulfide series: access to sulfur heterocycles." <u>Org Lett</u> **16**(11): 3060-3063.

Castillo-Lluva, S., *et al.* (2007). "Sustained cell polarity and virulence in the phytopathogenic fungus Ustilago maydis depends on an essential cyclin-dependent kinase from the Cdk5/Pho85 family." <u>Journal of cell science</u> **120**(Pt 9): 1584-1595.

Castillo-Lluva, S., *et al.* (2004). "A member of the Fizzy-related family of APC activators is regulated by cAMP and is required at different stages of plant infection by Ustilago maydis." <u>J Cell Sci</u> **117**(Pt 18): 4143-4156.

Castillo-Lluva, S. and J. Perez-Martin (2005). "The induction of the mating program in the phytopathogen Ustilago maydis is controlled by a G1 cyclin." <u>Plant Cell</u> **17**(12): 3544-3560.

Chang, F. and I. Herskowitz (1990). "Identification of a gene necessary for cell cycle arrest by a negative growth factor of yeast: FAR1 is an inhibitor of a G1 cyclin, CLN2." <u>Cell</u> **63**(5): 999-1011.

Chua, G., *et al.* (2002). "The sal3(+) gene encodes an importin-beta implicated in the nuclear import of Cdc25 in Schizosaccharomyces pombe." <u>Genetics</u> **162**(2): 689-703.

Conlon, P., *et al.* (2016). "Single-cell dynamics and variability of MAPK activity in a yeast differentiation pathway." <u>Proc Natl Acad Sci U S A</u> **113**(40): E5896-E5905.

Davey, J. (1998). "Fusion of a fission yeast." Yeast **14**(16): 1529-1566.

Davey, J. and O. Nielsen (1994). "Mutations in cyr1 and pat1 reveal pheromone-induced G1 arrest in the fission yeast Schizosaccharomyces pombe." Current genetics **26**(2): 105-112.

Elion, E. A*., et al.* (1993). "FUS3 phosphorylates multiple components of the mating signal transduction cascade: evidence for STE12 and FAR1." Molecular biology of the cell **4**(5): 495-510.

Feldbrugge, M.*, et al.* (2004). "Regulation of mating and pathogenic development in Ustilago maydis." Current opinion in microbiology **7**(6): 666-672.

Flor-Parra, I.*, et al.* (2007). "Polar growth in the infectious hyphae of the phytopathogen ustilago maydis depends on a virulence-specific cyclin." The Plant cell **19**(10): 3280-3296.

Flor-Parra, I.*, et al.* (2007). "Polar growth in the infectious hyphae of the phytopathogen ustilago maydis depends on a virulence-specific cyclin." Plant Cell **19**(10): 3280-3296.

Flores, K. and R. Seger (2013). "Stimulated nuclear import by beta-like importins." F1000Prime Rep **5**: 41.

Garcia-Muse, T.*, et al.* (2003). "Pheromone-induced G2 arrest in the phytopathogenic fungus Ustilago maydis." Eukaryotic cell **2**(3): 494-500.

Garcia-Muse, T.*, et al.* (2004). "Characterization of B-type cyclins in the smut fungus Ustilago maydis: roles in morphogenesis and pathogenicity." Journal of cell science **117**(Pt 3): 487-506.

Garcia-Muse, T.*, et al.* (2004). "Characterization of B-type cyclins in the smut fungus Ustilago maydis: roles in morphogenesis and pathogenicity." J Cell Sci **117**(Pt 3): 487-506.

Garrido, E. and J. Perez-Martin (2003). "The crk1 gene encodes an Ime2-related protein that is required for morphogenesis in the plant pathogen Ustilago maydis." Mol Microbiol **47**(3): 729-743.

Garrido, E. and J. Perez-Martin (2003). "The crk1 gene encodes an Ime2-related protein that is required for morphogenesis in the plant pathogen Ustilago maydis." <u>Molecular microbiology</u> **47**(3): 729-743.

Garrido, E.*, et al.* (2004). "The induction of sexual development and virulence in the smut fungus Ustilago maydis depends on Crk1, a novel MAPK protein." <u>Genes & development</u> **18**(24): 3117-3130.

Garrido, E.*, et al.* (2004). "The induction of sexual development and virulence in the smut fungus Ustilago maydis depends on Crk1, a novel MAPK protein." <u>Genes Dev</u> **18**(24): 3117-3130.

Gillissen, B.*, et al.* (1992). "A two-component regulatory system for self/non-self recognition in Ustilago maydis." <u>Cell</u> **68**(4): 647-657.

Graves, P. R.*, et al.* (2001). "Localization of human Cdc25C is regulated both by nuclear export and 14-3-3 protein binding." <u>Oncogene</u> **20**(15): 1839-1851.

Hanahan, D. (1983). "Studies on transformation of Escherichia coli with plasmids." <u>J Mol Biol</u> **166**(4): 557-580.

Harel, A. and D. J. Forbes (2004). "Importin beta: conducting a much larger cellular symphony." <u>Mol Cell</u> **16**(3): 319-330.

Hartmann, H. A.*, et al.* (1996). "The pheromone response factor coordinates filamentous growth and pathogenicity in Ustilago maydis." <u>The EMBO journal</u> **15**(7): 1632-1641.

Heimel, K.*, et al.* (2010). "The Ustilago maydis Clp1 protein orchestrates pheromone and b-dependent signaling pathways to coordinate the cell cycle and pathogenic development." <u>The Plant cell</u> **22**(8): 2908-2922.

Heimel, K.*, et al.* (2010). "The transcription factor Rbf1 is the master regulator for b-mating type controlled pathogenic development in Ustilago maydis." <u>PLoS pathogens</u> **6**(8): e1001035.

Herskowitz, I. (1995). "MAP kinase pathways in yeast: for mating and more." <u>Cell</u> **80**(2): 187-197.

Isoda, M*., et al.* (2009). "The extracellular signal-regulated kinase-mitogen-activated protein kinase pathway phosphorylates and targets Cdc25A for SCF beta-TrCP-dependent degradation for cell cycle arrest." Mol Biol Cell **20**(8): 2186-2195.

Johnson, L. N*., et al.* (1996). "Active and inactive protein kinases: structural basis for regulation." Cell **85**(2): 149-158.

Kaffarnik, F*., et al.* (2003). "PKA and MAPK phosphorylation of Prf1 allows promoter discrimination in Ustilago maydis." The EMBO journal **22**(21): 5817-5826.

Kamper, J. (2004). "A PCR-based system for highly efficient generation of gene replacement mutants in Ustilago maydis." Molecular genetics and genomics : MGG **271**(1): 103-110.

Kamper, J*., et al.* (1995). "Multiallelic recognition: nonself-dependent dimerization of the bE and bW homeodomain proteins in Ustilago maydis." Cell **81**(1): 73-83.

Kerppola, T. K. (2008). "Bimolecular fluorescence complementation (BiFC) analysis as a probe of protein interactions in living cells." Annu Rev Biophys **37**: 465-487.

Kim, D. H. and D. M. Koepp (2012). "Hect E3 ubiquitin ligase Tom1 controls Dia2 degradation during the cell cycle." Mol Biol Cell **23**(21): 4203-4211.

Kumagai, A. and W. G. Dunphy (1997). "Regulation of Xenopus Cdc25 protein." Methods in enzymology **283**: 564-571.

Lamson, R. E*., et al.* (2006). "Dual role for membrane localization in yeast MAP kinase cascade activation and its contribution to signaling fidelity." Current biology : CB **16**(6): 618-623.

Lanver, D*., et al.* (2010). "Sho1 and Msb2-related proteins regulate appressorium development in the smut fungus Ustilago maydis." The Plant cell **22**(6): 2085-2101.

Lanver, D*., et al.* (2017). "Ustilago maydis effectors and their impact on virulence." Nat Rev Microbiol **15**(7): 409-421.

Leeuw, T.*, et al.* (1998). "Interaction of a G-protein beta-subunit with a conserved sequence in Ste20/PAK family protein kinases." Nature **391**(6663): 191-195.

Mielnichuk, N. and J. Perez-Martin (2008). "14-3-3 regulates the G2/M transition in the basidiomycete Ustilago maydis." Fungal genetics and biology : FG & B **45**(8): 1206-1215.

Mielnichuk, N.*, et al.* (2009). "A role for the DNA-damage checkpoint kinase Chk1 in the virulence program of the fungus Ustilago maydis." J Cell Sci **122**(Pt 22): 4130-4140.

Mielnichuk, N.*, et al.* (2009). "A role for the DNA-damage checkpoint kinase Chk1 in the virulence program of the fungus Ustilago maydis." Journal of cell science **122**(Pt 22): 4130-4140.

Miller, K. E.*, et al.* (2015). "Bimolecular Fluorescence Complementation (BiFC) Analysis: Advances and Recent Applications for Genome-Wide Interaction Studies." J Mol Biol **427**(11): 2039-2055.

Muller, P.*, et al.* (2003). "Mating and pathogenic development of the Smut fungus Ustilago maydis are regulated by one mitogen-activated protein kinase cascade." Eukaryot Cell **2**(6): 1187-1199.

Muller, P.*, et al.* (2003). "Mating and pathogenic development of the Smut fungus Ustilago maydis are regulated by one mitogen-activated protein kinase cascade." Eukaryotic cell **2**(6): 1187-1199.

Nern, A. and R. A. Arkowitz (1999). "A Cdc24p-Far1p-Gbetagamma protein complex required for yeast orientation during mating." J Cell Biol **144**(6): 1187-1202.

Nolen, B.*, et al.* (2004). "Regulation of protein kinases; controlling activity through activation segment conformation." Molecular cell **15**(5): 661-675.

Perez-Martin, J. (2009). "DNA-damage response in the basidiomycete fungus Ustilago maydis relies in a sole Chk1-like kinase." DNA repair **8**(6): 720-731.

Perez-Nadales, E.*, et al.* (2014). "Fungal model systems and the elucidation of pathogenicity determinants." Fungal Genet Biol **70**: 42-67.

Peter, M. and I. Herskowitz (1994). "Direct inhibition of the yeast cyclin-dependent kinase Cdc28-Cln by Far1." Science **265**(5176): 1228-1231.

Pope, P. A*., et al.* (2014). "Regulation of cyclin-substrate docking by a G1 arrest signaling pathway and the Cdk inhibitor Far1." Current biology : CB **24**(12): 1390-1396.

Pope, P. A*., et al.* (2014). "Regulation of cyclin-substrate docking by a G1 arrest signaling pathway and the Cdk inhibitor Far1." Current biology : CB **24**(12): 1390-1396.

Rout, M. P*., et al.* (1997). "A distinct nuclear import pathway used by ribosomal proteins." Cell **89**(5): 715-725.

Sgarlata, C. and J. Perez-Martin (2005). "The cdc25 phosphatase is essential for the G2/M phase transition in the basidiomycete yeast Ustilago maydis." Molecular microbiology **58**(5): 1482-1496.

Sgarlata, C. and J. Perez-Martin (2005). "The cdc25 phosphatase is essential for the G2/M phase transition in the basidiomycete yeast Ustilago maydis." Mol Microbiol **58**(5): 1482-1496.

Sgarlata, C. and J. Perez-Martin (2005). "Inhibitory phosphorylation of a mitotic cyclin-dependent kinase regulates the morphogenesis, cell size and virulence of the smut fungus Ustilago maydis." J Cell Sci **118**(Pt 16): 3607-3622.

Sgarlata, C. and J. Perez-Martin (2005). "Inhibitory phosphorylation of a mitotic cyclin-dependent kinase regulates the morphogenesis, cell size and virulence of the smut fungus Ustilago maydis." Journal of cell science **118**(Pt 16): 3607-3622.

Shimada, Y*., et al.* (2000). "Nuclear sequestration of the exchange factor Cdc24 by Far1 regulates cell polarity during yeast mating." Nat Cell Biol **2**(2): 117-124.

Singh, R. K*., et al.* (2012). "Novel E3 ubiquitin ligases that regulate histone protein levels in the budding yeast Saccharomyces cerevisiae." PLoS One **7**(5): e36295.

Steinberg, G. and J. Perez-Martin (2008). "Ustilago maydis, a new fungal model system for cell biology." Trends in cell biology **18**(2): 61-67.

Straube, A*., et al.* (2003). "Microtubule organization requires cell cycle-dependent nucleation at dispersed cytoplasmic sites: polar and perinuclear microtubule organizing centers in the plant pathogen Ustilago maydis." Molecular biology of the cell **14**(2): 642-657.

Sung, M. K*., et al.* (2016). "A conserved quality-control pathway that mediates degradation of unassembled ribosomal proteins." Elife **5**.

Terfruchte, M*., et al.* (2014). "Establishing a versatile Golden Gate cloning system for genetic engineering in fungi." Fungal Genet Biol **62**: 1-10.

Terfruchte, M*., et al.* (2014). "Establishing a versatile Golden Gate cloning system for genetic engineering in fungi." Fungal genetics and biology : FG & B **62**: 1-10.

Topp, C. N*., et al.* (2002). "Integration of the gene for carboxin resistance does not impact the Ustilago maydis-maize interaction." Current microbiology **44**(1): 67-70.

Whiteway, M. S*., et al.* (1995). "Association of the yeast pheromone response G protein beta gamma subunits with the MAP kinase scaffold Ste5p." Science **269**(5230): 1572-1575.

Wilkinson, M. G. and J. B. Millar (2000). "Control of the eukaryotic cell cycle by MAP kinase signaling pathways." FASEB J **14**(14): 2147-2157.

Zarnack, K*., et al.* (2008). "Pheromone-regulated target genes respond differentially to MAPK phosphorylation of transcription factor Prf1." Molecular microbiology **69**(4): 1041-1053.

Zavala-Gonzales, M. A*., et al.* (2014). "Validation and diagnostic usefulness of gastroesophageal reflux disease questionnaire in a primary care level in Mexico." J Neurogastroenterol Motil **20**(4): 475-482.

Zhao, X*., et al.* (2007). "Mitogen-activated protein kinase pathways and fungal pathogenesis." Eukaryotic cell **6**(10): 1701-1714.